ABSTRACT

Title of Document:	INVESTIGATION OF THIOLATED POLYMER IN GENE DELIVERY
	Irene Bacalocostantis
Directed By:	Professor Peter Kofinas, Fischell Department of Bioengineering

Thiol-containing bioreducible polymers show significant potential as delivery vectors in gene therapy, a rapidly growing field which seeks to treat genetic-based disorders by delivering functional synthetic genes to diseased cells. Studies have shown that thiolated polymers exhibit improved biodegradability and prolonged *in vivo* circulation times over non-thiolated polymers. However, the extent to which thiol concentrations impact the carrier's delivery potential has not been well explored. The aim of this dissertation is to investigate how relative concentrations of free thiols and disulfide crosslinks impact a polymeric carriers delivery performance with respect to DNA packaging, complex stability, cargo protection, gene release, internalization efficiency and cytotoxicity. To accomplish this goal, several fluorescent polymers containing varying concentrations of thiol groups were synthesized by conjugating thiol-pendant chains onto the primary amines of cationic poly(allylamine). *In vitro* delivery assays and characterization techniques were employed to assess the effect of thiols in gene delivery.

INVESTGATION OF THIOLATED POLYMER IN GENE DELIVERY

By

Irene Bacalocostantis

Dissertation submitted to the Faculty of the Graduate School of the
University of Maryland, College Park, in partial fulfillment
of the requirements for the degree of
Doctor of Philosophy
2012

Advisory Committee:
Professor Peter Kofinas, Chair
Professor Silvia Muro-Galindo
Professor William Bentley
Professor Robert Briber
Associate Professor Adam Hsieh

www.manaraa.com

Dedication

I dedicate this dissertation to my family.

To my parents, Kiriacos and Sofia: I could not have done this without your love,

understanding, and support. I am forever in your debt. Thank you.

To my sister, Eliana: Thank you for the laughs, the cries, the Kodak moments, but most

of all - Thank you for being someone I could always count on.

Acknowledgements

My first thanks goes to my advisor and committee chair, Professor Peter Kofinas, who, for five years, played the dual role of academic mentor and friend. Peter, I could not have asked for a better advisor, without your guidance and persistent help this dissertation would not have been possible. Thank you.

Next thanks goes to my co-advisor, Professor Silvia Muro-Galindo, who welcomed me into her research group and guided me every step of the way. Silvia: Your enthusiasm for research and commitment to mentoring is truly inspiring.

To my close friends Angela Mariani and Joyce Breger: Thank you for always being there, and know, that I will always cherish the memories we created together. To the Kofinas lab boys, past and present, Omar Ayyub, Adam Behrens, Von Cresce, Aaron Fisher, Ayan Ghosh, Daniel Janiak, Josh Silverstein, Mert Vural, and Ta-I Yang, thank you all for making every day interesting. Further thanks to my Muro-ite friends: Tridib Bhowmick, Rasa Ghaffarian, Janet Hsu, Jason Papademetriou, and Daniel Serrano for making me feel at home in their lab. A special thanks to Muro-ite Viraj Mane, for his mentorship and extraordinary patience. Bioengineering students Michael Kang, and Addison Goodley: Thank you for enduring countless hours with me in lab.

I would also like to thank my committee members Professor William Bentley, Professor Robert Briber, and Professor Adam Hsieh for being a part of this important part of my life. Thank you to Maria Klapa, Principle Researcher at the Foundation of Research and Technology in Patras, Greece, for encouraging me to embark on this long and fruitful journey. Finally, thank you to Foligo Therapeutics for their funding support.

Table of Contents

List of Tables

List of Figures

Chapter 1

1.1 Overview

With the recognition of inter-individual differences in drug response, the health industry is slowly moving towards the development of personalized medicine for optimal treatment with minimal side effects. The emerging field of gene therapy fulfills these needs and is considered the next generation in therapeutics.[1] The goal of gene therapy is to treat genetic-based disorders such as Alzheimer's, cystic fibrosis, and muscular dystrophy, by replacing the disease-causing gene with a functional synthetic gene. Gene therapy also aims to treat neurological, cardiovascular, and infectious diseases by developing synthetic genes that encode for cytotoxic proteins or prodrug activity.[2] Tumors, for example, can be targeted with tumoricidal or tumor suppressing genes.[3] Thus far, the therapeutic efficiency of synthetic genes has been proven in both animal and clinical studies.[4-10] However, the full potential of gene therapy has yet to be fulfilled due to challenges associated with delivery methods such as cell targeting specificity, transfection efficiency, gene expression regulation, and safety.[11] Statistics show that despite the therapeutic efficiency of synthetic genes, over 95% of clinical trials never reach phase III studies due to safety concerns involving gene delivery methods.[12]

Direct delivery of "naked DNA" into targeted tissues is by far the simplest delivery method used in gene delivery. Several challenges, associated with the size and charge of naked DNA, prevent this strategy from being applied with reasonable efficacy.[12-14] Studies have shown that the DNA's negative charge hinders cellular internalization. Further, due to its small size, naked DNA is readily degraded within the bloodstream upon systemic administration. Delivery vectors are therefore necessary for the successful

1

delivery of therapeutic genes to cells.[13, 15] Successful gene carriers must have the capability to overcome a number of intracellular and extracellular obstacles including gene packaging, serums stability, cell targeting, cellular uptake, endolysosomal escape, and cargo release.[2, 16]

Engineered viral capsids were the first vectors employed for gene delivery. Initial reports of clinical implementation showed that viral vectors had severe and even deadly side effects. In 2000, an 18 year old girl who participated in an ornithine transcarboxylase deficiency clinical trial at the University of Pennsylvania (UPenn) died as a result of an inflammatory reaction to an adenovirus based vector.[17] After the death of second UPenn volunteer, the US Food and Drug Administration (FDA) halted seven ongoing clinical trials at the university.[18] Then in 2002, a 3 year old boy treated with gene therapy at a hospital in France developed a leukemia-like clonal lymphocyte proliferation as a result of a retroviral vector.[19, 20] This time the US FDA halted over two dozen clinical trials.[20, 21]

The clinical challenges associated with viral vectors have motivated researchers to explore synthetic polymers as a safer delivery alternative.[22] Unlike viral vectors, polymeric carriers can be chemically and structurally modified to overcome several of the discussed challenges. The polymer's molecular weight, polydispersity, chain composition, and chain density can be altered to improve the carrier's delivery efficiency. In addition, polymers pose lesser risk of immunogenicity than viral vectors, carry no risk of integrating into the host chromosome, and can be produced in large quantities at low cost.[15, 23, 24]

1.2 Objectives

Thiol containing bioreducible polymers are especially attractive as delivery vectors because of their intrinsic ability to respond to environmental stimuli.[25, 26] Thiols (SH) readily form disulfide bonds (S-S) in an oxidation reaction which can be controlled by solution viscosity, pH, and temperature. The disulfides remain relatively stable in oxidizing environments such as the extracellular space, but are readily reduced in the intracellular reducing environment of cells.[25] Previously, studies have shown that polymer-gene complexes (polyplexes) formed with bioreducible polymers remain intact in the circulatory system, but degrade within the intracellular space for high cargo release.[15, 27] However, the extent to which thiol concentrations and degree of crosslinking impact the carriers delivery potential have not been well explored.

The aim of this dissertation is to investigate how relative concentrations of free thiols and disulfide crosslinks impact a polymeric carriers delivery performance with respect to DNA packaging, complex stability, cargo protection, gene release, internalization efficiency and cytotoxicity. To accomplish this goal, several fluorescent polymers containing varying concentrations of thiol groups were synthesized by conjugating thiol-pendant chains onto the primary amines of cationic poly (allylamine) PAA. Synthesis of thiolated polymers was verified by ^{1}H NMR. The relative concentration of thiol groups and the extent of disulfide crosslinking were determined by 5,5'-dithiobis-(2-nitrobenzoic acid) (DNTB) assay. Techniques such as gel electrophoresis, UV spectrophotometry, fluorescent microscopy, and dynamic light scattering were employed to characterize DNA binding/release, polyplex size and stability, and delivery potential. Transfection efficiency was determined by delivering plasmid DNA to breast cancer cells.

3

1.3 Mechanism of Polymeric Gene Delivery

Polymeric gene delivery begins with the packaging of genetic cargo by a polymer carrier. The resulting polyplexes are internalized by cells through non-specific adsorptive endocytosis or receptor-mediated endocytosis.[1, 11] In receptor-mediated endocytosis, polymer complexes carry targeting ligands that bind to specific receptors located on cell surfaces and trigger internalization.[11, 28] Non-specific endocytosis results from electrostatic interactions arising between positively charged polymeric carriers and negatively charged carboxylated glycosaminoglycans (GAGs) present on the cell's surface. Both ligand-receptor and polymer-GAG interactions cause the cellular membrane to invaginate, thus engulfing polyplexes in a membranous vesicle known as the endosome. Initially, the endosome has a pH~7. However, as the vesicle matures into a lysosome, the internal pH drops to ~4. Polyplexes that do not escape prior to maturation are degraded by lysosomal enzymes.[28] Many cationic polymers have the ability to escape the endolysosome through the proton sponge effect; a phenomenon in which polymers absorb protons from the incoming cytosol and swell, thereby rupturing the endolysosome and releasing the DNA cargo into the cell cytosol. Once released, the cargo is transported to the nucleus for transcription.[11] The mechanism of polymeric gene delivery is depicted in Figure 1.

4
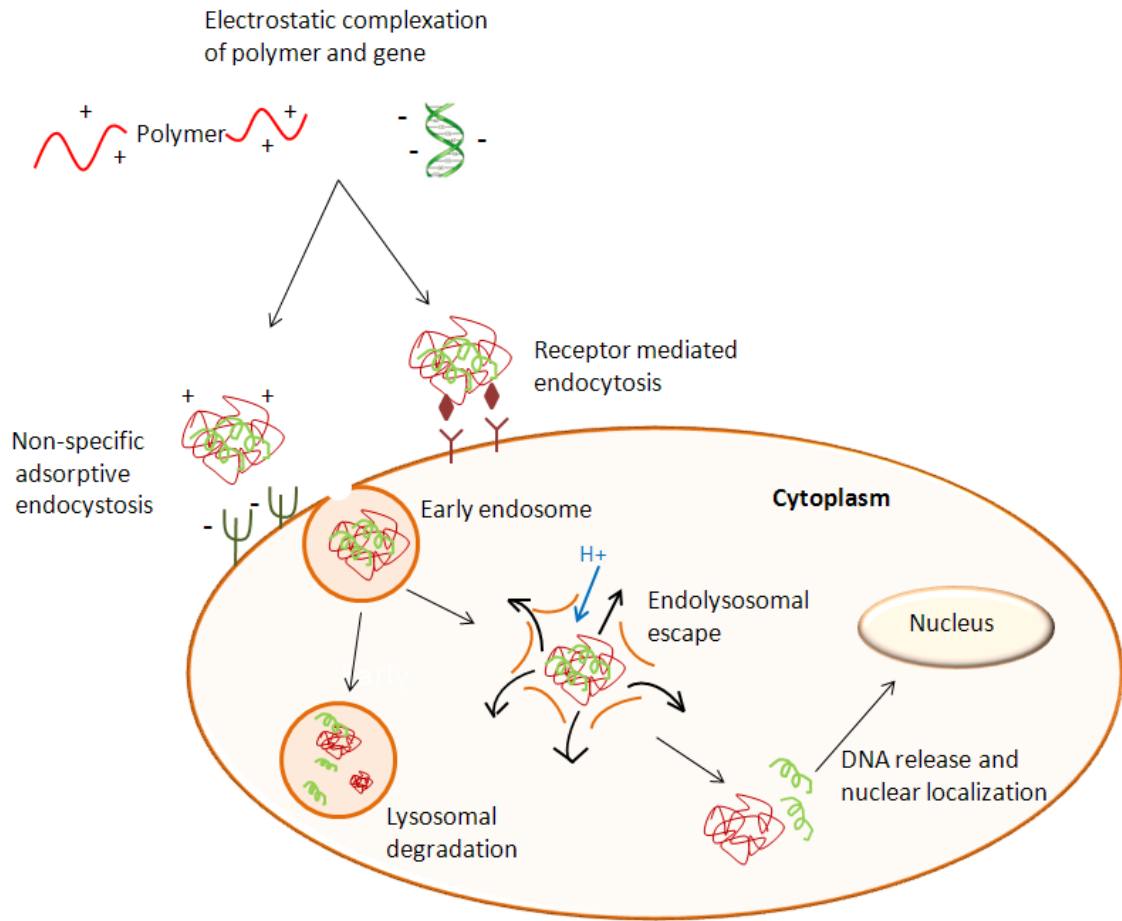
Figure 1. Schematic of polymeric gene delivery

1.4 Challenges in Gene Delivery

The extracellular and intracellular challenges associated with gene delivery are depicted in Figure 2.[29] This section reviews the primary challenges associated with polymeric gene delivery and discusses current methods employed to overcome them.

EXTRACELLULAR BARRIERS

Degradation of DNA in plasma
Uptake of DNA by reticuloendothelial system
Inability to target DNA to specific organs
Largely ineffective via the oral route – except for immunisation
Transfection inhibited by mucus

INTRACELLULAR BARRIERS

Endosomal escape of DNA
Lysosomal degradation of DNA
Cytoplasmic stability of DNA
Translocation of DNA to the nucleus

Figure 2: Intracellular and extracellular barriers in gene delivery [29]

1.4.1   Extracellular Barriers

1.4.1.1   *Gene Packaging*

The primary goal of gene packaging is to produce complexes of optimal size and composition for cellular uptake. There are three main packaging strategies that are currently being employed in polymeric gene delivery; electrostatic interaction, encapsulation, and adsorption (Figure 3).[11]
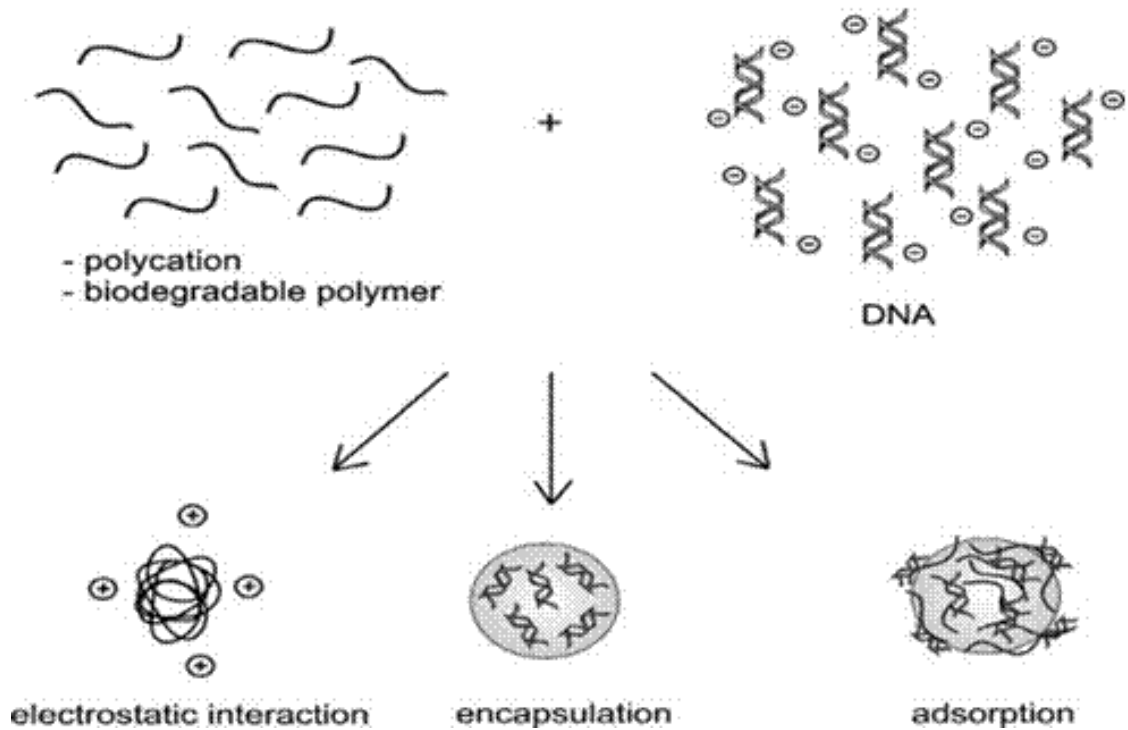
Figure 3. Main packaging strategies currently being employed in gene delivery [11]

Electrostatic interactions between the polymer's positively charged amines and the DNA's negatively charged phosphates are the primary driving forces behind DNA condensation.[30] Studies have shown that approximately 90% of the negative charges on the DNA phosphate backbone must be overcome for condensation to occur.[31] However, at a sufficient amine to phosphate ratio (N/P ratio), polyplexes form spontaneously upon mixing. The resulting particles have a toroidal or rod-like shape ranging from 30 to several hundred nm in diameter.[2] Polyplex size, charge, and stability can be altered by changing the N/P ratio.[32]

1.4.1.1.2   Encapsulation

An alternative packaging strategy is via hydrogel encapsulation. Hydrogels are crosslinked polymers with the ability absorb water without dissolving. The majority of hydrogels employed in gene delivery contain ester or disulfide linkages along their backbone. These bonds are readily hydrolyzed within the cell, allowing for more efficient DNA cargo release. The degradation kinetics of hydrogels can be modulated by altering the gels physicochemical properties, such as crosslink density. Hence, hydrogels can be customized to respond to environmental stimuli such as pH or temperature.[11]

Hydrogel-DNA particles in gene delivery are primarily formed by reverse emulsion, a technique in which monomer units and DNA strands are added to a hydrophobic solution containing amphiphilic emulsifier. Emulsifiers form micelles with non-ionic surfaces and charged cores. Since monomer units and DNA strands prefer the charged environment, they migrate into the micelle core. At this point, monomers and crosslinkers polymerize

8

to form a hydrogel structure loaded with DNA cargo. The major limitation of this method is that it requires high shear stresses, organic solvents, and extreme temperatures which degrade DNA.[11]

1.4.1.1.3 Adsorption

Adsorption involves conjugating cationic moieties onto the surface of biodegradable polymers so that DNA can electrostatically bind. The advantage of this technique is that it leaves the DNA readily available for release within the cell. However, because the DNA is located on the polymers surface, it can easily be accessed and degraded by enzymes.[11]

1.4.1.2 Serum Stability

The body's defense system is built so that it quickly identifies and eliminates foreign moieties. When systematically administered, cationic polymers interact with negatively charged serum proteins. As a result, polyplexes are rapidly cleared by the phagocytic cells of the mononuclear phagocyte system (MPS) in the liver, spleen, lungs and bone marrow.[2, 23] To minimize polymer-protein interactions, hydrophilic polymers, such as poly (ethylene) glycol (PEG) and N-(2-hydroxypropyl)methacrylamide (HPMA), can be grafted onto the polymer chain as a "brush" as shown in Figure 4.[2, 23] The molecular brush acts to sterically block polymer-protein interactions, thereby reducing particle aggregation and increasing the solubility of the polymer-DNA complexes. Studies have shown that the application of hydrophilic monomers can increase systemic circulation times of intravenously administered complexes.[1, 33]
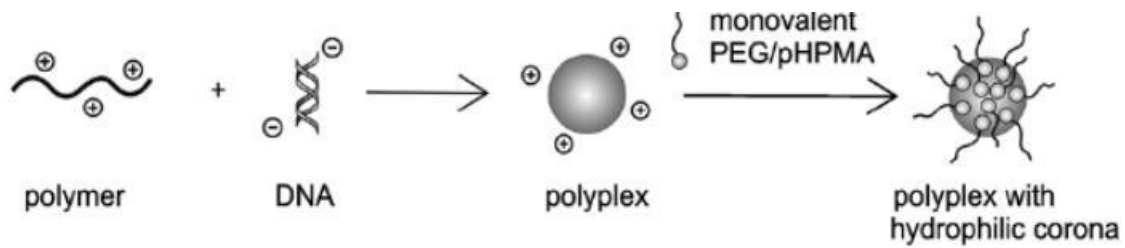
Figure 4. Polyplexes coated with PEG/pHMPA for prolonged circulation[11]

1.4.1.3 Cell Specific Targeting and Internalization

The relative importance of targeted cell specificity depends on the disease being treated. For some diseases, such as hemophilia, the identity of the transduced cells is not important so long as sufficient quantities of the delivered therapeutic gene are expressed. In other applications, such as in the treatment of tumors, cell specific delivery is imperative.[2]

To improve transfection cell specificity, targeting ligands are conjugated onto polyplex surfaces to facilitate receptor-mediated endocytosis.[11] Transferrin (Tf), for example, is a highly hydrophilic negatively charged protein that binds and delivers iron to cells through the transferrin receptor (Tf-R) located on cell surfaces. Dividing cancer cells exhibit elevated levels of transferrin receptors due to their need for iron, making Tf a potential targeting moiety for gene delivery to tumors.[34] Studies have demonstrated that in addition to actively targeting tumor cells, Tf also shields the surface charge of polyplexes, thereby decreasing interaction with plasma components, erythrocytes and non-target cells.[35] The success of ligand targeting depends on polymer-ligand conjugation

chemistry, distance between ligand and polymer complexes, ligand-receptor binding strength, and ligand density.[11]

In non-specific delivery, polyplexes are internalized by non-adsorptive endocytosis involving polymer-GAG interactions, as previously described.[1,11] Studies have shown that differences in proteoglycan distributions between cells types can lead to varying degrees of polymer-DNA uptake between cells.[11] Currently, cell-penetrating peptides (CPP) are being investigated for their ability to facilitate polymer internalization. It is hypothesized that these peptides work by one of three strategies; direct penetration of cellular membrane, induced endocytosis, and/or membrane pore formation. Originally derived from viral proteins these proteins are also being investigated for their potential immunogenicity.[11]

1.4.2 Intracellular Barriers

1.4.2.1 Endolysosomal Escape

Due to size restrictions, polymer complexes typically cannot diffuse into cells, and must therefore be internalized by endocytosis, a multistep process in which cells engulf molecules from the extracellular matrix. As polymers interact with the cell surface, a portion of the cell's membrane is invaginated and pinched off, forming a membrane bound vesicle called an endosome. Upon internalization, the endosome compartment has a pH~7, which ultimately drops to pH~4 as the vesicle matures from an endosome to a lysosome.[28] Polyplexes that do not escape the endolysosome are eventually degraded by enzymes present in the lysosome.[11]

The most commonly used method for endosomal escape is via pH-sensitive protonizable amino groups (i.e. 1°, 2° and 3° amines, imidazole) exhibiting pKa values between 5 and 7. Once in the acidic environment of the cell, amines located on the polymer backbone protonate by absorbing protons from the incoming cytosol. This phenomenon, also known as the proton sponge effect, induces osmotic swelling. As a result, the endolysosome ruptures and the genetic cargo is released into the cytosol.[1, 11] A polymer potential to escape the endosome is measured by its buffering capacity. Cationic polymers including poly(ethyleneimine), poly (2-dimethylamino) ethyl methacrylate (PDMAEMA), and polyamidoamines have high buffering capacities and can therefore escape the endolysosome through the proton sponge mechanism. Other cationic polymers, such as poly-L-lysine and poly(allylamine) have a low number of protonizable

12

amines and therefore a low buffering capacity. These polymers can only escape the endosome with the aid of a lysosomotropic agent, such as chloroquin.[36]

1.4.2.2 Cytotoxicity

Polymer biocompatibility and cell viability *in vitro* must be sufficiently demonstrated before polymer delivery systems can be introduced into clinic trials.[37] Studies have shown that polymer cationic charge is correlated to cell toxicity. The theory is that electrostatic interactions between the positively charged polymer and the negatively charged cell membrane cause the polymers to aggregate at the cell surface, thereby disturbing membrane structure and function.[38, 39] When systematically administered cationic polymers show high accumulation in the lungs, liver, and spleen. Not only does polyplex accumulation prevent gene cargo from reaching targeted cells, but it also results organ toxicity.[23]

Structural and non-structural parameters that promote polymer-cell and polymer-protein interaction, such as polymer molecular weight, degree of branching, charge density, polyplex size and stability, and ionic strength of solution, can intensify cytotoxic effects.[11, 40] Reports have demonstrated that high molecular weight (HMW) polymers exhibit higher cytotoxicities than low molecular weight polymers (LMW).[41-46] Researchers have tried to overcome this problem linking non-toxic LMW polymers via degradable linkages to form HMW polymers.[11,24]

Another common method of lowering cytotoxicty is by decreasing the polymer's cationic charge. This can be accomplished by grafting non-ionic molecules onto the cationic polymer. For example, when PEG is functionalized onto the backbone of a

13

cationic polymer, polyplex aggregation at the cell surface and cytotoxicity are decreased. At the same time, *in vivo* circulation time is increased due to minimized polyplex-protein interactions.[11] *In vitro* studies using COS-1 and HEK293 cell lines indicate that cell cultures transfected with PEGylated PAA have 10% more viability than PAA transfected cells. In addition, heterocyclic rings, such as imidazolyl and pyridinium, have been shown to lower toxicity by spreading the cationic charge of the headgroup.[47, 48]

Finally, there is also evidence that polymer interactions with cell proteins can affect protein function and cell function.[39] Polymer amines have been shown to disrupt the function of protein kinase C, a family of enzymes involved in a range of regulatory activities including receptor desensitization, cell growth, and transcription, through the disturbance of protein kinase activity.[38]

1.5   Cationic Polymers

Amine-rich cationic polymers have been given a lot of attention in gene delivery due to their ability to condense DNA into nanosized complexes. Studies have shown that at a sufficient N/P ratio, polyplexes form spontaneously upon mixing. The size of the resulting particles ranges from 30 to several hundred nm, depending on N/P ratio.[2, 32] In addition, cationic polymers have the ability to escape endolysosomal degradation via the proton sponge effect. Although more than 95% of cells in a culture internalize polyplexes during a given transfection, less than 50% of cells express the gene. From this standpoint, a polymers success is dependent upon its ability to buffer at endolysosomal pH.[2]

The following section briefly reviews several of the most commonly employed cationic polymer vectors and outlines the advantages and challenges associated with each.

15

1.5.1 Common Cationic Polymers

1.5.1.1 Poly(ethylene imine)

$$H_3C\text{-}CH_2\text{-}NH\text{-}[CH_2\text{-}CH_2\text{-}NH]_n\text{-}CH_2\text{-}CH_2\text{-}NH_3^+$$
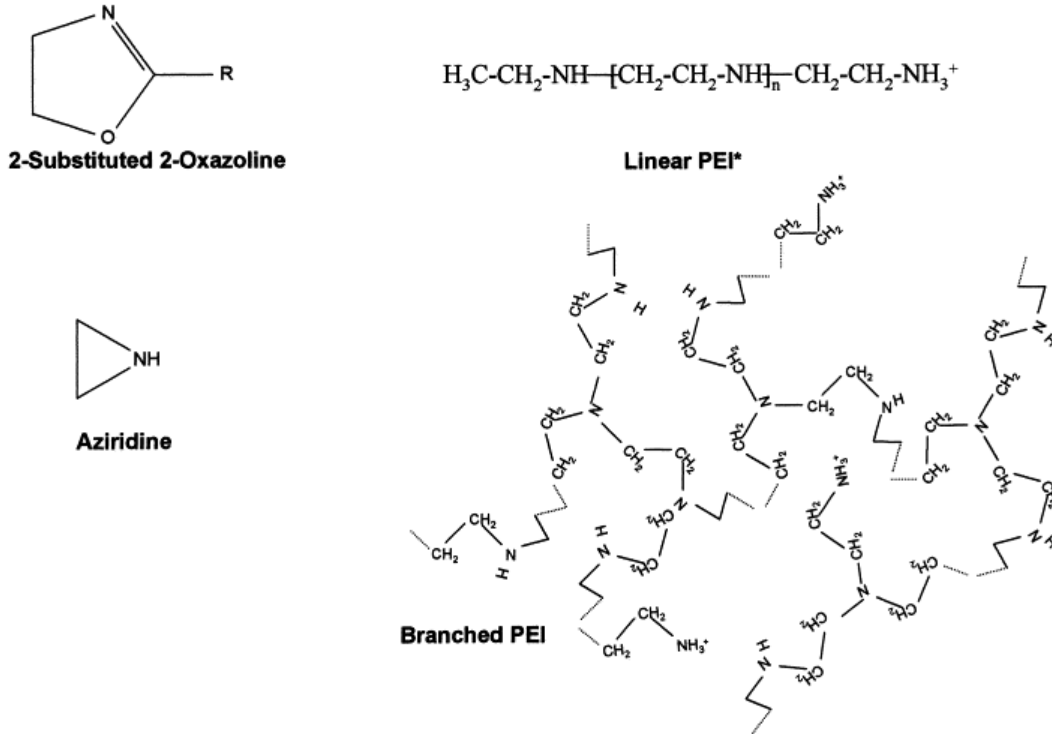
Figure 5. PEI precursors and products [49]

Polyethyleneimine (PEI) is perhaps the most commonly used cationic polymer due to its extraordinary buffering capacity.[48, 49] PEI comes in two forms: linear (l-PEI) and branched (b-PEI), as shown in Figure 5.[49] Branched PEI is synthesized by an acid catalyzed ring opening polymerization of aziridine monomers. The resulting polymer has a high number of unprotonated amine groups, which are responsible for b-PEIs high buffering capacity. Linear PEI is formed via cationic polymerization of 2-oxazoline monomer. Unlike b-PEI, 90% of l-PEI amines are already protonated at physiological pH.[49] As a result, l-PEI has a high cationic density which allows it to bind and condense DNA into small particles. However, the already protonated amines hinder l-PEI's

16

buffering capacity. Since transfection success if highly dependent on buffering capacity, b-PEI has significantly greater delivery rates than l-PEI.[1]

The transfection success of PEI has been well documented. Boussif *et al*.,[50] for example, demonstrated transfection of PEI polymers in over 25 cell lines, including 18 human cell lines. Reports have shown that PEI's molecular weight, which can be controlled through initiator concentrations and temperature during the polymerization process, is directly proportional to the carrier's cytotoxicity and transfection efficiency.[11, 49] In a series of experiments, Xiong *et al*.,[51] compared low molecular weight PEI with 800 Da (PEI 800) with high molecular weight PEI (PEI25k) Results showed that PEI25k–DNA complexes were more compact, with particle diameters averaging less than 100 nm at N/P ratios between 10 and 40. Under similar conditions, PEI800 could not form condense DNA, most likely because the polymer was unable to wrap around the plasmid DNA. As a result, PEI800 exhibited much lower transfection efficiencies. However, PEI25 also exhibited much greater cytotoxicity than PEI800.[42]

Transfection efficiency and biodegradability of b-PEI can be improved by linking together short PEI segments via biodegradable linkages. Studies have shown that peptide based analogues of PEI800 can reach transfection efficiencies similar to those of PEI25k, while maintaining low cytotoxicity levels.[42]
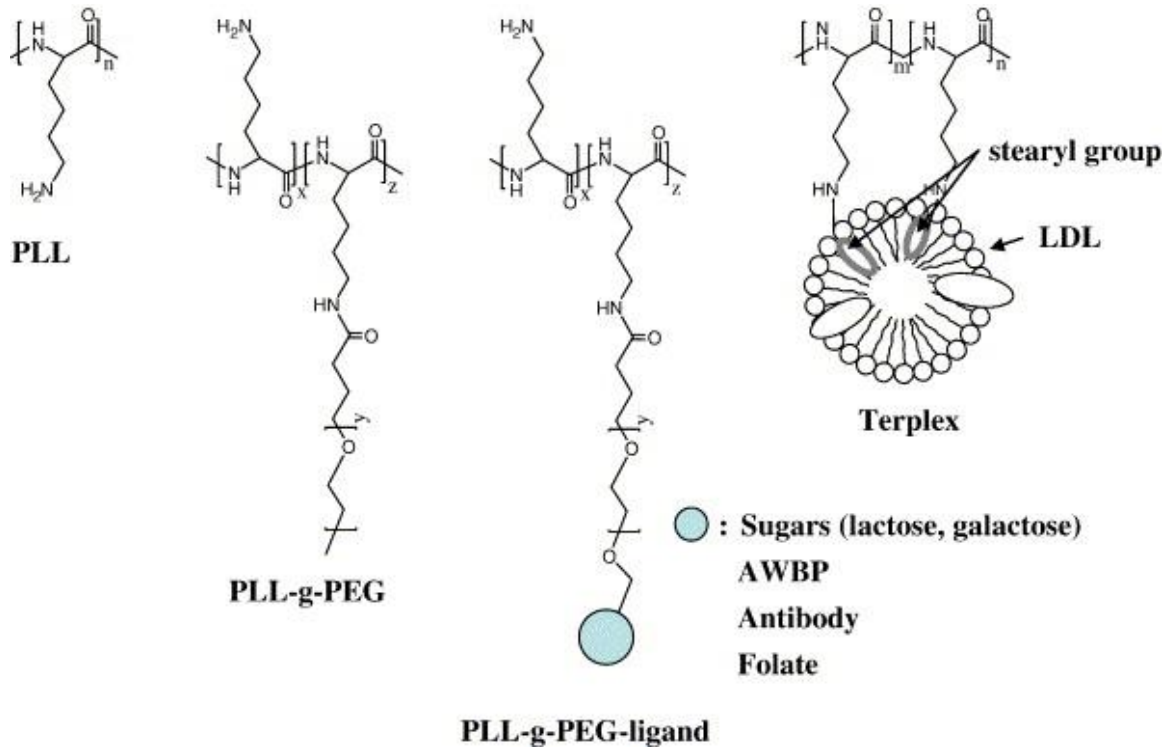
Figure 6: Chemical structure of PLL and some of its derivatives [52]

Cationic poly-L-lysine (PLL) is one of the first polymers investigated for its application in gene therapy.[1] PLL synthesis begins with the conversion of an e-amino lysine monomer into lysine anhydride. Ring opening polymerization is performed using an initiator containing l-lysine anhydride. The molecular weight is controlled by changing the feed ratio of monomer to initiator.

In general, HMW PLL is capable of condensing and protecting DNA. However, much like PEI, low molecular weight PLLs do not form stable complexes with DNA. Further, HMW PLLs elicit significant toxicity, making them unsuitable delivery carriers. In addition, since all of the e-amino groups of PLL are protonated at physiological pH, PLL polyplexes exhibit poor endolysosomal escape and low transfection.[1, 52]

18

In attempt to improve the safety profiles of PLL vectors, targeting moieties including sugars, antibodies, and peptides, have been conjugated onto the polymer's backbone as a means of increasing cell specificity and reducing polyplex aggregation. PEGylation has also been shown to ameliorate PLL's toxic effects.[52] In addition, amino acids with low pka values can be grafted onto the PLL chain to improve transfection rates.[53]

Finally, studies have also investigated how the structural differences between dendritic PLL (D-PLL) and linear PLL (l-PLL) affect the functionality and efficiency of the polymers in gene delivery. Yamagate *et al.*,[54] demonstrated that cells transfected with l-PLL internalized nearly 3x more DNA than cells transfected with d-PLL, but still had exhibited lower gene expression than d-PLL transfected cells. From these data it can be inferred that the low delivery success of PLL polymers does not result from inefficient uptake, but rather ineffective endolysosomal escape.[54]
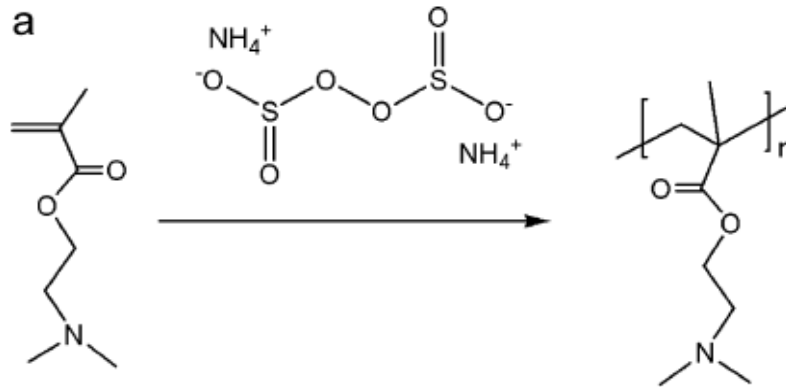
Figure 7. Synthesis of Poly(2-dimethylamino) ethyl methacrylate (pDMAEMA) [1]

Methacrylate polymers have excellent biocompatibility and have already been employed for medical purposes, such as the fabrication of contact lenses. Gene delivery studies have focused on one type of methacrylate polymer, (2dimethylamino) ethyl methacrylate (pDMAEMA), due to its superior transfection efficiency.[55]

pDMAEMA is synthesized by radical polymerization with an ammonium peroxide sulfate initiator as shown in Figure 7.[1] In comparison to other methacrylates, pDMAEMA exhibits higher transfection rates and lower cytotoxicity, most likely due to the presence of protonizable tertiary amines (pKa 7.5).[55] Studies show that primary and secondary amines are mainly responsible for high degrees of cytotoxicity, while polymers with tertiary amines are significantly less toxic but still transfectionally competent. Unfortunately, *in vivo* transfection of pDMAEMA is not as successful as *in vitro* studies. In ovarian cancer studies pDMAEMA has a 10% transfection efficiency *in vitro*, but only a 1-2% efficiency *in vivo*.[56]

20

1.5.2 Bioreducible Polymers

In an attempt to create safe and efficient delivery vectors, researchers have turned their focus to disulfide-containing polymers capable of responding to environmental stimuli.[24, 57, 58] Disulfides (-S-S-) are formed by thiols (S-H) in an oxidation reaction. These linkages are relatively stable within the oxidizing extracellular environment of the cells, but are readily reduced back into thiols in the reducing intracellular environment of cells.[58] As a result, thiol-containing polyplexes not only exhibit higher complex stability under extracellular conditions, but also have greater intracellular cargo release and lower cytotoxicity than non-thiolated carriers.[15, 57] Previously, disulfide bonds have been used to link non-toxic low molecular weight (LMW) polymer units to develop biocompatible high molecular weight (HMW) carriers.[24] Disulfide bonds have also been used to improve carrier stability *in vivo* by linking hydrophilic, non-ionic polymers with cationic polymeric carriers.[24]

Studies have demonstrated that complexes formed by HMW polymers have higher transfection efficiencies and greater steric stabilization than LMW polyplexes, but also impart greater cytoxicities.[41-46] Several explanations have been given as to why HMW polymers have greater transfection efficiencies. Van de Watering *et al*. proposed that the smaller polyplex size formed by HMW polymers is more conducive to internalization.[45] Godbey *et al*. suggested that HMW polymers are more capable of protecting genetic cargo from nucleases.[43] Finally, Georgiou *et al.* explained that larger polymers can destabilize the cellular membrane more effectively than smaller polymers, thereby facilitating internalization.[44] It is possible that membrane destabilization not only leads to greater transfection efficiencies, but also cell death. Pafiti *et al.* suggested that the

21

accumulation of HMW polymers at the cellular membrane leads to localized membrane destabilization and decreased cell viability.[46] The effect of HMW polymeric carriers has been demonstrated in both linear and star polymers.[43, 44, 46] To achieve the high transfection efficiency levels of HMW polymers while maintaining the relative safety of LMW polymers, researchers have developed bioreducible polymers, which primarily possess disulfide linkages in their backbone.[24] Disulfide bonds are relatively stable in the oxidizing extracellular space, allowing bioreducible polymers to maintain polyplex structure and stability.[24, 58] Within the reducing intracellular compartments, the disulfide bonds are reduced back into thiols and the polymer degrades into its LMW biocompatible segments. It is expected than that bioreducible polyplexes can achieve the high transfection success of HMW polymers while maintaining the lower cytotoxicity of LMW carriers.[59]

Disulfide bonds can also be used to increase polyplex stability by linking cationic polymers with hydrophilic, non-ionic polymers such as poly(ethylene)glycol (PEG) and N-(2-hydroxypropyl) methacrylamide (HMPA).[24] Polyplex stability depends on polymer structure and N/P ratio, or polyplex charge.[32] *In vivo*, cationic polymers electrostatically interact with negatively charged serum proteins, resulting in polyplex destabilization and rapid clearance by the phagocytic cells of the MPS.[2, 23] It is therefore useful to avoid polymer-protein interactions by masking the polymers cationic charge with non-ionic polymers such as PEG and HMPA.[23] This can be achieved by linking hydrophilic polymer segments onto a cationic polymer via disulfide linkages.[2, 24] Studies have shown PEGylated polyplexes to have lower toxicity levels and prolonged circulation times in comparison to non-PEGylated complexes.[33]

Chapter 2

2. 1   Abstract

Previous studies have focused on incorporating disulfide linkages either within the polymer backbone, or as direct linkages between cationic and non-ionic polymers in order to increase biocompatibility and serum stability. However, the potential of disulfide crosslinks extending from the polymer chain as a means of improving DNA binding efficiency, complex stability, and gene release has not been explored. Using poly(allylamine) (PAA) as a model, we investigated how pH sensitive disulfide crosslinked polymer networks can improve the delivery potential of cationic polymer carriers. To accomplish this, we conjugated thiol-terminated pendant chains onto the primary amines of PAA using 2-iminothiolane, developing three new polymer vectors with 5%, 13%, or 20% thiol modification. Polymer synthesis was verified by 5,5'-dithiobis-(2-nitrobenzoic acid) (DNTB, Ellman's Reagent) and H ^{1}NMR. Polymer fluorescence was determined by UV plate readings. Complex size and stability was measured by dynamic light scattering (DLS) and zeta potential, respectively. Extent of disulfide formation and buffering capacity were demonstrated by DAPI assay. Cargo packaging and protection was determined by gel electrophoresis.

2.2 Experimental

2.2.1 Materials

Poly(allylamine) solution (PAA; MW 15000) was purchased from PolySciences Inc. 2-Iminothiolane (2-IT, Traut's reagent) and 5,5′-dithiobis-(2-nitrobenzoic acid) (DNTB; Ellman's reagent) were purchased from Thermo Scientific. Millipore-Amicon Centrifugal Filter Units (MW cutoff of 5000 Da) were purchased from Millipore. pEGFP-N1 (4700 base pairs) was donated by the Dr. Bentley Research Group at the University of Maryland who acquired the plasmid from CLONTECH Laboratories and cloned it with Top 10 competent cells from Invitrogen. Extractions were carried out by HiSpeed Plasmid Maxi Kit purchased from Qiagen. Ethidium bromide and ethylenediaminetetraacetic acid powder (EDTA) were purchased from Fisher Scientific. Heparin sodium salt, phosphate-buffered saline (PBS), pH 7.4, molecular grade, 4′,6-diamidino-2-phenylindole (DAPI), DNase I amplification grade, hydrochloric acid (HCl), and sodium hydroxide (NaOH) were purchased from Sigma. A 1kb DNA Ladder, 10X TAE, and agarose were purchased from New England Biolabs, Promega, and Research Products International Corp, respectively. Folded capillary cells and stoppers were purchased from Malvern.

2.2.2 Methods

2.2.2.1 Synthesis of Thiol-PAA

Thiolation of cationic PAA is described in Figure 8. Briefly, PAA was dissolved in 4 mL of PBS, pH 7.4, with 1.75 mg/mL EDTA and reacted with 0.375, 0.75, or 1.5 mg/mL 2-iminothiolane (2-IT) so that 5, 13, or 20% of PAA's primary amines were replaced with thiol-pendant chains. EDTA does not take part in the thiolation reaction but was used to chelate divalent metals in solution, thereby preventing thiol oxidation. The reaction was run at room temperature (RT) for 2 h with continuous shaking on a tabletop orbital shaker. After 2 h, samples were washed twice with PBS using Millipore-Amicon Centrifugal Filter Units. Centrifugation was carried out at $8000g$. Washed samples were resuspended in PBS and stored at −80 °C.

Thiolated polymers were characterized by ^{1}H NMR in D_2O. Degree of thiolation was quantified by a 5,5′-dithiobis-(2-nitrobenzoic acid) (DNTB, Ellman's reagent) assay and verified by ^{1}H NMR. The DNTB assay was prepared according to manufacturer protocol. Ellman's reagent has been previously used to quantify thiol concentration on thiolated polymers.[60] Briefly, 72 μg polymer was suspended in 1 mL of Ellman's buffer with 50 μL of DNTB reagent (2 mg/mL). The absorbance of the polymer solution was measured at 412 nm and the thiol concentration was determined by solving for $c = A \div bE$, where A is the absorbance at 412 nm, b is the path length in centimeters, E is the molar absorptivity, and c is the concentration in mol/liter (M).

2.2.2.2   Polyplex Preparation

pEGFP-N1 plasmid (MW 2.9×10^6 Da, 4700 base pairs) was extracted from *E. coli* using the HiSpeed Plasmid Maxi Kit by Qiagen according to kit protocol. pEGFP-N1 is commonly used in delivery studies because it expresses green fluorescent protein (GFP) only upon successful transfection, which is easily detected by UV and fluorescent microscopy.

Polymer–plasmid complexation was carried out by incubating the polymer and plasmid at RT for 45 min at N/P ratios of 1, 5, 10, 20, and 40. The extent of disulfide formation in polyplexes was tested by measuring the concentration of reactive thiols present in solution at initial mixing and after the 45 min incubation period using the previously described DNTB assay.

2.2.2.3   DNA Binding Efficiency

A DAPI displacement assay was used to determine how thiol crosslinks affect the DNA binding efficiency of cationic polymers. Briefly, DAPI was added to pEGFP plasmid and incubated at RT for 30 min to allow the DAPI stain to intercalate into the plasmid strands. For complexation, polymers and DAPI-stained plasmid were mixed and incubated in a 96 well plate at N/P ratios of 1, 5, 10, 20, and 40. Each well consisted of 1 µg plasmid and was brought to a total volume of 100 µl with PBS. Complexation was carried out at RT for 45 min. Fluorescence was read at $\lambda_{ex}= 360$ nm and $\lambda_{em}= 455$ nm. Relative fluorescence was determined using the following equation:

$$F_{REL}= 100* (F_{pol}-F_o)/(F_{DNA}-F_o)$$ [61]

26

Where F_{pol} is the fluorescence of the polymer-plasmid/DAPI solution, F_{DNA} is the fluorescence of DAPI complexed with plasmid, and F_o is the fluorescence of uncomplexed DAPI.

Polyplex formation was further verified by gel electrophoresis. The electrostatic interactions between polymers and plasmid neutralize the DNA's negative charge and polyplex migration down the agarose gel is retarded.[48] Polymer-plasmid complexation was carried out in PBS as previously described under "Polyplex Preparation." Gels were composed of 0.7% agarose and contained ethidium bromide (EtBr). Polyplexes were run at 100 V for 1 h against a 1 kb ladder and a plasmid control. A second gel electrophoresis, in which polymer and plasmid were complexed in the presence of 4 mg/mL heparin, was also performed for comparison purposes. Heparin is a negatively charged polysaccharide used to mimic *in vivo* interactions between cationic polymers and negatively charged proteins proteins.[62]

2.2.2.4 *Polyplex Size and Zeta Potential*

To determine polyplex size, polymer and pEGFP-N1 were complexed in 2 mL deionized water at N/P ratios of 1, 5, 10, 20, and 40. Hydrodynamic size measurements of polymer-plasmid complexes were obtained by dynamic light scattering (DLS). The hydrodynamic radius measured by the DLS is calculated from the Stokes-Einstein equation, $D = kT \div 6\pi\eta Rh$ where k is the Boltzmann constant, T is the temperature, η is the medium viscosity, and $f = 6\pi\eta Rh$ is the frictional coefficient for a hard sphere in a viscous medium.[63]

For zeta potential measurements, polymer-plasmid solutions were prepared at N/P ratios of 1, 5, 10, 20, and 40 in 0.8 mL deionized water. Zeta potential measurements were performed using a Malvern Zetasizer Nano ZS 90 particle analyzer.

2.2.2.5 Serum Stability

Gel electrophoresis was used to determine polyplex stability under *in vivo* mimicking conditions. Briefly, polymer-plasmid complexes were incubated in PBS, pH 7.4 for 45 min at RT for complexation to occur. After the initial complexation time, heparin was added to the polyplex solution at a final volume of 4 mg/mL heparin and the polyplexes were incubated for another 30 min at RT. Complexes were then run on a 0.7% agarose gel containing EtBr against a 1 kb ladder and a plasmid control for 1 h at 100 V.

2.2.2.6 DNase Protection Assay

A DNase I protection assay was performed to determine the DNA protection potential of thiolated polymers relative to the unmodified polymer. Briefly, polymer-plasmid complexation was carried out in PBS as previously described. Polyplexes were subsequently added to a solution of 4 mg/mL heparin containing 0.1 unit/µl DNase (human serum ranges between 2.0×10^{-4} and 8.2×10^{-2} unit/µl enzyme activity) to mimic *in vivo* conditions.[64] After a 30 min incubation, complexes were run by gel electrophoresis described above.

28

2.2.2.7   Buffering Capacity

A polymeric carrier's buffering capacity can affect its potential for endolysosomal escape and its delivery success.[65] Buffering capacity is defined as the percentage of positively charged groups that become protonated from pH 7.5-5.1.[66] It can be determined with an acid-base titration assay. Briefly, unmodified, 5%, 13%, and 20% thiol-modified polymers were added to 150 mM NaCl solution at a concentration of 0.2 mg/mL and the solutions were brought to a pH~11 with NaOH. Then, 0.1 M HCl was added to polymer solutions in increments of 25 μl and the pH was measured at each point. The buffering capacity was calculated using the following equation:

$$\text{Buffering capacity (\%)} = (\delta V_{HCl} \times 0.1M)/N(mmol) * 100 \ ^{[66]}$$

Where δV_{HCl} is the volume of the HCl solution (mL) needed to bring the pH from 7.4 to 5.1, 0.1 M is the concentration of the HCl, and N (mmol) is the total moles of polymer amines in each titration.

2.2.2.8   pH-Sensitive Gene Release

A DAPI assay was used to assess the polymer's potential to release the DNA cargo within the acidic environment of the cell. Briefly, polymer and plasmid were complexed at N/P ratios of 1, 5, 10, 20, and 40. Polyplex solutions were then brought to a pH of ~5.5 (late endosomal pH) using 0.1 M HCl and incubated for 30 min to allow for plasmid release. After the initial incubation period, DAPI was added to the solutions which were then incubated for an additional 30 min period. DAPI fluorescence was read at λ_{ex}= 360 nm and λ_{em}= 455 nm.

29

2.2.2.9 *Statistical Analysis*

All experiments were performed in triplicate. Data is presented as the average and corresponding standard deviation (error bar) of three (n = 3) separate sample trials. For zeta potential and DLS runs, multiple values were collected from each sample and outliers were identified by Grubb's test and eliminated.

2.3 Results and Discussion

2.3.1 Characterization of Thiolated Polymers

Using PAA as a model for a cationic polymer delivery vector, our goal was to improve the delivery potential of cationic polymers by generating pH-sensitive disulfide crosslinked modifications. By altering the concentration of 2-IT used in the synthesis reaction, we synthesized three thiolated polymers with 5, 13, or 20% thiol conjugation (Figure 8). The thiol percentage is a measure of how many primary amines on the PAA backbone were successfully conjugated with thiol-pendant chains. Thiolation was verified and quantified by a DNTB assay and by ^{1}H NMR.

According to the DNTB assay, 0.375, 0.75, and 1.5 mg/mL 2-IT synthesizes 5, 13, and 20% thiolated polymers, respectively (Table 1). ^{1}H NMR was performed on unmodified and 20% thiol-modified polymer in D_2O to verify thiolation. In the unmodified polymer, the methyl peak, adjacent to the primary amine, is located at 3.5 ppm. Thiol conjugation results in the formation of an additional peak at 2.6 ppm which signifies the presence of the methyl group adjacent to the thiol. An integration of the relative area under these two peaks verifies that the approximate 20% thiolation determined by the DNTB.

31
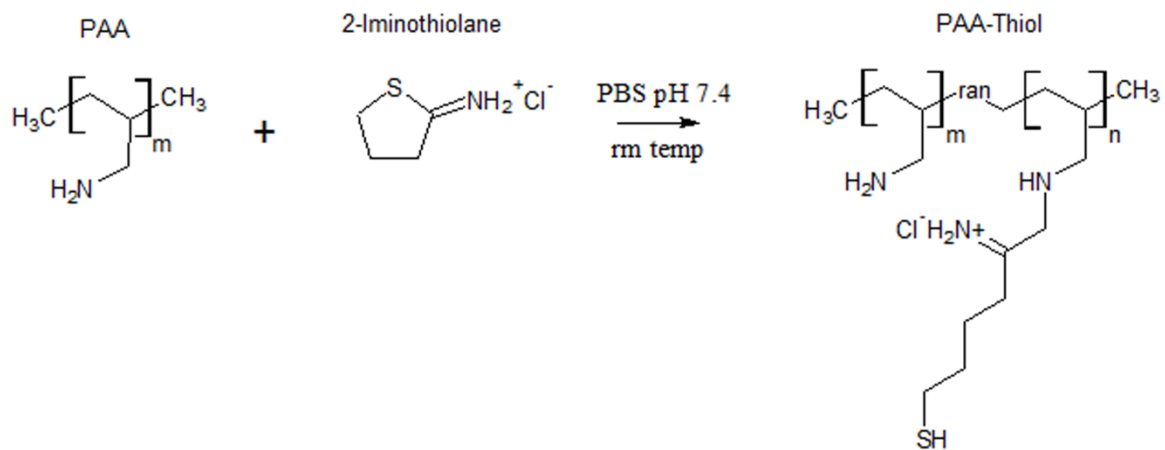
Figure 8. Synthesis of thiolated polymer by 2-iminothiolane

Table 1. Percent thiolation determined by concentration of 2-IT

Sample	PAA (mg/mL)	2-Iminothiolane (mg/mL)	% of 1$^{\text{o}}$ amines thiolated
1	1	0	0
2	1	0.375	4.59 ± 2.43
3	1	0.75	13.07 ± 1.61
4	1	1.5	19.27 ± 0.074

2.3.2 Validation of Disulfide Bonding

Other studies have shown that thiol conjugates can readily form crosslinked disulfide networks. PEGylated peptides can condense DNA through ionic interactions, as well as crosslinked networks formed by the spontaneous oxidation of cysteine thiols.[24] Correlations between disulfide formation and solution viscosity indicate that thiol oxidation occurs more rapidly in viscous solutions. It is presumed that the close proximity of thiols in viscous solutions facilitates disulfide bonding.[60]

Table 2 shows the percent of free thiols present in solution after the 45 min incubation period as determined by DNTB. For 5% and 13% polymers, the general trend showed that the percentage of free thiols decreased, and therefore the number of disulfides increased, with increasing N/P ratio. We believe that increased disulfide bonding in higher N/P complexes resulted from the close proximity of thiols, as previously suggested by Maraschutz *et al*.[60] Overall, 5% thiolated polymers exhibited the highest degrees disulfide formation, followed by the 13% thiolated polymers. The exception was the N/P 40, 13% polyplexes which achieved the highest degree of crosslinking among all polyplexes. Interestingly, 20% thiolated polymers achieved very low disulfide binding. We believe that the additional amines from 2-IT increased the polymer's cationic charge, leading to greater repulsion among polymer chains and hindering disulfide formation.

Table 2. Percentage of thiols present in solutions after polymer-plasmid complexation

N/P	5% Thiol	13% Thiol	20%Thiol
1	97.19 ± 0.97	90.14 ± 3.90	91.32 ± 3.85
5	77.66 ± 0.76	90.39 ± 2.13	84.10 ± 6.95
10	52.26 ± 0.52	74.94 ± 3.43	55.37 ± 19.5
20	55.66 ± 0.48	66.54 ± 2.44	87.90 ± 6.46
40	69. 41± 0.93	41.72 ± 3.32	84.44 ± 10.5

34

2.3.3 DNA Binding Efficiency

Cationic polymers bind their genetic cargo through electrostatic interactions between the positively charged amines of the polymer and the negatively charged phosphates of the DNA backbone. The amines of a polymer backbone, however, have been linked to high cytotoxicity.[39, 67] Therefore, it would be beneficial to develop a carrier that can carry larger amounts of DNA cargo at lower polymer concentrations. To determine whether thiol crosslinks can increase the amount of genetic cargo held by each carrier, the binding efficiencies of the unmodified and thiol-modified polymers were assessed using a DAPI displacement assay. DAPI is a fluorescent probe that interacts strongly with A-T base pairs of DNA. When bound to DNA, DAPI displays intense fluorescence at ex/em ~360/455 nm. The electrostatic interaction and complexation between polymer and DNA displaces DAPI and decreases fluorescence intensity. Hence, as DAPI fluorescence decreases, the polymer binding efficiency increases.[61]

The effect that thiolation and polymer concentration have on the fluorescence of DAPI-DNA is represented in Figure 9. Unmodified PAA had the least effect on fluorescence across all N/P ratios, suggesting weak PAA-DNA binding. This result was confirmed by gel electrophoresis on an agarose gel containing EtBr. Like DAPI, EtBr is an intercalating dye that only binds to free DNA, or DNA that is not complexed with polymer. As a result, only free DNA is visible by gel electrophoresis.[68] The gel assay demonstrated that PAA cannot adequately bind DNA cargo (Figure 10). PAA is a weak polyelectrolyte that has previously been shown to exhibit aggregation properties dependent on concentration, environmental pH, and aging times.[69] In a study by Zhou *et al.*,[70] discrete nanoparticles between PAA and DNA were formed at N/P values between

35

0.8-1.0, as determined by changes in light scattering. Further analysis by an EtBr displacement assay showed that at N/P ratios between 0.67 and 1.0 PAA decreased EtBr-DNA interactions, confirming some complexation. However, increasing the N/P ratio from 1.0 to 1.67 had no affect EtBr-DNA binding. Zhou *et al.*[70] concluded that at higher PAA concentrations EtBr-DNA interactions are independent of changes in the polymer concentration. In another study, Pathak *et al.*[48] demonstrated that PAA-DNA complexation occurs only at very high polymer concentrations. This was done by running PAA-DNA complexes with polymer/plasmid weight ratios of 0.1, 0.2, and 0.3 μg/μg on an agorose gel. According to the data, polyplex retardation occurred only at the highest polymer concentration, which is nearly 10-fold higher than that of our N/P 40 complexes.

Thiolation improves the polymer's ability to displace DAPI and bind with plasmid DNA. According to Figure 9, all thiolated polymers demonstrated greater efficiency in displacing DAPI than PAA across all N/P ratios. When 5%, 13%, and 20% thiolated polymer concentrations are increased from N/P 1 to N/P 5, there is a sharp decrease in DAPI fluorescence. At N/P 10, DAPI fluorescence drops to values as low as ~40 a.u. for all thiolated polymers. At N/P 20 and 40, DAPI fluorescence intensity is maintained between ~35-45 a.u. This suggests that past N/P 10 polymer-DNA binding is not greatly affected by the increasing polymer concentration.

Gel electrophoresis yielded similar results. While PAA complexes exhibited no retardation, migration of thiolated polyplexes was impeded at high N/P ratios. As seen on Figure 10, thiolated polymers could not complex DNA at N/P 1 regardless of percent thiolation. Referring to the DAPI results (Figure 9), we see that at N/P 1, even the highly

thiolated 20% polymer decreases fluoresce by only 20 a.u. with respect to the unmodified polymer. All thiolated polymers exhibited minimal crosslinking at N/P 1 (Table 2), which could potentially explain why complexation was unsuccessful. At higher N/P ratios, thiolated polyplexes exhibited either partial or complete complexation. Partial complexation was evident by a faded plasmid strand, which suggests that only some of the DNA migrated through the gel. For some polyplexes, the DAPI assay and gel electrophoresis showed conflicting results. For example, the 20% thiolated polymer displaced DAPI just as efficiently at N/P 5 as it did at N/P 40. However, at N/P 5, 20% thiolated polymers did not completely retard plasmid migration, whereas N/P 40 complexes did. We believe that the low DAPI fluorescence of 20% thiolated complexes can be attributed to the large size of the polymer. It is possible that the larger chain density of 20% thiolated polymers sterically hinders DAPI-plasmid interaction, thereby decreasing DAPI fluorescence. At the same time, the greater degree of disulfide crosslinks in 5% and 13% thiolated complexes (Table 2) may have prevented plasmid migration along the gel.

Polymer-plasmid complexation was also performed in the presence of heparin to determine whether the negative charge of heparin would inhibit complexation. Resulting gel assays showed that in the presence of heparin, neither PAA nor thiolated polymers can complex DNA (Figure 11). The strong negative charge of heparin inhibited the electrostatic interaction of the polymer with the plasmid across all N/P ratios and thiol concentrations.

37
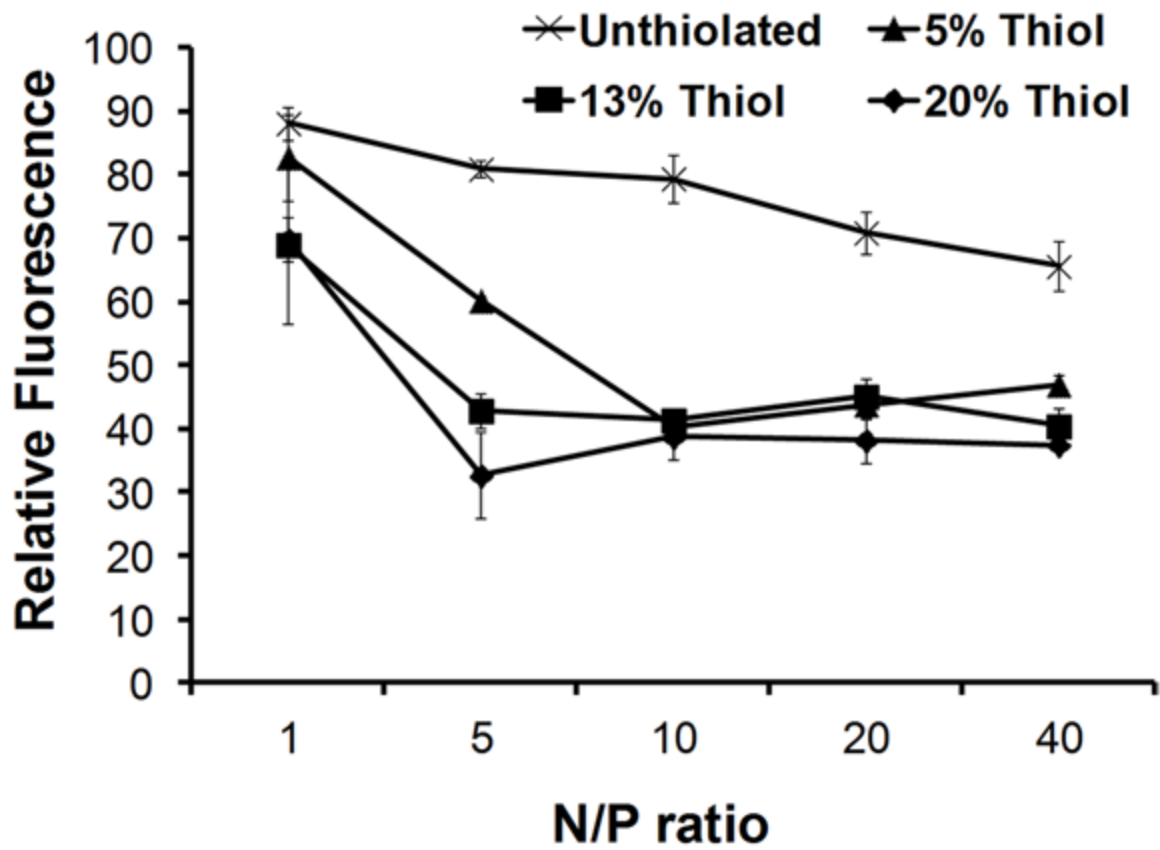
Figure 9. Displacement of DAPI from pEGFP-N1 by unmodified and thiolated polymers shows that thiolated polymers displaced DAPI more efficiently than unthiolated PAA, suggesting greater DNA packaging by thiolated polymers.
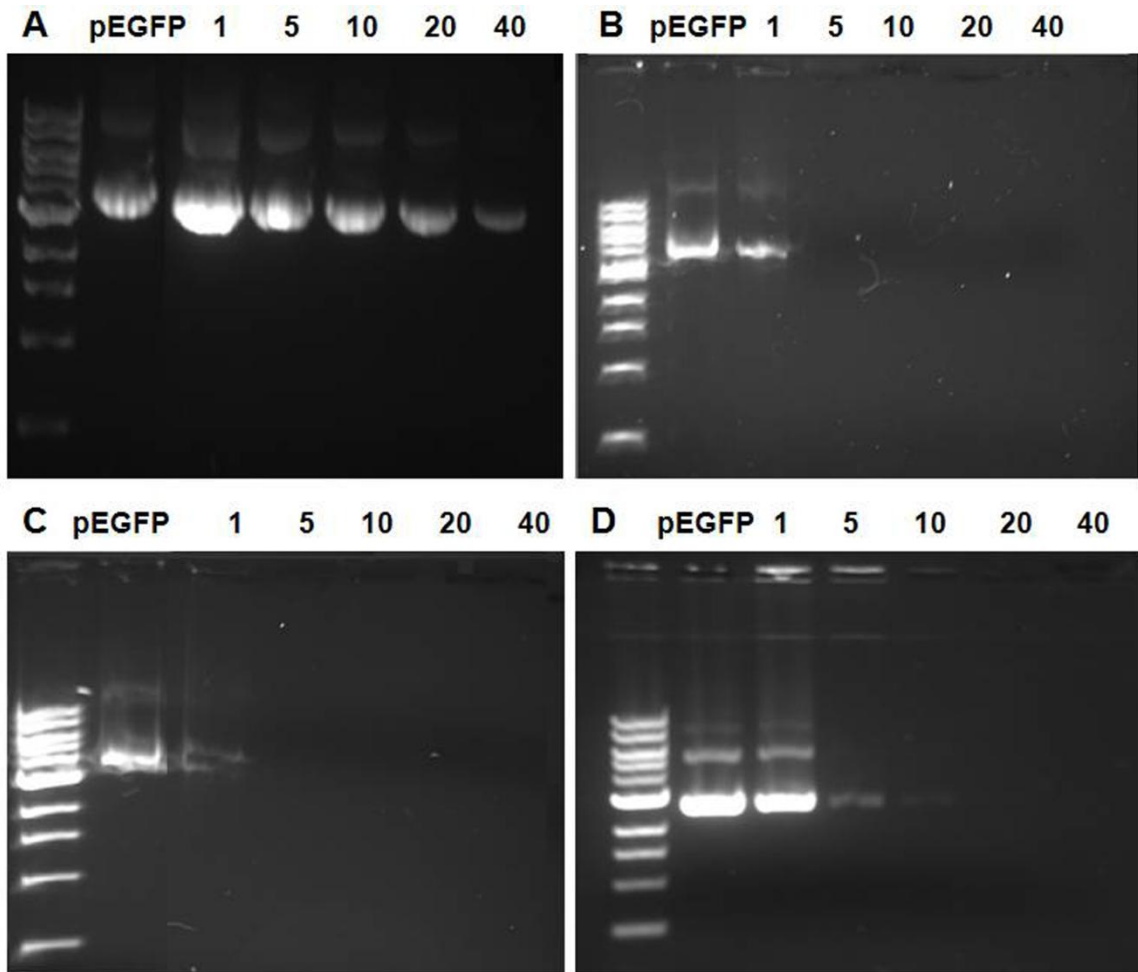
Figure 10. Gel electrophoresis of PAA (A), 5% (B), 13% (C), and 20% (D) thiol-polyplexes complexed in PBS indicate that PAA does not adequately package DN, whereas all thiolatd polymers were able to package DNA.
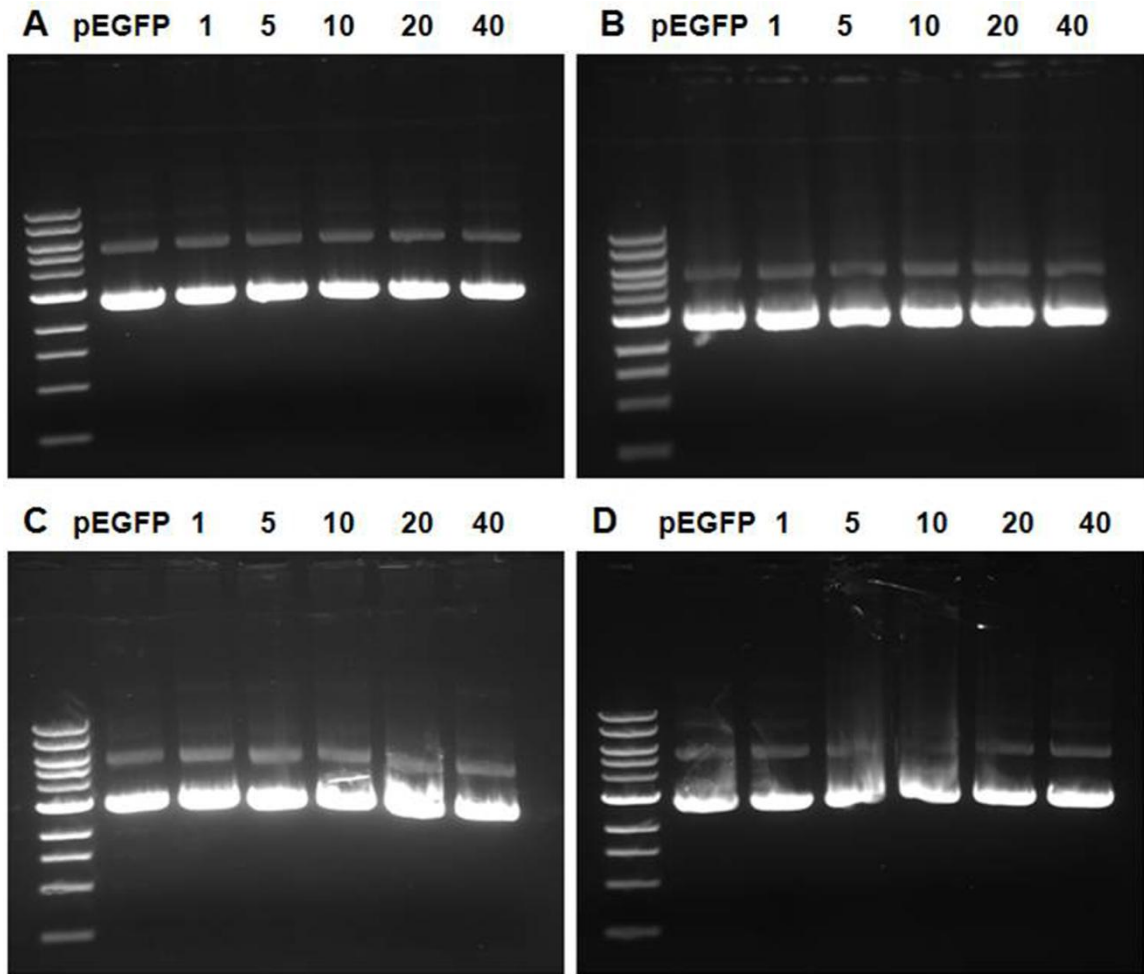
Figure 11. Gel electrophoresis of PAA (A), 5% (B), 13% (C), and 20% (D) thiol-polyplexes complexed in heparin shows that PAA and thiolated polymers could not complex in heparin solution.

2.3.4   Complex Size and Stability

Formation of stable, nanosized polyplexes is an important prerequisite for successful cellular internalization. Optimal complex size varies between cell types, but spherical particles of ~100 nm are more amenable for internalization in cell culture and *in vivo*.[71] Polyplex stability, or the complex's ability to resist aggregation, also plays a vital role in successful gene delivery. Polyplex aggregation results in particles that are too large for efficient cellular uptake. In addition, polymer aggregates that accumulate at the cell surface can damage the plasma membrane. *In vivo*, polyplex aggregation prevents cargo from reaching target cells, and results in increased toxicity levels at the site of accumulation.[23, 39, 72]

Polyplex size and stability were determined using dynamic light scattering (DLS) and zeta potential, respectively. The magnitude of the zeta potential indicates the stability of a colloidal system. Large negative or positive zeta potentials indicate that the particles repel each other. Repulsion limits particle aggregation and allows for a stable suspension to form. Generally, zeta potentials greater than +30 mV or lower than -30 mV indicate good stablity. As zeta potentials approache zero, particles in suspension aggregate.[73]

DLS data (Table 3) showed no consistent pattern for 5%, 13%, and unmodified polymer complexes. The size of unmodified PAA and 5% thiolated PAA polyplexes could not be determined at N/P 1 and N/P 5 due to large fluctuations in complex size. Based on the low zeta potentials corresponding to unmodified and 5% thiolated polymers at N/P 5, we believe the large polydispersity of these complexes results from complex instability. However, at N/P 1 both unmodified and 5% thiolated polymers have zeta

41

potentials that are quite negative and thereby do not support the DLS data. The smallest complexes were formed by N/P 10-40, 5% polyplexes, which can be explained by the high degree of crosslinking in these polyplexes. 13% and 20% thiolated polymers show more consistency between DLS and zeta potential measurements than the unmodified and 5% thiolated polymers. At N/P ratios of 1, 20, and 40, 13% thiolated polymers formed polyplexes of ~100 nm with a small standard deviation. N/P 5, 13% polyplexes, on the other hand exhibited a large size range which can be explained by the low zeta potential of these complexes. The exception to this set of polyplexes were the N/P 10 complexes which were nearly twice as large in size. Finally, the 20% thiolated polymers showed the greatest consistency between DLS and zeta potential data. Complexes obtained from the 20% thiol-modified polymer reached absolute zeta potential values between 25 and 40 mV, and ranged between 80-125 nm. Since 20% thiolated polymers did not demonstrate high degrees of thiol crosslinking, we believe that polyplex formation resulted primarily from electrostatic interactions between polymer strands and plasmid cargo.

42

Table 3. Polyplex size and zeta potenials

% thiol	N/P	Size (nm)	ζ (mV)
0	1	-	-20.00 ± 2.07
0	5	-	-6.75 ± 3.24
0	10	122.50 ±33.45	4.74 ± 4.47
0	20	100.85 ± 21.88	10.75 ± 3.07
0	40	105.48 ± 7.55	16.00 ± 0.53
5%	1	-	-27.53 ± 1.16
5%	5	-	-15.68 ± 5.63
5%	10	63.05 ± 23.22	11.36 ± 3.79
5%	20	71.45 ± 20.09	17.83 ± 1.63
5%	40	91.63 ± 14.03	19.73 ± 0.21
13%	1	104.05 ± 5.72	-34.00 ± 1.87
13%	5	91.94 ± 48.51	4.26 ± 0.52
13%	10	191.85 ± 24.17	35.90 ± 1.25
13%	20	100.56 ± 8.98	38.23 ± 0.75
13%	40	105.05 ± 4.80	41.77 ± 2.67
20%	1	80.76 ± 10.01	-35.37 ± 1.07
20%	5	87.72 ± 7.95	24.13 ± 2.76
20%	10	99.72 ± 5.02	31.87 ± 2.82
20%	20	117.61 ± 5.25	38.87 ± 5.79
20%	40	124.09 ± 2.74	41.40 ± 1.57

2.3.5   Heparin-Induced Decomplexation

Typically, *in vitro* polymeric gene delivery assays are carried out in serum free medium to avoid the polymer-protein interactions that inhibit polyplex internalization. *In vivo*, however, cationic polymer-protein interactions cannot be avoided. Negatively charged serum proteins aggregate around polymer-plasmid complexes. As a result, polyplexes are destabilized, and the DNA is left susceptible to enzymatic degradation. Hence, we evaluated the polymers potential to maintain complex stability in a more physiologically-relevant system, e.g., in the presence of heparin, a negatively charged polysaccharide used to mimic potential polyplex interactions with serum proteins.[62]

Thiolated polymers were complexed in PBS, then exposed to heparin for 30 min, and finally run on an agarose gel to evaluate the degree of decomplexation. Figure 12 shows that thiolated polymers decomplexed at low N/P ratios but remained intact at higher N/P ratios. 5% and 20% thiolated polymers maintained polyplex stability at N/P ratios of 10, 20, and 40, decomplexing only at N/P 1 and 5. The 13% thiolated polyplxes decomplexed only at N/P 1. Unmodified PAA showed complete decomplexation. However, from the complexation assay (Figure 10), we know that PAA never complexed with plasmid. Further, when comparing the complexation and decomplexation assays, it becomes evident that polyplexes that were only partially complexed in the complexation assay (Figure 10) completely decomplexed in the presence of heparin (Figure 12). From the data, it appears that overall the 13% thiolated polymer would be a better carrier choice for improved gene binding and release.
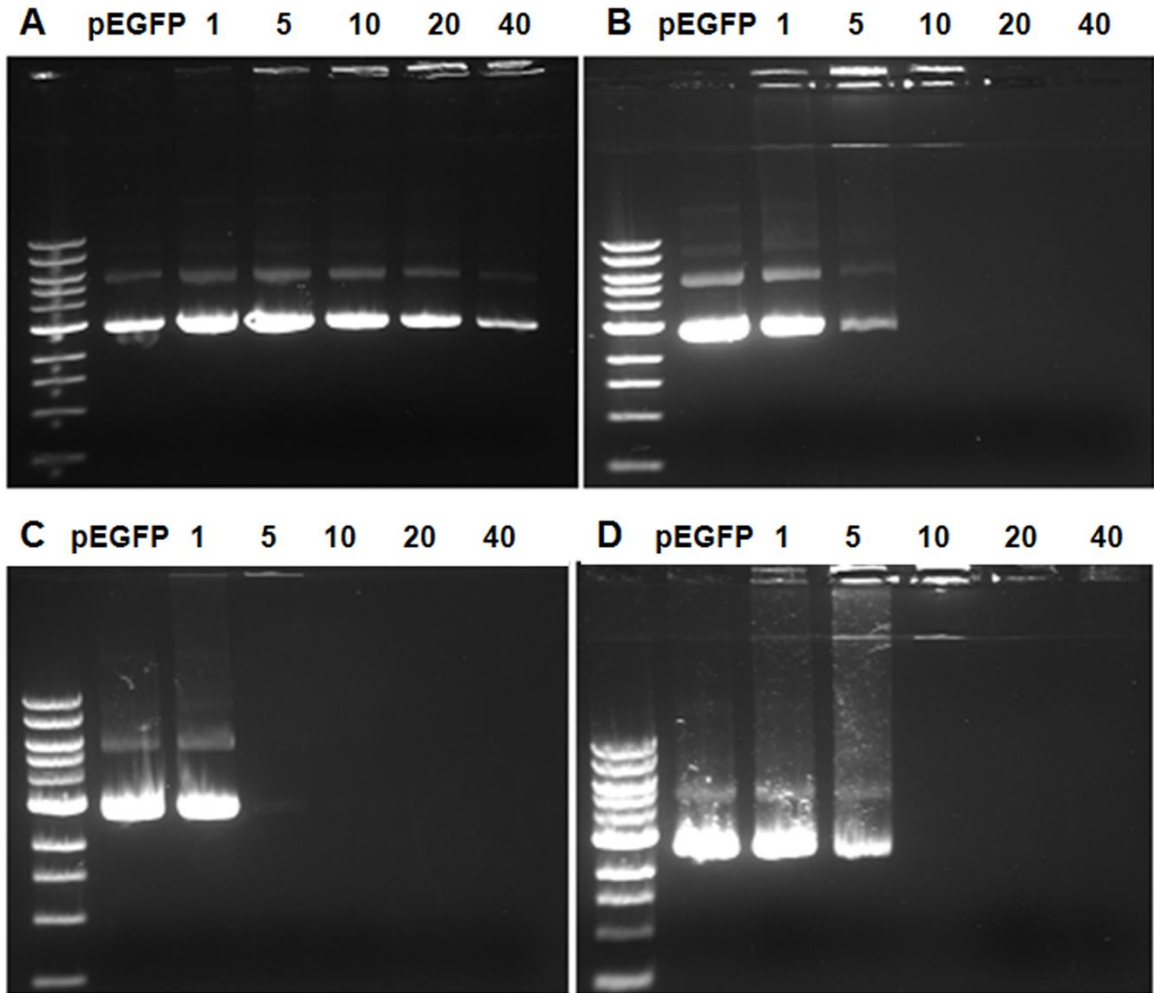
44

Figure 12. Gel electrophoresis of unmodified PAA (A), 5% (B), 13% (C), and 20% (D) thiol-polyplexes after suspension in a heparin solution. Results indicate that all thiolated polymers were able to resist decomplexation at high N/P ratios.

2.3.6 Cargo Protection

For a polymeric delivery vector to be clinically successful, it must not only bind DNA, but must also protect the cargo from degradative enzymes present in the host circulatory system. Results obtained from the heparin induced decomplexation assay suggested that at higher N/P ratios thiolated polymers have the ability to maintain polyplex structure in the presence of serum proteins. These polymers should therefore also be more efficient at protecting gene cargo than unmodified polymer carriers. To determine whether thiol crosslinks improve gene protection, a DNase I protection assay was performed. *In vivo*, human serum contains between 2.0×10^{-4} and 8.2×10^{-2} unit/μl enzyme activity. To mimic these conditions, polyplexes were complexed in plasmid, then added to a heparin solution, and finally treated with 0.1 unit/μl DNase I.[64] Samples were subsequently run on a 0.7% agarose gel to determine DNA degradation.

Results showed that weakly bound PAA (Figure 13) could not protect plasmid from DNase degradation across all N/P ratios. Thiolated polymers, on the other hand, successfully protected the plasmid at N/P ratios of 20 and 40, but left the plasmid susceptible to degradation at lower N/P ratios. The 20% thiolated polyplexes completely degraded at N/P 1, 5, and 10, which could potentially be explained by the poor disulfide-linking of these polyplexes. 5% and 13% thiolated polymers, performed better than the 20% complexes, exhibiting only partial plasmid degradation. Partial degradation is evident by the presence of two bands, a degraded DNA band and an intact DNA band. The 13% thiolated polymers showed some enzymatic degradation at N/P 1-20, but completely protected the DNA with the highly crosslinked N/P 40 polyplexes. The 5%

46

thiolated polyplexes exhibited partial degradation across all N/P ratios. It is possible that the greater enzymatic protection in 5% and 13% polyplexes resulted from the higher degree of disulfide crosslinking.

When comparing the data aquired from the "Heparin-Induced Decomplexation" assay and the "DNase I Protection Assay", it becomes evident that some samples which resisted decomplexation in the presence of heparin, did not completely protect the DNA cargo in the DNase I assay. For example, 13% thiolated polyplexes with N/P>5 remained intact in the presence of heparin (Figure 12c). Based on this data, it could be inferred that these complexes would completely resist DNase I degradation. However, Figure 13c shows partial DNA degradation in these samples. We believe that heparin-polymer interactions were not strong enough to completely decomplex polyplexes and release plasmid cargo, but that the presence of heparin was sufficient to destabilize complexes leaving some of the DNA suscpetible to degradation.
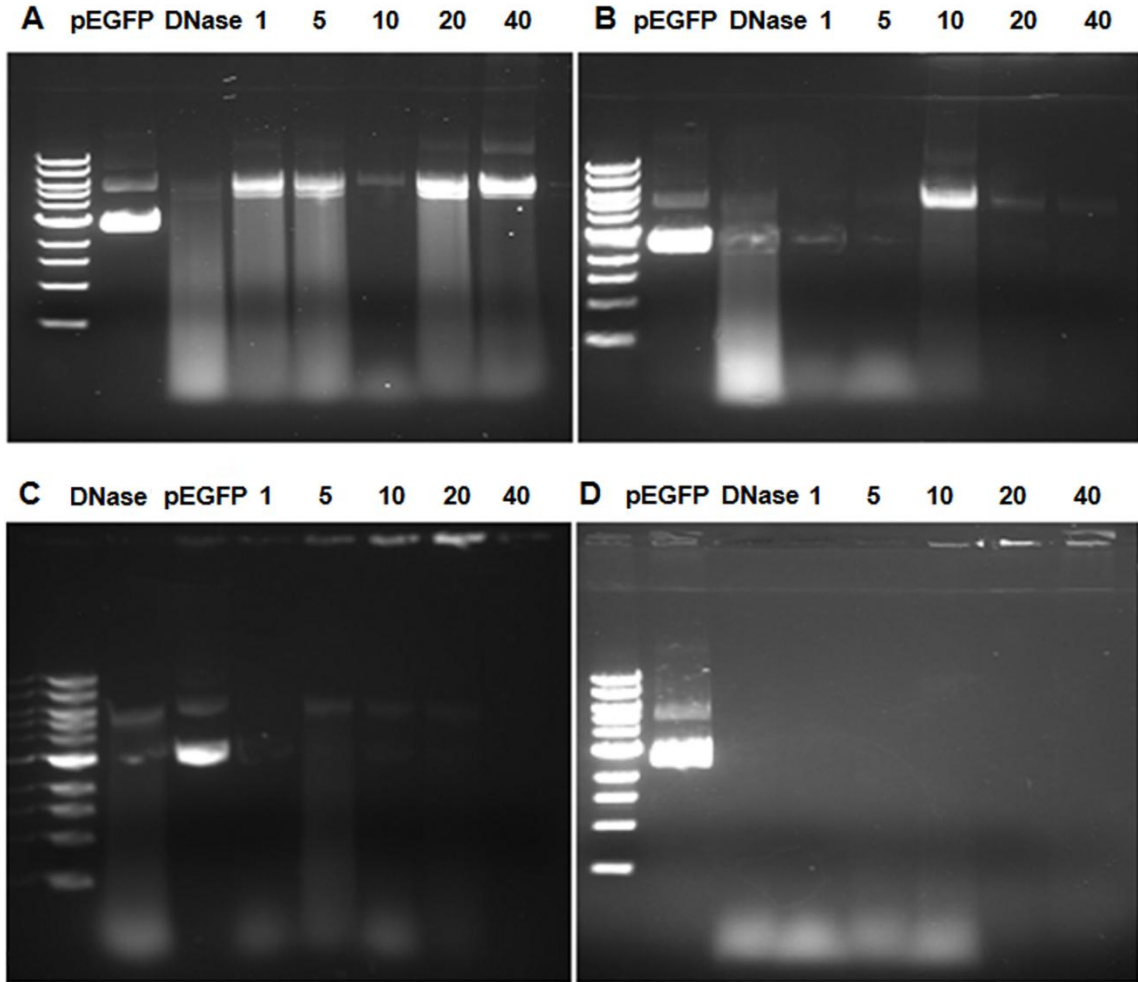
47

Figure 13. Gel electrophoresis of unmodified PAA (A), 5 (B), 13% (C), and 20% (D) thiol-polyplexes after exposure to DNase I in a heparin solution. Results show that PAA could not protect plasmid DNA, however, thiolated polyplexes prevented DNA degradation at N/P ratios of 20 and 40.

2.3.7 Buffering Capacity and Endolysosomal Escape

Due to size restrictions, polyplexes typically cannot diffuse into cells and must be taken up by endocytosis, a multistep process in which cells internalize molecules from the extracellular space by engulfing them within the cell membrane. A portion of the membrane invaginates and pinches off from the cell forming a membrane bound vesicle known as the endosome. Upon internalization, the endosome has a pH ~7 which ultimately drops to pH~4 as the vesicle matures from an endosome to a lysosome.[28] Polyplexes that do not escape the endolysosome are eventually degraded. Although more than 95% of cells in a culture internalize polyplexes during a given transfection, less than 50% of cells express the gene.[2] From this standpoint, a polymers success is dependent upon its ability to buffer the endolysosomal pH, which has been shown to facilitate polyplex escape into the cell cytosol via the proton-sponge effect.[2, 13] To determine whether thiol groups can improve the buffering capacity of cationic polymers, we performed a titration assay in which 0.1 M HCl was added to polymer solutions in increments of 25 µl and the change in pH was recorded. Polymers with a high buffering capacity contain larger amounts of protonizable groups. As a result of this buffering effect, a greater amount of protons, or acid, must be added to the solution for the pH to drop. Since disulfides are readily reduced in the presence of protons, increasing the number of thiols conjugated onto the polymer backbone improves the polymers buffering capacity. Each polymer's buffering capacity was calculated as the percentage of amine groups being protonated when the pH drops from pH 7.0 to 5.1, conditions mimicking the change from the extracellular environment to the low pH of the endosome.[66] The results showed that the presence of thiols can drastically improve the polymers buffering

49

capacity. 20% thiolated polymers had a buffering capacity of ~47%, which was more than double the buffering capacity of unmodified polymer (~19%). The 5% and 13% polymers attained buffering capacities of ~30 and ~36, respectively. The improvement in buffering capacity is evident in the titration curves obtained (Figure 14).
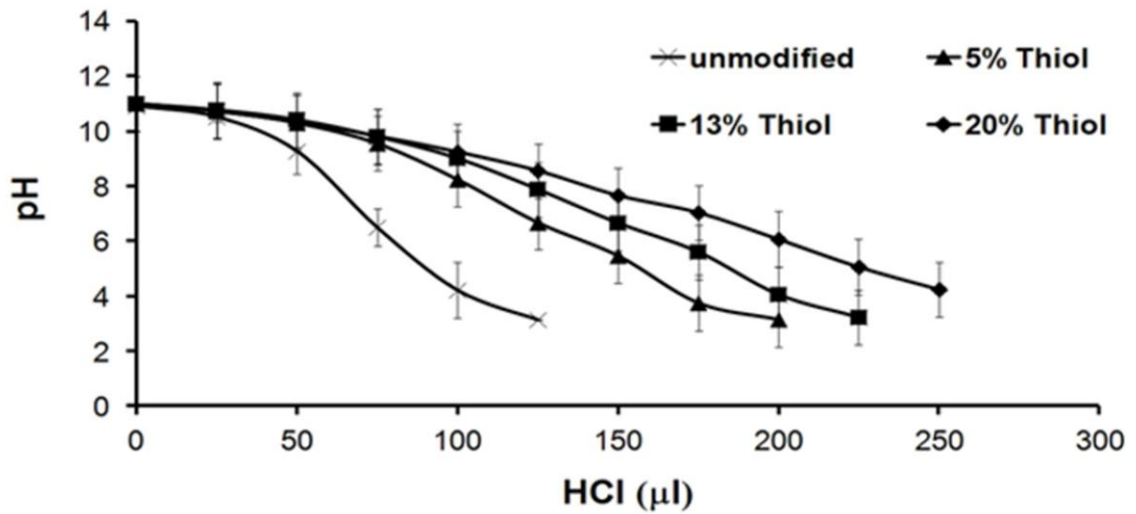

Figure 14. Titration assay of unmodified PAA, 5, 13, and 20% thiolated polymers shows that thiolation improves buffering capacity.

2.3.8 pH-Sensitive Gene Release

Polymeric carriers that depend solely on strong electrostatic interactions to bind gene cargo often experience inefficient cargo release; the polymer remains bound to the DNA even within the cell. As a result, the delivered DNA never reaches the nucleus where gene expression takes place. The binding efficiency studies showed that at higher N/P ratios thiolated polymers were able to successfully complex DNA. A pH-sensitive gene release assay was performed to determine whether thiolated polymer could release its cargo within the endosome before reaching lysosomal degradation. Figure 15 shows the relative fluorescence of DAPI-labeled DNA of unmodified and thiolated polyplexes at N/P ratios of 1, 5, 10, 20, and 40. At endosomal pH 5.5, unmodified and 5% thiolated polymers showed very low (if any) gene release. The high fluorescence intensities observed in the unmodified polyplex solutions once again verified that PAA does not adequately bind DNA. 5% thiolated polyplexes, on the other hand, exhibited low fluorescence intensities at pH 7.0, suggesting high binding efficiency. The previous DAPI displacement and gel assays demonstrated that the 5% thiolated polymer was the most efficient at binding DNA. This data verified that result and also showed that 5% polyplexes did not adequately release DNA; polymer-plasmid complexes remained bound even at the low pH of 5.5. The 20% thiol polyplexes exhibited high cargo binding and release only at N/P ratios of 20 and 40. At N/P 1, 5, and 10, 20% thiolated polymers did not appear to sufficiently bind cargo DNA. This result can also be seen in the gel assay (Figure 10). Finally, the 13% polymer appeared to have the highest binding-release capabilities out of all thiolated polymers, with the N/P 40 ratio being the exception. As demonstrated by the DNTB assay, 13%, N/P 5 polyplexes displayed the greatest amount

51

of crosslinking amongst all polymer samples. Based on this data it can be inferred that an optimal combination of charge ratio and thiol crosslinks are required for high binding and release kinetics.
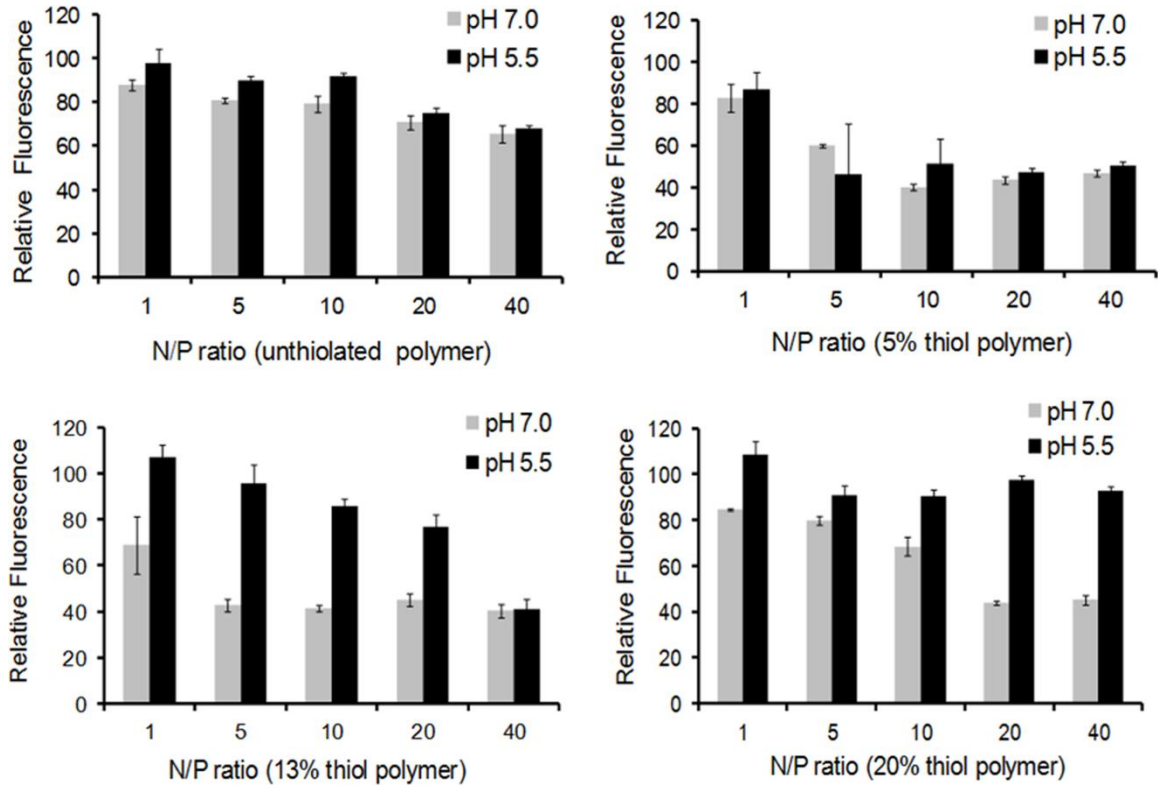
Figure 15. pH-sensitive plasmid release determined by a DAPI dispacement assay. Results show that 13% (NP 1-40) and 20% (NP 20-40) polyplex formulations were most efficient at binding DNA at pH of 7 and releasing cargo at pH 5.5.

2.4 Conclusions

Our data demonstrates that a certain degree of thiolation can significantly improve the carrier's *in vivo* potential. From our results we can conclude that the 5% thiolated complexes would be inefficient polymeric carriers because of their low gene release. Although these complexes bind and protect DNA more efficiently than 13% and 20% thiolated polymers, they exhibit minimal (if any) gene release at endosomal pH. 5% thiolated polyplexes also demonstrated the greatest amount of crosslinking overall. We therefore believe that too many crosslinks hinder the polymer's delivery potential. At the same time, the 20% thiolated polymer, which had the greatest buffering capacity and potential for endolysosomal escape, was also inefficient at DNA binding and release. Further, 20% thiolated polymers were the least effective in protecting gene cargo. The N/P 20 and 40, 20% thiolated polyplexes were the exception to the 20% polyplex formulations, exhibiting high binding and release kinetics. Therefore, the polyplexes with the greatest delivery potential overall, were the 13% thiolated polymers. Although 13% polyplexes showed partial degradation in the presence of DNase, they also achieved approximately twice the buffering capacity of PAA and were typically better at binding and releasing DNA.

Chapter 3

3.1 Abstract

This study investigates the extent of disulfide linking in a thiol-containing polymer and determines the impact that free thiols have on the polymer's delivery potential. A fluorescent cationic polymer containing thiol-pendant chains was prepared from poly(allylamine) (PAA) and 2-iminothiolate (Traut's Reagent) as described in chapter 2. Polymer fluorescence was determined by UV plate readings. Complex size and stability was measured by dynamic light scattering (DLS) and zeta potential, respectively. Transfection efficiency and cytotoxicity were assessed in MCF-7 breast cancer cells. Results show that polymers containing thiol crosslinks form smaller, more stable complexes than non-thiolated PAA. Fluorescent measurements, microscopy imaging, and DNA electrophoresis show that thiolated polymers are not internalized by cells in a culture, yet, they bind to the cell surface, perhaps valuable for applications requiring cell adhesion. Therefore, the extent of disulfide formation in thiolated polymers must be evaluated and the resulting effects of free thiols documented, prior to use as delivery vectors.

3.2 Experimental

3.2.1 Materials

Poly(allylamine) solution (PAA) (MW 15000) was purchased from PolySciences Inc. 2-iminothiolane (2-IT, Traut's reagent) and 5,5'-dithiobis-(2-nitrobenzoic acid) (DNTB) (Ellman's reagent) were purchased from Thermo Scientific. Millipore-Amicon® Centrifugal Filter Units (MW cutoff of 5000 Da) were purchased from Millipore. The DNA plasmid pEGFP-N1 (4700 base pairs) was purchased from CLONTECH Laboratories and cloned with Top 10 competent cells from Invitrogen. MCF-7 cells (Cat No. HTB-22) were purchased from ATCC. Extractions were carried out by HiSpeed Plasmid Maxi Kit purchased from Qiagen. Ethidium bromide, ethylenediaminetetraacetic acid powder (EDTA), Texas red-dextran (MW 10,000), paraformaldehyde (PFA), cover-slips, and glass slides purchased from Fisher Scientific. Dulbecco's Modified Eagle Medium and Lipofectamine2000 were purchased from Invitrogen. Phosphate buffered saline (PBS) molecular grade pH 7.4, 4',6-diamidino-2-phenylindole (DAPI), mowiol, filipin, amiloride, and monodansylcadaverine (MDC) were purchased from Sigma. Trypsin and penicillin/streptomycin were acquired from Gibco. Fetal bovine serum (FBS) was purchased from Cellgro. 1kb DNA Ladder, 10X Tris-Acetate-EDTA buffer (TAE), and agarose were purchased from New England Biolabs, Promega, and Research Products International Corp, respectively. Folded capillary cells and stoppers were purchased from Malvern.

3.2.2. Methods

3.2.2.1 Polymer Synthesis and Complexation

Thiolated polymers were synthesized and complexed with plasmid DNA as described in chapter 2. Briefly, PAA (MW 15,000) was dissolved in 4 ml PBS 4 at 1 mg/mL,with 1.75 mg/mL EDTA, and 1.5 mg/mL 2-iminothiolane. The reaction was run at room temperature (RT) for 2 h with continuous stirring on table-top orbital shaker. Synthesized thiolated polymers were washed with PBS using Milipore-Amicon Centrifugal Filter Units and stored at -80°C.

pEGFP-N1 plasmid (MW 2.9 x 10^6 Da, 4700 base pairs) was extracted from *E. coli* using the HiSpeed Plasmid Maxi Kit by Qiagen according to kit protocol. Polymer-plasmid complexation was carried out by incubating the polymer and plasmid at RT for 45 min at N/P ratios of 1, 5, 10, 20, and 40.

3.2.2.2 Polymer Fluorescence

Thiolated and unthiolated polymer were added to 40 µl PBS at concentrations of 0.005, 0.025, 0.05, 0.10, and 0.20 mg/mL in a 96 well plate. These concentrations correspond to those used in polyplexes with N/P (nitrogen/phosphate) ratios of 1, 5, 10, 20, and 40 delivered to MCF-7 cells. The fluorescence intensity of polymeric samples was measured with a plate reader at ex/em ~ 595/620 nm. A model red fluorescent polymer, Texas red dextran, was used as a positive control. All samples were run in triplicate.

3.2.2.3 *Measuring GFP Expression*

Transfection efficiency of thiolated and non-thiolated polymers was determined by GFP expression. Briefly, MCF-7 cells were plated on gelatin coated cover-slips in 24-well plates at 200,000 cells/well and incubated overnight in 1x Dulbecco's Modified Eagle Medium (DMEM) supplemented with 10% Fetal Bovine Serum (FBS) and 1% streptomycin/penicillin at 37°C for cell adherence. After 24 h, confluent cells were incubated for 4 h at 37°C in serum free media containing non-thiolated or 20% thiolated polyplexes with N/P ratios of 1, 5, 10, 20, and 40. Positive control cells were treated with commercial transfection reagent lipofectamine2000, according to supplier protocol. Negative control groups included untreated and plasmid (no polymer) treated cells. Cells were then washed and incubated in serum-supplemented DMEM for 48 h to allow for GFP expression. After 48 h, cells were washed, followed by staining with DAPI, cell fixation with 2% paraformaldehyde (PFA), and mounting on glass slides using Mowiol. Samples were visualized using an Olympus IX81 fluorescence microscope (Olympus) and a 40X objective. Fluorescent images were obtained with an ORCA-ER camera (Hamamatsu Corporation) and SlideBook™ 4.2 software (Intelligent Imaging Innovations, Inc.). Fluorescence images were analyzed using Image-Pro 6.3 software (Media Cybernetics, Inc).

3.2.2.4 *Gel Electrophoresis*

Gel electrophoresis was performed on DNA samples isolated from cell media and transfected cells to determine whether gene cargo was completely internalized. Briefly, cells were plated and transfected with thiolated polyplexes as described above. After the

57

4 h transfection period, media was collected from wells. Cells were collected with trypsin and plasmid and chromosomal DNA were extracted and purified with the PuregeneCore Kit (Qiagen) according to kit protocol. Plasmid that did not internalize was similarly purified from cell media. DNA samples were run at 100 V for 1 h on a .07% agarose gel containing ethidium bromide (EthBr) and loading dye, against a 1 kb ladder.

3.2.2.5 *Uptake Inhibition*

Filipin, amiloride, and MDC inhibit caveolae assisted internalization, macropinocytosis, and clathrin-mediated endocytosis, respectively.[74, 75] To determine potential polyplex internalization by any of these pathways, cells were treated with filipin, amiloride, and MDC prior to transfection. MCF-7 cells were plated on gelatin coated cover-slips in 24-well plates at 200,000 cells/well and allowed to adhere overnight. The following day, cells were treated with filipin (1 μg/ml), amiloride (3 mM), or MDC (50 μM) for 30 min at 37°C as previously described.[76] Then, N/P 40, 20% thiolated polyplexes were added and incubated for 4 h with inhibitors present. Control groups included untreated cells and cells treated only with polyplexes (no inhibitors). Post-transfection washing, staining, fixation, and visualization were carried out as described above. Polymer fluorescence intensities were calculated by analyzing the sum fluorescence intensity using Image-Pro 6.3 software. The average fluorescence intensity was then calculated by dividing the sum fluorescence intensity of each image by the number of cells.

58

Polymer-cell membrane interactions were studied by incubating cells with thiolated polyplexes or uncomplexed (no plasmid) thiolated polymers for 4 h as done in the above transfection assays. Cell preparations, transfections, and calculations for polymer fluorescence intensities were carried out as described above. Untreated cells were used as a control.

To determine whether incubation time plays a role on polymer-cell binding, a time dependent transfection was performed. Polyplex internalization was determined by fluorescence microscopy. Cell plating and polyplex transfection were carried out as previously described. However, instead of the 4 h incubation period previously used, polyplexes were incubated with cells for 30 min, 1 h, 2 h, 4 h, and 24 h. At each of these times points, cells were washed, stained with DAPI, fixed, and mounted as described above. The average fluorescence intensities were calculated and compared to an untreated control group.

Temperature effects on polymer-cell membrane binding were determined by performing transfection assays at 4°C or 37°C for 4 h. Cell preparation and transfections were carried out as previously described. After the 4 h incubation period, cells were washed, stained, fixed, mounted, and visualized as described above. The average fluorescence intensities were calculated and compared to untreated control cells incubated at either 4°C or 37°C for 4 h.

3.2.2.7   Cell Count

To determine the effects of thiol-pendant chains on cell viability, MCF-7 cells were transfected with non-thiolated PAA or 20% thiolated polyplexes at N/P ratios 1-40 as previously described. Control cells were treated with Lipofectamine2000 in order to assess polymer toxicity relative to a commercial reagent. Commercial surfactant Triton X was used as a positive cytotoxic control. Untreated cells were used as a negative control for toxicity. Gross cell viability was inferred by determining cell counts in the culture 48 h post transfection. Ten images were obtained from each well; cell nuclei were counted and averaged. Cell count was calculated relative to untreated control cells.

3.2.2.8   Statistical Analysis

For all transfection assays, analysis was performed on ≥ 2 cover slips, using 10 images per cover slip, and ≥ 40 cells per image.

The data are expressed as the mean $\pm$ standard error of the mean (SEM). Outliers were identified using Grubb's outlier test. The criterion for statistical significance was p values < 0.05.

3.3 Results and Discussion

3.3.1 Polymer Fluorescence

Figures 16 and 17 show the fluorescent intensities of unthiolated and thiolated PAA as measured by UV plate readings. Polymer fluorescence was tested at 5 different polymer concentrations and compared to a model fluorescently-labeled polymer, Texas red dextran, a positive control. As shown in Figure 16, unthiolated PAA did not demonstrate any photosensitivity at ex/em ~595/620 nm. Thiolated polymer on the other hand reached fluorescent intensities ~1000 a.u. We believe that the fluorescence of thiolated polymers resulted from interactions between the strongly nucleophilic thiolates and π-electrons associated with the C=N. Literature shows that thiolates form in solution from thiols.[77] Further, it is well documented that molecules containing 'π' electrons (also known as delocalized electrons) or 'lone pair' electrons (particularly those associated with N, O, P, and S atoms) are capable of fluorescence.[78] The fluorescent characteristics of the thiolated polymer are explained in further detail in chapter 4.
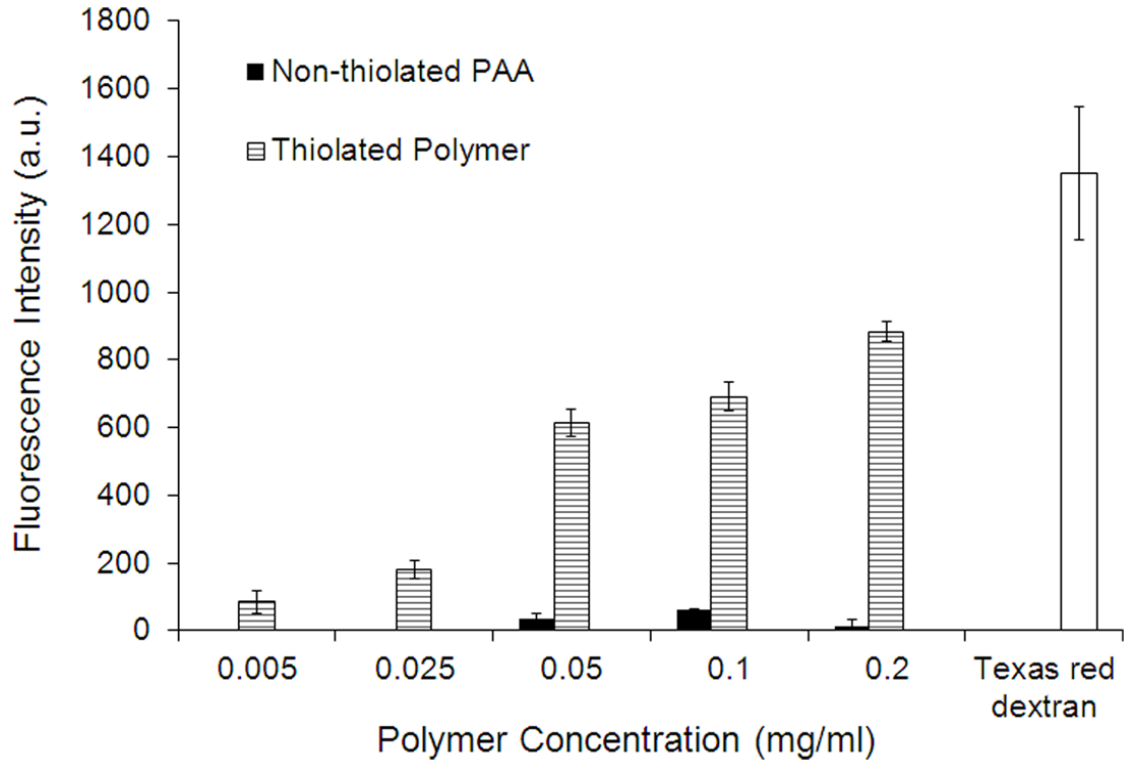
61

Figure 16. Fluorescence intensity of non-thiolated PAA, thiolated polymer, and Texas red dextran control determined by UV plate reader show that thiolated polymers exhibit a concentration dependent fluorescence. No fluorescence is observed by non-thiolated polymers.

3.3.2 Polyplex Delivery and GFP Expression

PAA has been proven to be a poor gene delivery vector due the polymer's low buffering capacity at endosomal pH.[48] Unlike more efficient delivery vectors, such as poly(ethyleneimine) and poly(amidoamine) dendrimers, which possess titratable secondary and tertiary groups, PAA only contains non-titratable primary amines.[38, 48] As a result, upon cellular internalization PAA cannot escape the endosome through the proton sponge effect: a phenomenon in which endosomal osmotic swelling, brought on by the presence of hydrolysable amine groups on the polymer, causes the endosome to rupture, releasing the polymer-DNA complexes into the cell cytosol.[48, 79]

Previously we demonstrated that thiolated polymers efficiently complexed plasmid DNA, obtaining size values between 80-120 nm, whereas non-thiolated polymers were not as efficient at binding cargo. To determine whether thiol-pendant chains impact the transfection success of cationic polymers, transfection assays were performed in MCF-7 breast cancer cells. Fluorescent images of MCF-7 cells treated with non-thiolated and thiolated polyplexes show that all polyplex treated cells and negative control groups did not express GFP. In contrast, positive control cells treated with commercial lipofectamine successfully expressed GFP. Figure 17, shows a set of fluorescent images collected from cells treated with 20% polyplexes at N/P ratios 1, 5, 10, 20, and 40, and control groups. The green fluorescence visible only in lipofectamine treated cells results from GFP expression. The red fluorescence is emitted by the thiolated polymer.

From Figure 17, it is evident that polymer-plasmid treated cells show an increase of polymer uptake (red) with increasing N/P ratio, but that GFP was not expressed in these

63

cells, as opposed to lipofectamine treated cells. However, no conclusions can be made regarding polyplex internalization. To determine whether plasmid was delivered into the cells, gel electrophoresis was performed on DNA extracted from transfected cells and cell media. The red fluorescence observed by thiolated polyplexes indicates that polymer is still present in the samples. Whether the polymer is located within or on the surface of cells cannot be determined from this assay.
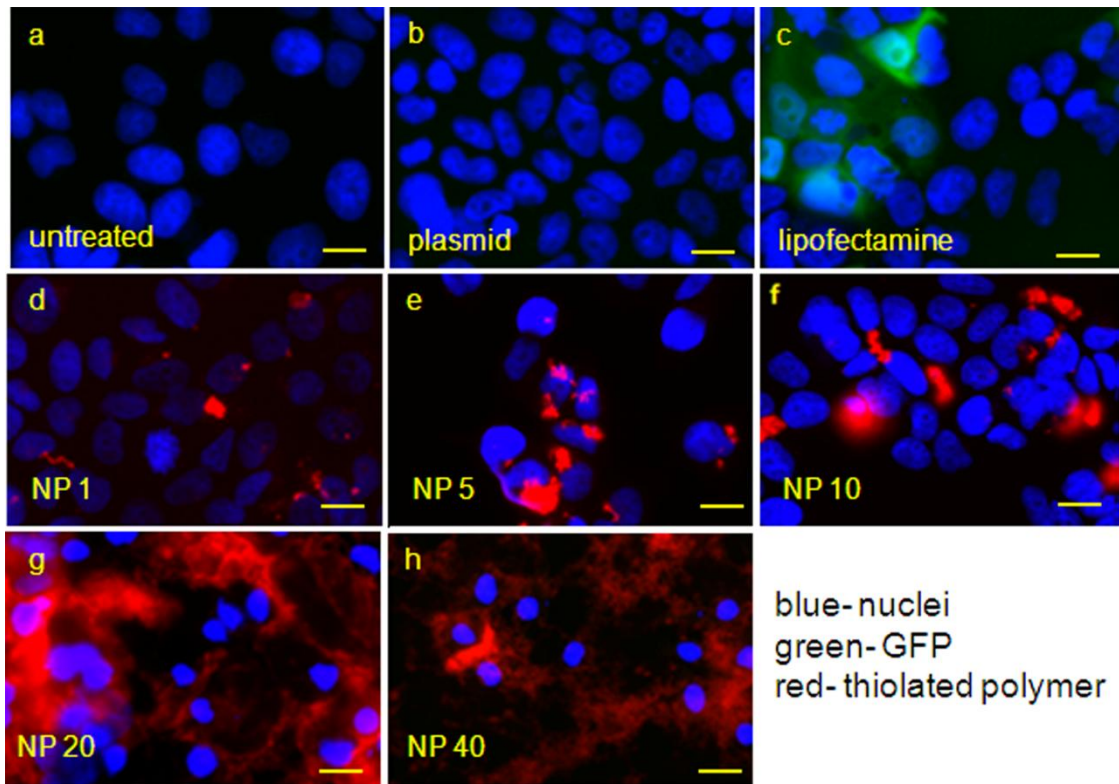

Figure 17. MCF-7 cells transfected with 20% thiolated NP1-40 polyplexes (a-e). Control groups (a) untreated, (b) plasmid and (c) lipofectamine. Incubation: 4 h at 37°C. 40 X objective; scale bar, 15 μm. GFP expression only observed in lipofectamine treated cells.

3.3.3 Plasmid Internalization

Upon internalization, polymeric carriers must overcome a number of intracellular challenges, including endolysosomal escape and cargo release, before the delivered genes can be expressed.[1, 2, 28, 80] Typically, more than 95% of the cells in a culture internalize over 100,000 copies of the vector, but less than 50% the cells express the cargo.[2]

To determine whether thiolated polyplexes were internalized, DNA was extracted from polyplex treated cells versus cell media. DNA samples were run on an agarose gel in order to assess the relative concentration of plasmid internalized by cells, versus the concentration of polymer still present in the cell media. Figure 18 shows the DNA extracted from cells and media in polyplex treated samples and control groups. Untreated cells and cells treated with polyplexes show only chromosomal DNA, as indicated by the bright upper band. The media samples collected from NP 1-10 polymer treated cells, on the other hand, show evidence of plasmid DNA, indicating that plasmid DNA did not internalize during the transfection. The upper and lower bands in these wells correspond to supercoiled and relaxed plasmid, respectively. This effect is also seen in the plasmid control group. Plasmid is not visible in media collected from N/P 20 and 40 transfections. We believe that the high electrostatic binding at these concentrations prevented plasmid release from polymer carriers. As a result, plasmid DNA and polymer bound to cell membrane were removed as part of cell debris in the purification process. Positive control lipofectamine samples exhibit plasmid and media, suggesting that some of the plasmid in these samples was internalized by cells.
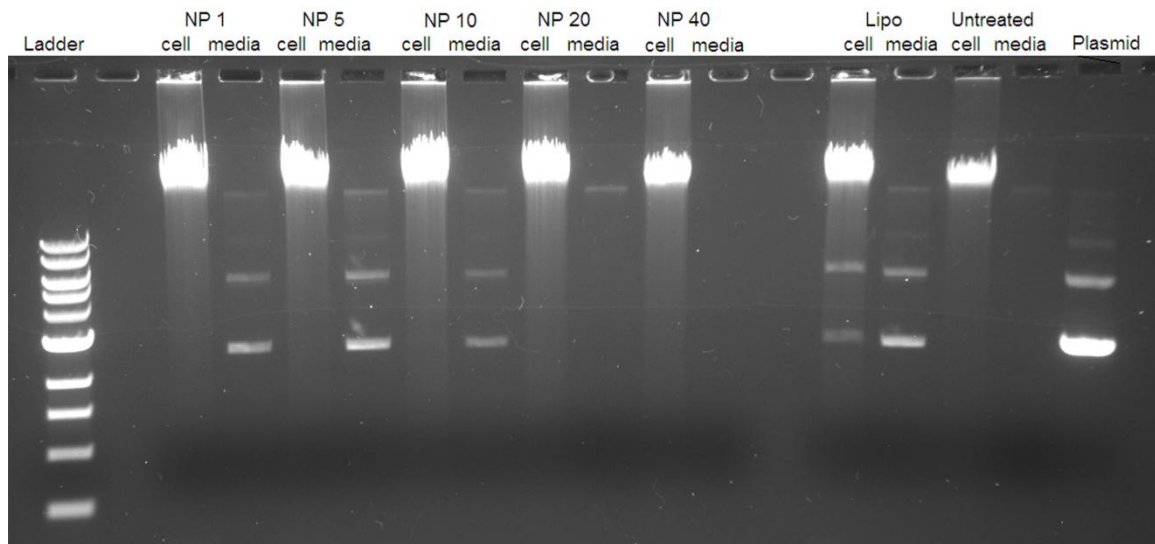
65

Figure 18. Gel electrophoresis of DNA purified from cells and cell media shows that only lipofectamine treated cells internalized DNA. Incubation: 4 h at 37°C.

3.3.4 Uptake Inhibition

The results obtained from GFP expression and gel electrophoresis suggest that thiolated polyplexes are not internalized by cells. Fluorescent images from the GFP expression assay, however, show that the red fluorescing polymer is present in cell samples. Since transfected cells are thoroughly washed with PBS post-transfection, we believe that the thiolated polymeric carriers have attached to the cell surface via disulfide linkages. A pathway inhibition assay, in which cells were treated with one of three pathway inhibitors prior to polyplex transfection, was performed to demonstrate the polyplexes bind to the cell's surface.

Endocytosis is subdivided into four main categories; (i) clathrin-mediated endocytosis, (ii) caveolae, (iii) macropinocytosis and (iv) phagocytosis.[74] The first three pathways can be inhibited with monodansylcadaverine (MDC), filipin, and amiloride, respectively. MDC is an agent that blocks formation clathrin-coated pits. Filipin affects cholesterol, thereby inhibiting caveolar-assisted endocytosis. Amiloride hinders Na^+/H^+ exchange in macropinocytosis and non-classical CAM-mediated endocytosis.[74, 75] Phagocytosis is more specific of immune cells and hence is less relevant to our system.[81]

MCF-7 cells were treated with MDC, filipin, or amiloride prior to transfection. Figure 19 shows that polyplex treated cells exhibited similar average fluorescence intensities regardless of inhibition. In all cases, fluorescence was significantly increased as compared to untreated cells, which exhibited minimal background fluorescence. These data validate that the inhibitors don't affect potential binding of polyplexes to the cell surface, and further confirm that polymers are not internalized by cells.

67
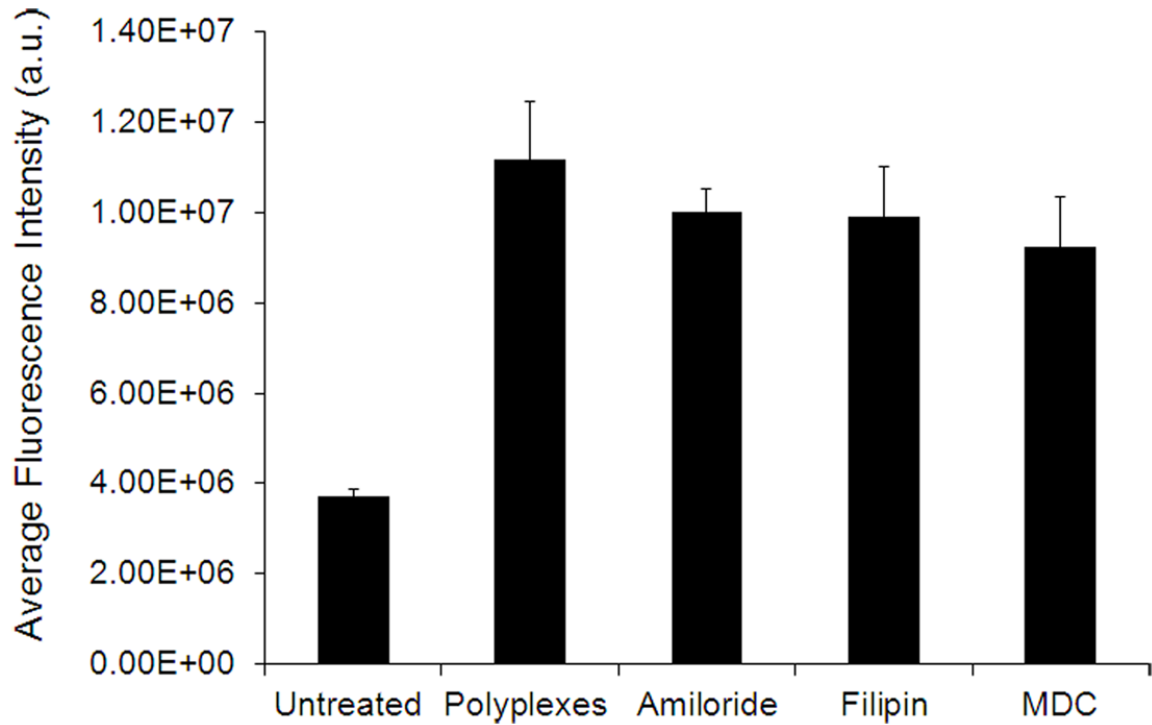
Figure 19. Average fluorescence intensities obtained from untreated cells, un-inhibited polyplex treated cells, and polyplex treated cells inhibited with Filipin, MDC, an Amiloride treated cells after 4 h transfection with 20%, N/P 40 thiolated polyplexes. Incubation: 4 h at 37°C. Results show that polyplexes are not internalized by the clathrin-mediated, caveolae assisted, or macropinocytosis pathways, and thereby suggest that polymer-cell surface binding.

3.3.5 Polymer-Cell Membrane Binding

Electrostatic interactions between thiolated cationic polymers and DNA condense cargo into nanosized particles amenable for *in vivo* delivery. It is generally accepted that particles less than 150 nm are optimal for internalization.[82] Studies have shown that free PAA with MW 15000 has a hydrodynamic radius of over 4.8-6.5 nm in the pH range of 6.0-9.5.[83] Internalization of uncomplexed free polymer would therefore be hindered by the polymers large size. Hence, to further verify polyplex binding to cell surfaces, uncomplexed polymer and polymer-plasmid complexes were delivered to cells. Uncomplexed thiolated polymer that doesn't bind to the cell's surface would be removed during PBS wash. As a result, fluorescent images of these cells would show little (if any) fluorescence.

Figure 20 shows that average fluorescence intensities in polyplex-treated, polymer-treated, and untreated control cells. At low N/P ratios the same fluorescence intensities are observed in treated and untreated cells. This low fluorescence is attributed to background noise and suggests that polymer binding at these N/P ratios is minimal. As N/P ratio increases, the average fluorescence also increases. We believe that the greater number of thiols present in these samples facilitate the formation of disulfide linkages between the polymer and proteins present on the cell membrane. In addition, Figure 20 shows that polymer-treated cells display similar fluorescence intensities as cells transfected with polyplexes. This data once again suggests that polyplexes are not internalized by cells. We believe that the polymer binds to the cell membrane via disulfide bonds, which prevent the un-internalized polyplexes from being removed in the wash step prior to cell fixation and fluorescent microscopy.
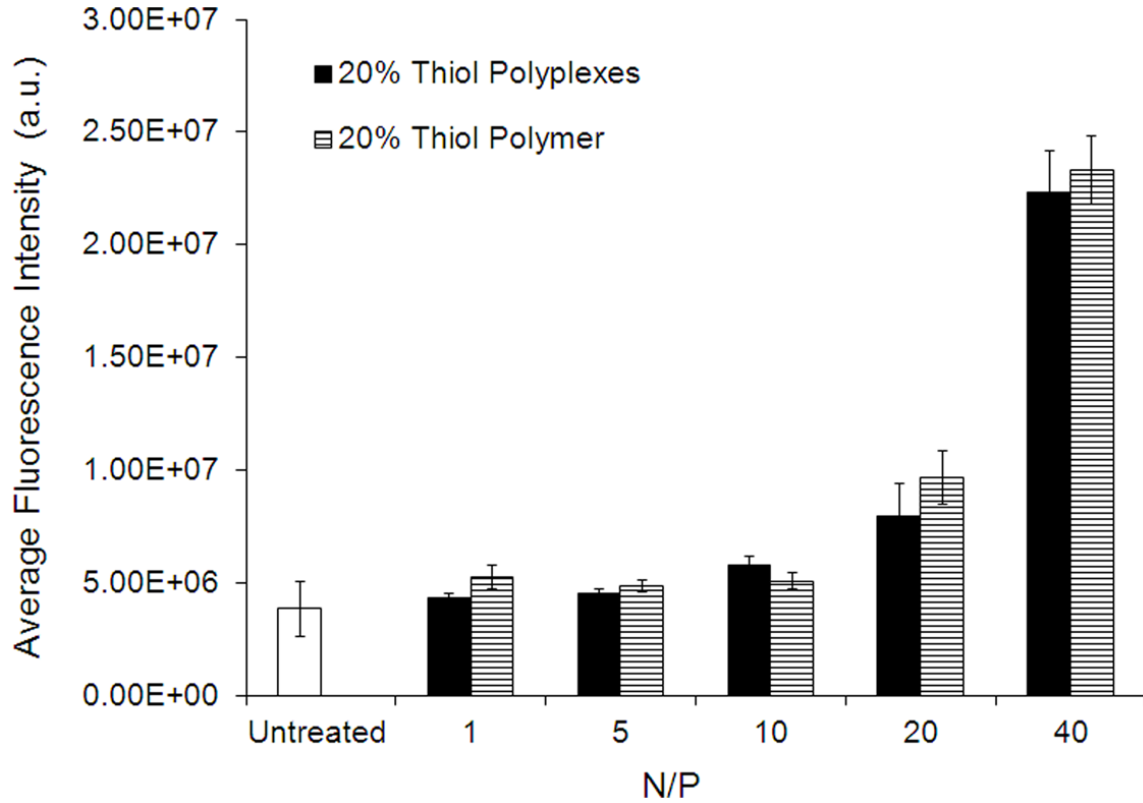
69

Figure 20. Average fluorescence intensities obtained from cells treated with 20% thiolated polyplexes, 20% tholated polymers (no plasmid), and untreated controls indicate no significant difference in polymer concentration between polyplex and polymer treated cells, suggesting that polyplexes are not internalized. Incubation: 4 h at 37°C.

3.3.6 Binding Kinetics

To determine whether polymer-membrane binding is a time dependent reaction, MCF-7 cells were incubated with polyplexes for over 30 min, 1 h, 2 h, and 4 h at 37^oC. In addition, another set of MCF-7 cells was treated with thiolated polyplexes and incubated at 4^oC to determine whether temperature affects the kinetics of polymer-membrane disulfide linking. N/P 40, 20% thiolated polyplexes were used for all time and temperature dependent assays because of their high fluorescence intensities.

Data demonstrate that cell surface binding is time and temperature dependent. Figure 21 shows that the average fluorescence intensities observed in polyplex treated samples increases with incubation time. Transfections carried out for 30 min, 1 h, and 2 h show no discernible difference in average fluorescence from untreated control groups. However, after 4 h of incubation fluorescence intensities doubled and remained relatively constant between the 4 h and 24 h time points. This data suggests that initial the polymer-cell membrane interactions are minimal. As a result, the polymer is removed in the wash step and the observed fluorescence is primarily due to background noise. At the 4 h time period there is a significant increase in average fluorescence intensity values, which we attribute to increased polymer-cell interactions. Since there is no further increase in fluorescence over the next 24 h, we conclude that the majority of polymer-cell interactions occur between 2-4 h of incubation.

The temperature-dependent assay demonstrated that polymer-membrane binding is hindered at 4^oC. As shown in Figure 22, cells treated with polyplexes at 4^oC exhibit the same noise fluorescence intensity as untreated cells. Studies show that the thiol-disulfide

71

exchange is highly dependent on temperature, with elevated temperatures facilitating the reaction.[84] It is expected, therefore, that at 4°C there would be minimal (if any) disulfide interactions between thiolated polymers and cell surfaces.

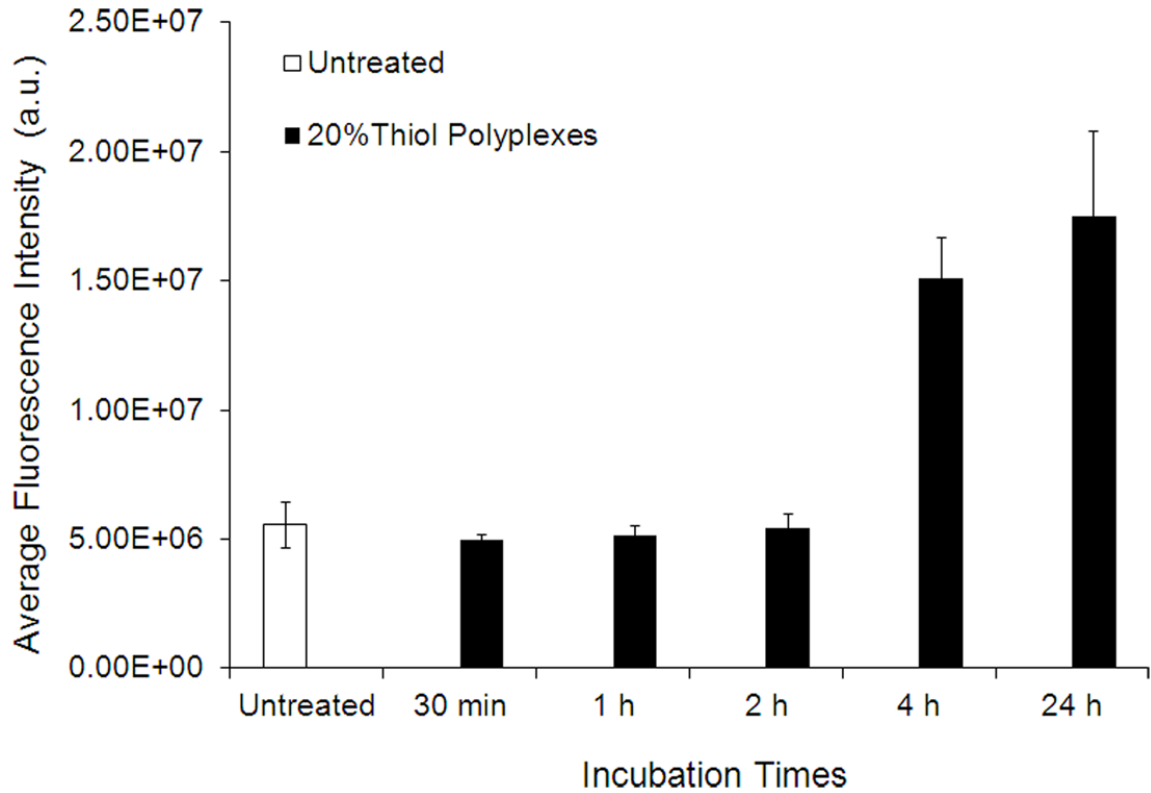**Figure 21. Average fluorescence intensities obtained from polyplex treated cells suggest that polymer-cell surface binding occurs between 2-4 h. Incubation temperature: 37°C**
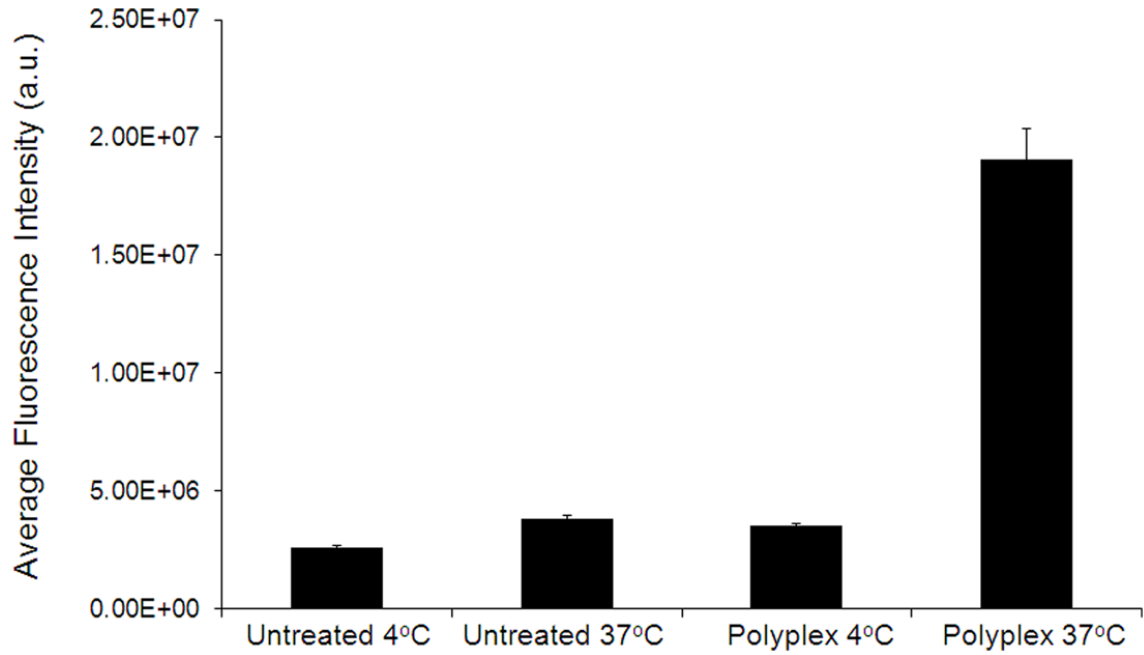
Figure 22. Average fluorescence intensities observed in untreated and polyplex treated cells at 4°C and 37°C indicate that polyplexes do not attach to cell surface at 4°C. Incubation: 4 h at 37°C.

3.3.7 Cell Count

Cell count was performed on with 20% thiolated polyplexes and non-thiolated PAA to determine whether thiols affect cytotoxicity. Control cells were treated with lipofectamine to compare the toxicity of polymers relative to a commercial transfection reagent. Untreated cells were used a negative control for toxicity. Cells treated with Triton X, which permeabilizes cells by disrupting membranes, were used as a positive control. Gross toxicity was determined by performing a cell count of treated cells relative to the untreated control group. Figure 23 shows that at N/P ratios 1-20, there is no significant difference in cell count between polyplex treated cells, lipofectamine and untreated controls. At N/P 40, the viability of cells treated with thiolated polyplexes drops to ~60%. We believe that the excess amount of polymer binding onto the cell surface significantly impacts cell viability.
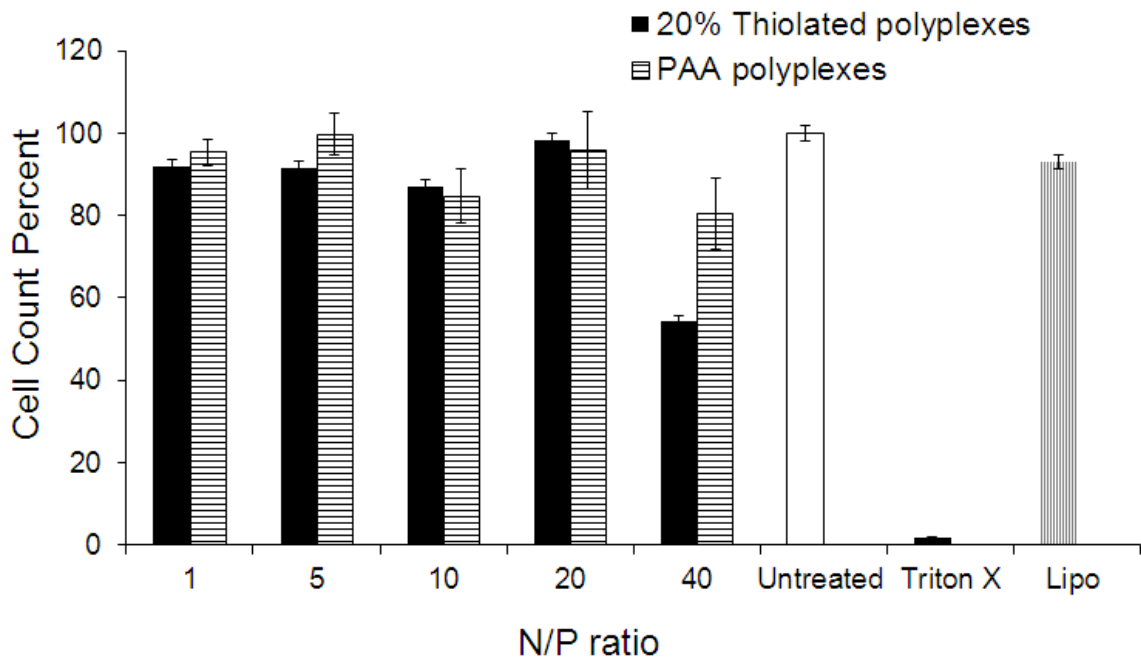
Figure 23. Percent cell count of polymer treated cells relative to an untreated control, suggests minimal toxicity at NP 1-40. Viability of thiolated polyplex treated cells decreases by ~40% at N/P 40. Count 48 h post-transfection.

3.4 Conclusions

Although thiol-pendant chains improved the complex size and stability of polyplexes, as demonstrated by DLS and zeta potential data, cell transfection assays showed that free thiols impede polyplex internalization due to polymer-cell surface attachments. The extent of attachment is determined by the concentration of thiols present, with higher concentrated polymers binding more readily to cell surfaces. Cytotoxicity is also affected by thiolated polymers. At lower polyplex concentrations, polymers do not exhibit significant toxicity. However, at higher thiolated polymer concentrations the viability of cells drops to nearly half. The effects of thiols as determined by this study should be taken under consideration when synthesizing thiol-containing cationic polymers for gene delivery. The high binding between free thiols and polymer cell surfaces impedes internalization but may have potential in other applications such as tissue engineering, medical implants, and biosensors where cell adhesion is necessary.

Chapter 4

4.1 Abstract

Fluorescent polymers have attracted much attention in a variety of biomedical applications including biosensing, immunology, tissue engineering and gene delivery.[85] In cellular studies, fluorescent polymers are employed in an attempt to gain a deeper understanding of cellular processes, such as gene expression, protein transport, signaling and regulatory processes.[86]

The concept of using fluorescence in intracellular trafficking and cell imaging is not limited to fluorescent polymers. Organic dyes, fluorescent proteins, and lanthanide chelates are often employed in the biological field.[85] However, the success of these biomaterials is limited due to challenges including photostability and toxicity.[85, 87, 88] In gene delivery, for example, fluorescent dyes are conjugated onto delivery complexes to assess internalization efficiency and aid in the optimization of drug carriers.[88, 89] The large size of the probes often interferes with the carrier's delivery efficiency. Studies have shown that attachment of a dye onto the polymer carrier can reduce expression by as much as 95%.[89] Protein reporters, such as green fluorescent protein (GFP) and its derivatives, have also been used to monitor gene expression.[86, 90] However, the fluorescent signals of GFP and similar protein reporters, diffuse quickly within the cytoplasm of the cell during imaging, making it difficult to discern a single reporter molecule.[90] Aggregation of fluorescent proteins within the cell can lead to cell toxicity.[85] Finally, fluorescent markers, such as fluorescein, are susceptible to photobleaching, thereby compromising image contrast, quality, and prohibiting long-term monitoring of cells.[87, 88]

76

Fluorescent polymers offer the same advantages as fluorescent probes while avoiding the problem of delivery interference, the additional cost of probes, and potential photobleaching. As a result, fluorescent polymers are being investigated for a number of biological applications. Highly fluorescent nanoparticles, also known as "polymer dots", for example, show higher photostability than molecular florescent probes and can be applied to cell imaging, ultrathin films or structured particles.[87, 91] Fluorescent polymers that quench upon protein interaction can used to identify biomarker proteins in early disease detection.[92, 93] Finally, fluorescent polymers offer the opportunity for more reliable and less costly detection methods than the commonly used ELISA assay and high through put microarrays.[93, 94, 95]

The application of fluorescent polymers in cellular assays would greatly improve the quality of cell imaging and significantly impact our understanding of cellular processes, allowing for the development of new and more reliable techniques. However studies show that the optical and electrochemical properties of fluorescent polymers are strongly affected by small perturbations in the environment, including changes in temperature, pH, and solvent.[96, 97] Fluorescent conjugated polymers, for example, can be quenched very quickly in the presence of charged molecules.[97] In this paper we explore optical changes in a thiol-containing fluorescent polymer with respect to inter- and intra- polymer chain interactions and non-specific interactions in solutions.

4.2 Experimental

4.2.1 Materials

Poly(allylamine) solution (PAA) (MW 15000) was purchased from PolySciences Inc. 2-iminothiolane (2-IT, Traut's reagent) and 5,5'-dithiobis-(2-nitrobenzoic acid) (DNTB) (Ellman's reagent) were purchased from Thermo Scientific. Millipore-Amicon Centrifugal Filter Units (MW cutoff of 5000 Da) were purchased from Millipore. pEGFP-N1 (4700 base pairs) plasmid was purchased from CLONTECH Laboratories and cloned it with Top 10 competent cells from Invitrogen. Extractions were carried out by HiSpeed Plasmid Maxi Kit purchased from Qiagen. Ethidium bromide, ethylenediaminetetraacetic acid powder (EDTA), dextran, Texas red dextran (MW 10,000), were purchased from Fisher Scientific. Dulbecco's Modified Eagle Medium and was purchased from Invitrogen. Phosphate buffered saline (PBS) pH 7.4, molecular grade was purchased from Sigma. Fetal bovine serum (FBS) was purchased from Cellgro. *Label* IT Tracker Intracellular Nucleic Acid Localization Kit, Fluorescein was purchased from Mirus Bio LLC.

4.2.2 Methods

4.2.2.1 Polymer Synthesis

Thiolated polymers were synthesized by functionalizing 20% of the amines on a poly(allylamine) (PAA) backbone as previously described. Briefly, PAA was suspended in solution containing ethylenediaminetetraacetic acid powder (EDTA) and 2-Iminothiolane (Traut's reagent). The reaction was run at room temperature (RT) for 2 h to allow for conjugation of thiol chains onto the primary amines of PAA. Synthesized polymers were washed with PBS using Milipore Centrifugal Filter units at 8000 g. Filtered samples were suspended in PBS and stored at -80°C. Synthesis was verified by DNTB and ^{1}H NMR.

4.2.2.2 Polymer Fluorescence

Fluorescence of thiolated polymers was verified by UV plate reader. Briefly, 0.005, 0.025, 0.05, 0.10, and 0.20 mg/mL of thiolated and non-thiolated polymers, 2-IT, and EDTA were suspended in PBS, pH 7.4 in a 96 well plate. Polymer concentrations correspond to polyplex N/P ratios previously used. The fluorescence intensity of all samples was measured with a plate reader at ex/em ~595/620 nm. Fluorescently labeled polymer, Texas red dextran, was used as a positive control. The fluorescence intensity of PBS was also measured and subtracted from sample readings to remove background noise.

Fluorescence was measured at various time points over a 24 h time period to assess fluorescence stability. After 24 h, 10 μl 0.1 M HCl was added to all solutions to

79

determine whether acidic environments affect fluorescence. Fluorescence intensities were measured again and calculated as previously described.

4.2.2.3 Fluorescent Microscope

Thiolated polymer fluorescence was confirmed by fluorescent microscopy. Briefly, thiolated polymers were fixed at concentrations mentioned above on gelatin coated coverslips using 2% paraformaldehyde (PFA). Subsequently, coverslips were attached to glass slides using Mowiol. Samples were visualized using an Olympus IX81 fluorescence microscope (Olympus) and a 40X objective. Fluorescent images were obtained with an ORCA-ER camera (Hamamatsu Corporation) and SlideBook™ 4.2 software (Intelligent Imaging Innovations, Inc.). Fluorescence images were analyzed using Image-Pro 6.3 software (Media Cybernetics, Inc).

4.2.2.4 Protein Induced Fluorescent Quenching

Polymer-protein quenching was demonstrated by incubating thiolated polymers in Dulbecco's Modified Eagle Medium (DMEM) containing fetal bovine serum (FBS). Briefly, thiolated polymers were suspended at the concentrations mentioned above in phenol-free or phenol-supplemented media containing 10% FBS. Fluorescence was measured at the same polymer concentrations and with the same control group as above.

4.2.2.5 Polymer-Plasmid Interactions

Often in in-vitro delivery studies, DNA cargo is labeled with a molecular probe so that the DNA's pathway within the cell can be visualized. Intracellular trafficking allows researchers to identify the rate-limiting step in the transfection process. To determine

80

whether polymer-plasmid interaction affect the probe's fluorescence properties, thiolated polymer and fluorescein labeled plasmid DNA were complexed (polyplexes) at N/P ratios of 1, 5, 10, 20, and 40 in a 96-well plate at RT for 45 min. Plasmid labeling was carried out by Mirus Label IT kit according to manufacturer protocol. After incubation, fluorescent intensities of polyplexes were determined by plate reader at an ex/em ~492/523 and compared to uncomplexed plasmid. The experiment was performed in PBS and serum-free DMEM.

4.2.2.6   *Statistical Analysis*

All experiments were performed in quadruplicate. Data is presented as the average and corresponding standard deviation of the mean (SEM) of four (n= 4) separate sample trials. Grubb's test with $p < .05$ was used to determine significant outliers.

4.3 Results and Discussion

4.3.1 Polymer Fluorescence

Fluorescence is a phenomenon in which certain electrons in a molecule transition from ground state to excited state by absorbed light. As the electron return to ground state, some of the energy absorbed is emitted as fluorescence. Literature shows that molecules containing 'π' electrons (also known as delocalized electrons) or 'lone pair' electrons (particularly those associated with N, O, P, and S atoms) are capable of fluorescence.[98] In the present study, we developed a fluorescent polymer by conjugating thiol pendant chains onto the primary amines of PAA using 2-IT as previously described.[99] The resulting fluorescent polymer contained 'π' bonds as well as lone pair electrons associated with thiolates, and demonstrated increased photosensitivity at ex/em ~595/620 nm.

To verify fluorescence of thiol containing polymers, fluorescent intensities of thiolated and non-thiolated polymers, as well as EDTA and 2-IT were measured by plate reader. EDTA and 2-IT were utilized in the synthesis of thiolated polymers. Hence, the fluorescence intensities of these reagents were measured to ensure that the fluorescent properties observed in thiolated polymer samples resulted from the polymer itself, rather than residual reagents in solution. Fluorescently labeled polymer, Texas-red dextran, was used as a positive control. As shown in Figure 24, non-thiolated PAA, EDTA, and 2-IT did not display any fluorescence. Thiolated polymers displayed a concentration dependent increase in fluorescence. At low polymer concentrations, minimal (if any)

fluorescence was observed in thiolated polymers. However, at the highest .2 mg/ml concentration, fluorescence values reached ~1000 a.u.

We attribute polymer fluorescence to interactions between thiolate lone pair electrons and 'π' orbitals of C=N bonds. Previous studies have shown that thiols (SH) form highly nucleophilic thiolates (S-) in aqueous solution.[100] Thiolates contain three lone pair electrons and are capable of charge transfer-transitions.[101]The active role of thiolates in fluorescence has been well documented. Farrar *et al*.,[101] for example, demonstrated that charge energy transfers between thiolate lone pair electrons and 'π' orbitals of copper(II) give rise to the optical properties of copper proteins, known as cupredoxins. We believe that thiolates, formed from conjugated thiol groups, destabilized the 'π' orbitals of C=N bonds, giving rise to the polymers fluorescence. In general, any influence that destabilizes 'π' electrons increases fluorescence a molecule's fluorescence, whereas 'π' orbital stabilization diminishes fluorescence.[98] Further, we reason that larger concentration of thiols and double bonds in higher concentrated polymer samples facilitated 'π' electron destabilization, resulting in higher fluorescence intensities.

Thiolated polymer fluorescence was further verified by fluorescence microscopy. As with UV readings, fluorescent microscopy showed that fluorescence intensity increased with polymer concentration. Figure 25 shows the sum fluorescence intensities of thiolated polymer samples as determined by Image-Pro 6.3 software. The polymer can be visualized in Figure 26.

83

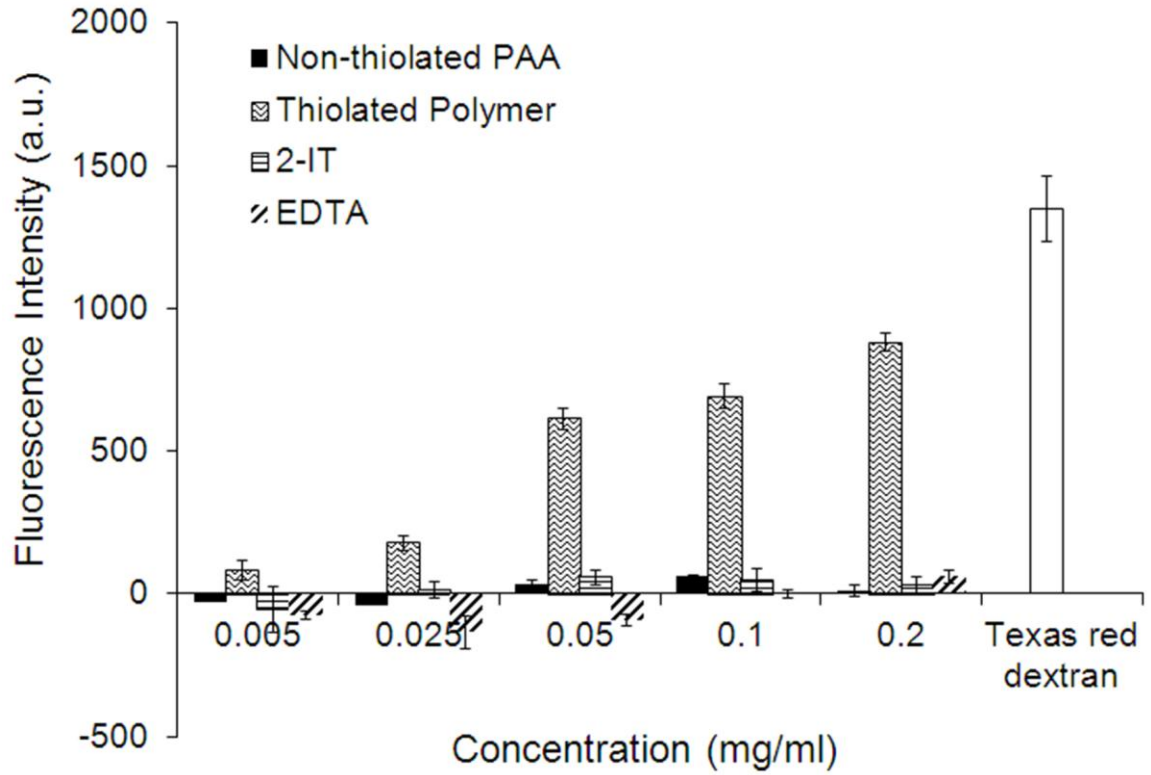**Figure 24. Fluorescence intensities of thiolated and non-thiolated polymers, EDTA, 2-IT, and Texas red dextran control show that thiolated polymer, but not PAA or reagents fluoresce at ex/em 595/620.**
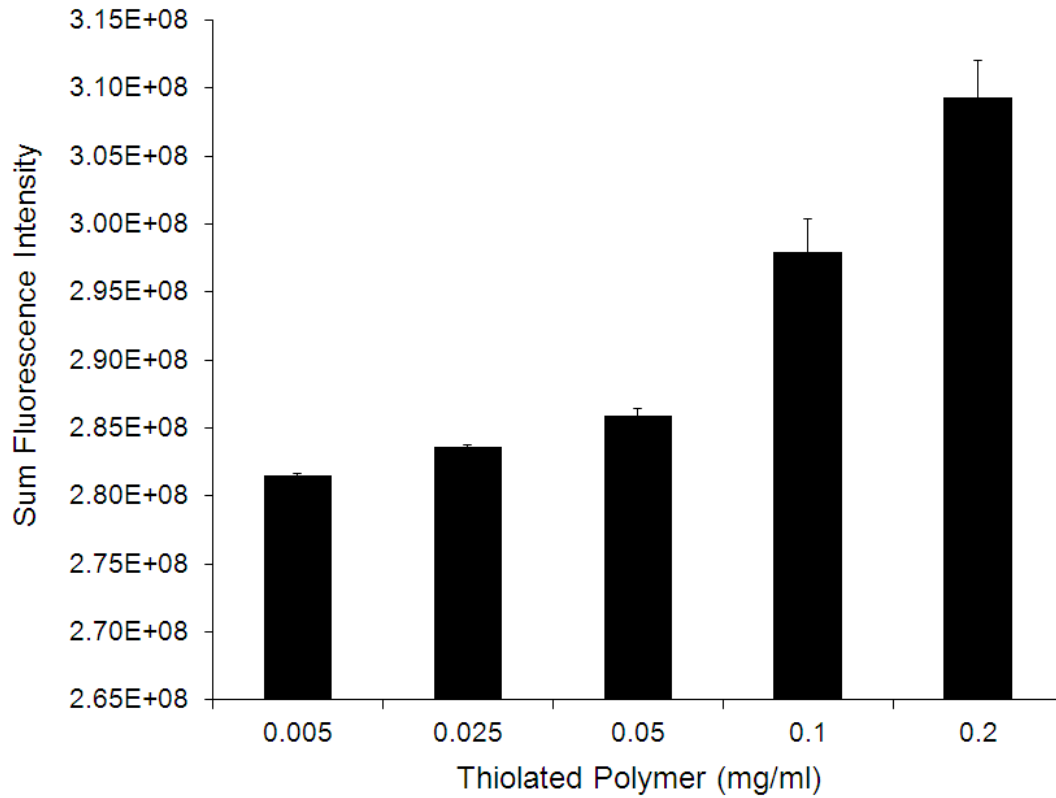
Figure 25. Sum fluorescence intensities obtained by fluorescent microscope confirm fluorescence of thiolated polymer.
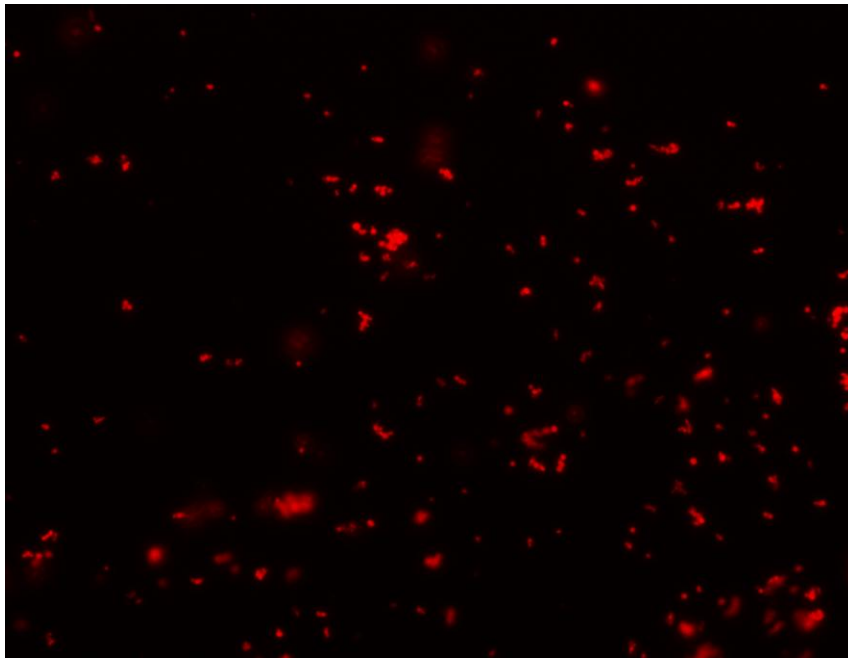

Figure 26. Image of thiolated polymer obtained by fluorescent microscope

85

4.3.2 Fluorescence Stability

Over time, a decrease in fluorescence intensities was observed in thiolated polymer samples. The phenomenon by which a molecule's fluorescence intensity decreases is also known as "quenching".[102] Figure 27 shows that thiolated polymers fluoresced at t=0, but exhibited a rapid decline in intensity over a 24 h period. The fluorescence decrease was more rapid in higher concentrated polymer solutions. Within 1 h of incubation, the highest concentrated sample dropped from ~1000 a.u. to ~250 a.u., whereas minimal fluorescence decrease was observed at other concentrations. After 24 h the fluorescence intensity of all samples dropped below ~250 a.u. Non-thiolated PAA did not show any change in fluorescence over time (Figure 28).

We attribute the fluorescent quenching in thiolated polymers to the formation of disulfide bonds. Previous studies have shown disulfide (S-S) form from thiols in an oxidation reaction. The reaction is spontaneous, but also time dependent, with the majority of thiol formation occuring within a 24 h period.[60] Based on our knowledge of thiolate activity in fluorescence, we believe that the reduction of thiolates, due to disulfide formation, diminished 'π' electron destabilization and hence decreased polymer fluorescence. Finally, we believe that high concentration polymer solutions exhibited a more rapid decline in fluorescence because disulfide formation occurs more rapidly as thiol concentration increases. Previous studies have demonstrated the correlations between disulfide formation and solution viscosity, suggesting that the close proximity of thiols in concentrated solutions facilitates disulfide bonding.[60]
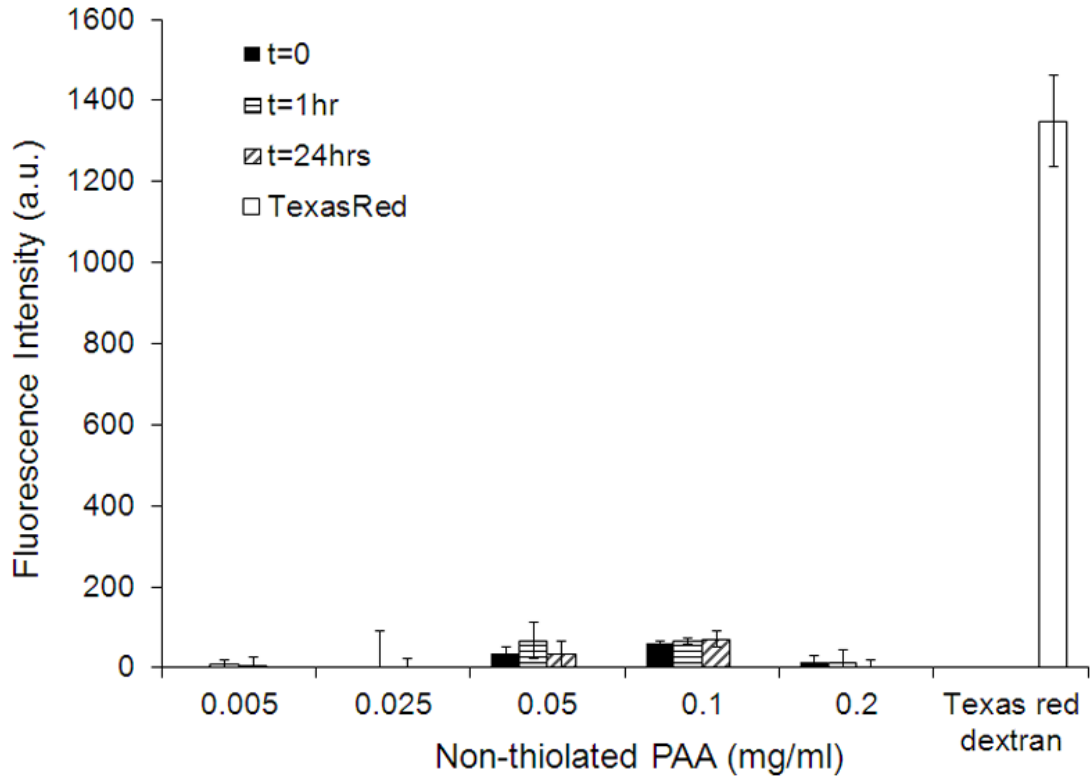
86

Figure 27. Fluorescence intensities of unmodfied PAA inidcate no fluorescence at ex/em ~595/620
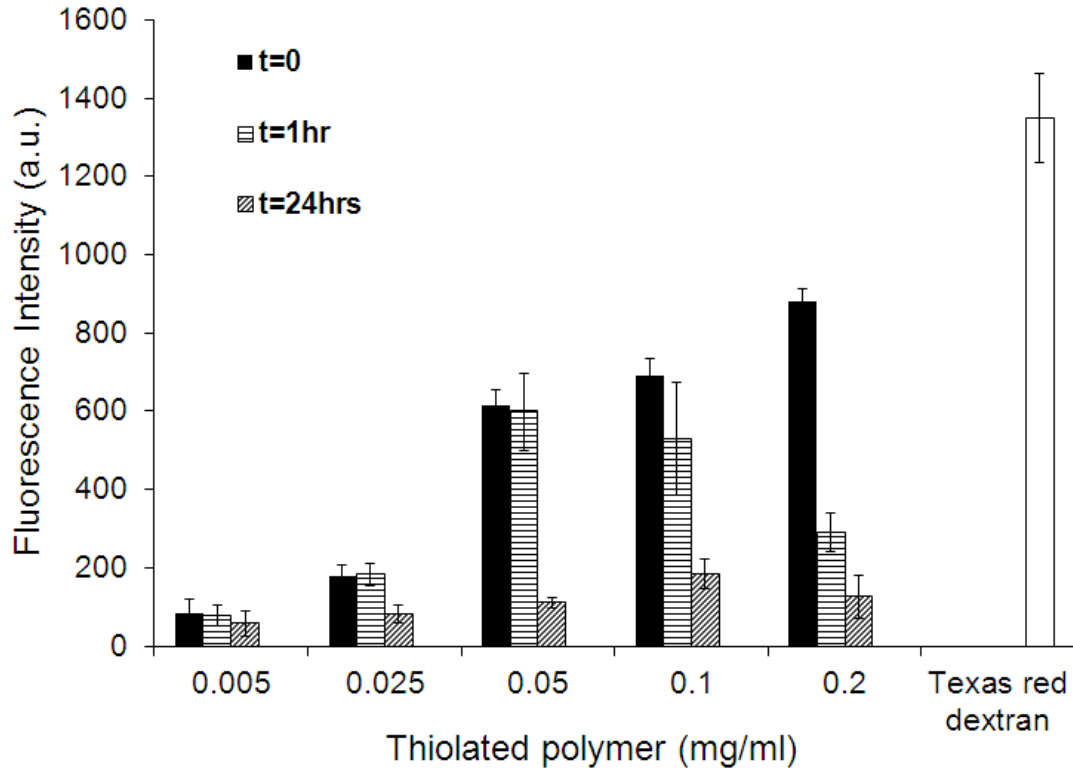

Figure 28. Fluorescence intensities of thiolated polymer indicate fluorescence instability at ex/em 595/620. Quenching attributed to reduction of thiolates in solution due to disulfide bond formation.

87

4.3.3 Acid Effects

pH-sensitive polymeric materials are often applied in drug delivery systems to trigger cargo release within the acidic environment of the lysosome.[103] Our studies showed that the addition of HCl to already quenched thiolated polymers temporarily increased fluorescence values. As shown in Figure 29, quenched thiolated polymers demonstrate a brief rise in flurescence upon the addition of HCl (t=0). However, within the first 15 min of HCl treatment, fluorescence values decreased between 200-600 a.u. After another 15 min, fluorescence intensities dropped to zero. This effect was not obsereved in non-thiolated polymers (Figure 30).

When studying the effects of thiolates on the emission of nanocrystal quantum dots (NQD), Jeong *et al*., concluded that thiol-thiolate concentrations, which are influenced by absolute initial thiol concentrations, pH, and reaction times, significanlty impact the systems photoluminescence. Overall, the study suggested that thiolates, rather than thiols, were responsible for NQD optical proerties. However, thiolates played a dual role, both enhancing and decreasing photoluminescnece.[100] We believe that the fluorescent effects exhibited upon titration resulted from shifts in the thiol-thiolate conentrations resulting from the addition of HCl. Acidic environments favor the protonated thiol form over thiolate groups. However, the mechanism behind the drastic but brief increase in fluorescence exhibited by thiolated polymers remains unclear.
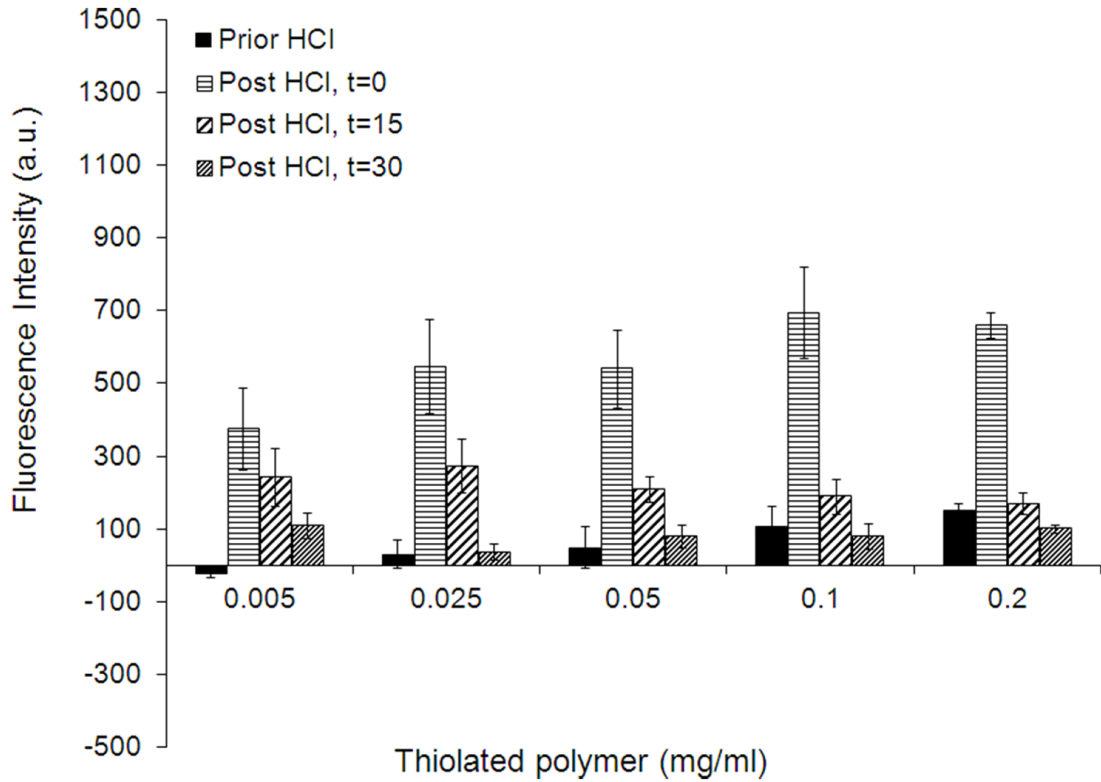
88

Figure 29. Fluorescent intensities of quenched thiolated polymers indicate rapid but brief increase in fluorescence at ex/em 595/620 after addition of HCl.
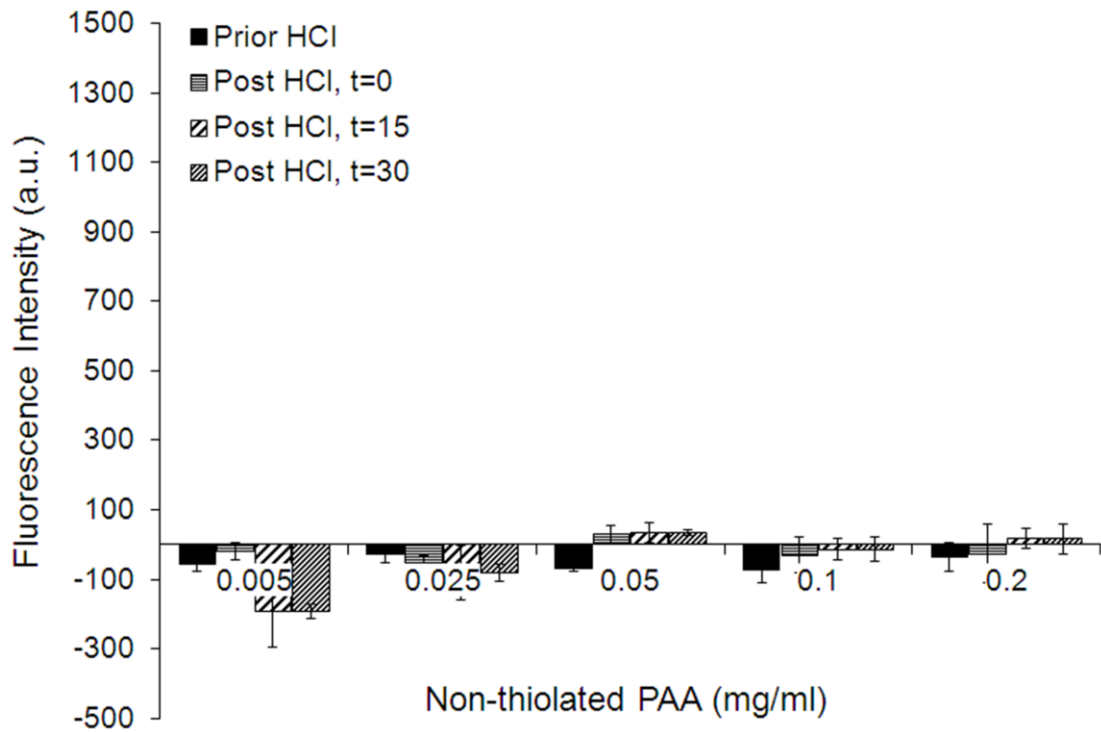

Figure 30. Fluorescence intensities of non-thiolated PAA do not change upon addition of HCl.

4.3.4 Protein Interactions

Conjugated fluorescent polymers have generated significant interest in sensor applications because of their efficient quenching in the presence of small molecule energy and electron acceptors.[104] In studies requiring cellular imaging, such as in-vitro polymeric gene delivery, polymer quenching could significanlty impact data accuracy. To determine whether serum proteins could affect the fluorescent proerties of thiolated polymers, polymers were suspended in DMEM(-phenol) and DMEM(+phenol) containing 10% FBS. Figure 31, shows that the presence of serum proteins immediately quenches polymer fluorescence in both phenol supplemented and phenol free media. Although it is possible that quenching occurs as a result of disulfide binding between thiolaed polymers and serum proteins containing thiol groups, we believe that the process is primarily driven by polymer-protein electrostatic interactions. In the previous assays, it took 24 h for complete quenching to occur in phenol-supplemeneted and phenol-free medias. In the presence of FBS, however, quenching is instantaneous in both media types. The rapidity of this reaction leads us to believe that static quenching due to polymer-protein electrostatic interactions, not disulfide bonding, is the primary drive behind the quenching effect. Previous studies have shown that static quenching, which requires the formation of a polymer-quencher complex, can from coulomb driven interactions between proteins and fluorescent polymers.[105]
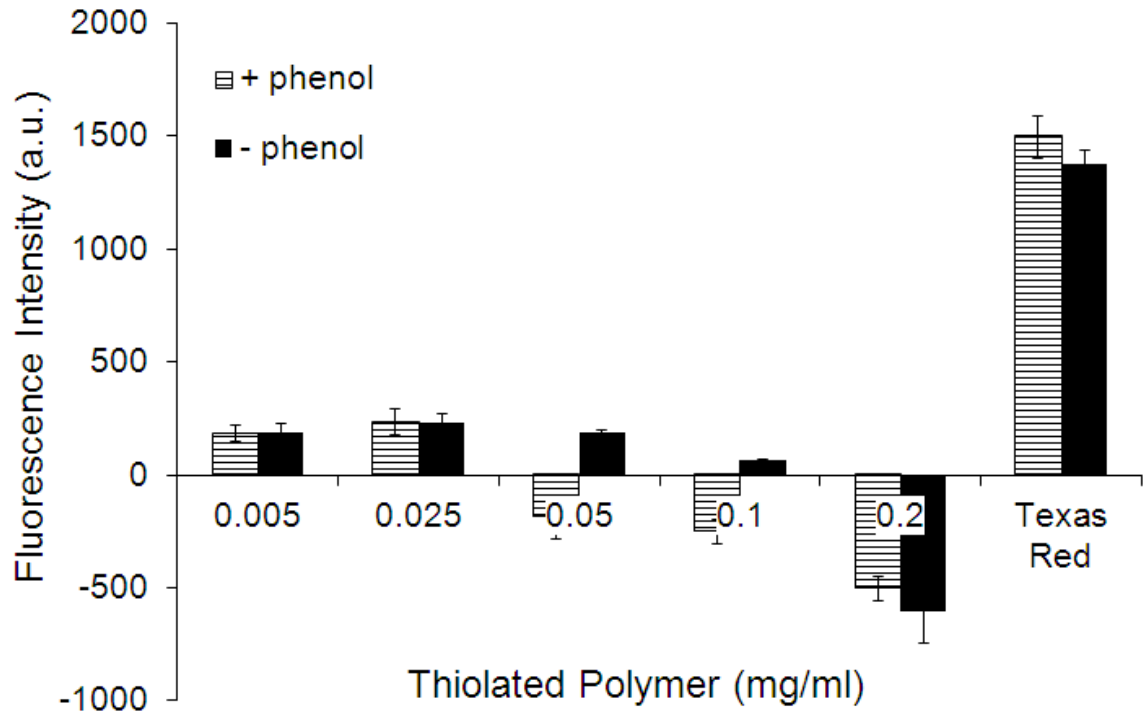
Figure 31. Flurecence intensities of thiolated polymer in +/ –phenol FBS supplemented media inidcate fluorescence quenching.

4.3.5 Polymer-Probe Interactions

In addition to polymer quenching, the quenching of fluorescent probes required for intracellular trafficking applications may also lead to incorrect data analysis. Previous studies have demonstrated probe quenching in the presence of two fluorescent reporters. Mishra *et al.*[106] showed that the fluorescence signal of YOYO-1 labeled plasmid DNA was quenched upon complexation with a rhodamine labeled beta-cyclodextrin containing polymer. This quenching effect was not observed when labeled plasmid was complexed with non-rhodamine labeled DNA.[106] To our knowledge, potential quenching of a molecular probe upon contact with a fluorescent polymer has not been investigated.

In the case of gene delivery, fluorescent molecular probes are often conjugated onto the genetic cargo for intracellular trafficking. In this study, plasmids were labeled with fluorescein reporter molecules prior to complexation with polymer in DMEM or PBS. Fluorescence intensities of labeled plasmid complexes were compared to uncomplexed fluorescein-plasmid controls. Results demonstrate that complexation quenched fluorescein in DMEM but not PBS. In DMEM, fluorescein labeled plasmid displays fluorescent intensity values of ~225 a.u. (Figure 32). At N/P 1 complexes solutions display about half the fluorescence intensity of the uncomplexed plasmid control. At N/P 5, the fluorescein signal is reduced to nearly 20%. Finally, at N/P values 10, 20, 40 the fluorescein is nearly undetectable. Polyplexes formed in PBS, on the other hand, did not display any fluorescein quenching (Figure 33).
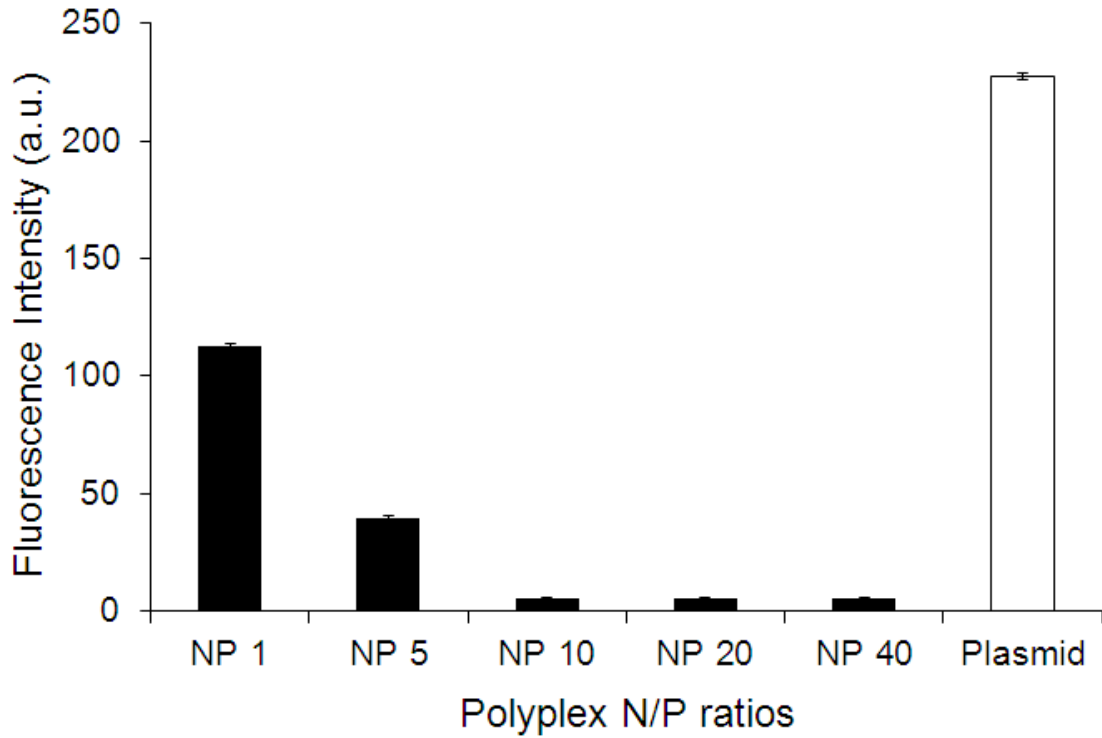
Figure 32. Fluorescein signal of labeled plasmid is quenched after complexation in DMEM.
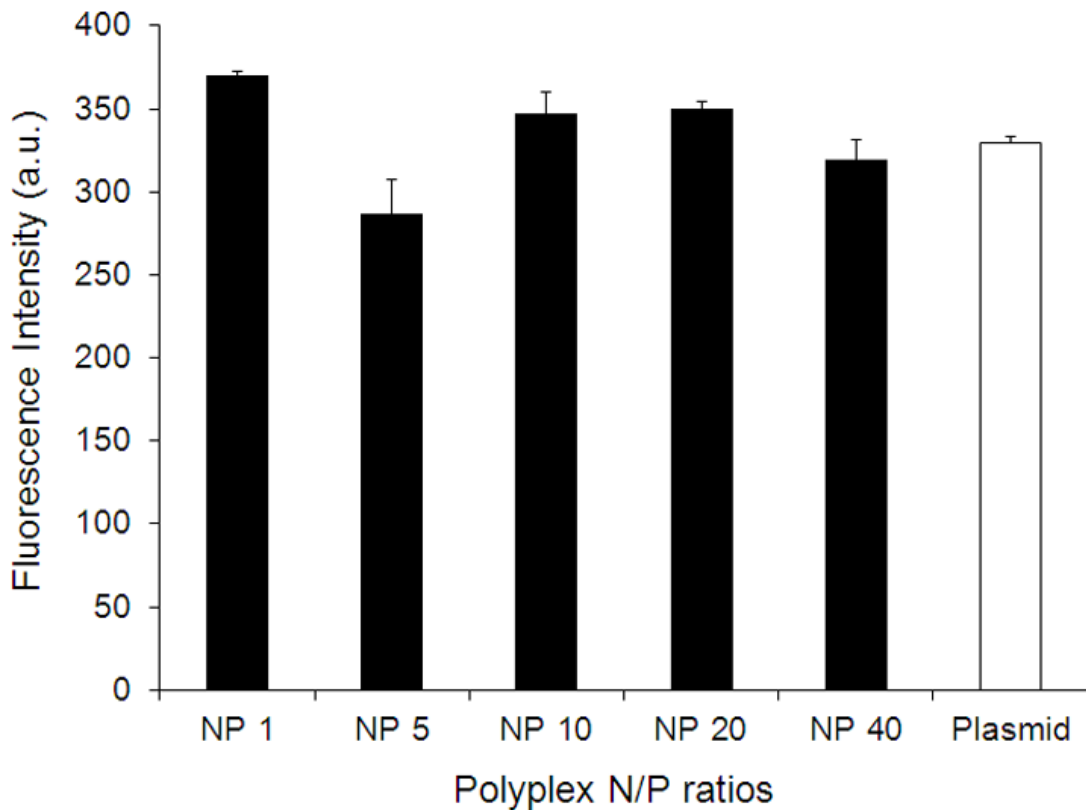
Figure 33. Fluorescein signal of labeled plasmids remains stable upon complexation in PBS.

93

4.4 Conclusions

Fluorescent polymers have the potential to simplify intracellular trafficking assays by eliminating the need for fluorescent molecular probes. In gene delivery, for example, fluorescent polymers can be used to visualize the polyplex delivery pathway intracellularly and identify any potential rate-limiting steps that inhibit successful and efficient gene expression. However, the fluorescent properties of such polymers have not been adequately studied.

Our research shows that environmental conditions can alter the polymers fluorescent qualities. Thiol-PAA exhibits its highest fluorescent intensities in PBS. We attribute the polymer's fluorescence to arise from destabilization of 'π' bonds by lone pair electrons of thiolates. Further, we believe that disulfide bond formation over time is responsible for fluorescence in quenching. Lowering the pH in this instance shifts the thiol-thiolate concentration and results in a rapid but brief increase in fluorescence. We also observed that the fluorescent signal quenches in the presence of proteins. Finally, we determined that the polymers will quench the signal of a plasmid labeled with a molecular probe in DMEM. This affect is not observed in PBS.

The data presented here signifies the importance of fully understanding a fluorescent polymers system prior to applying it in *in vitro* investigations. Preliminary experiments testing for changes in fluorescence under varying external conditions will allow for the elimination of potential background noise and result in more accurate analysis of cell transfection success.

Conclusions

A successful polymeric carrier for non-viral gene delivery must overcome a number of challenging extracellular and intracellular obstacles. Our preliminary data suggested that thiolated polymers are more suitable DNA carriers than non-thiolated polymers. For example, unlike unmodified PAA, all thiolated polymers were able to condense DNA. Further, at high N/P ratios, thiolated polymers were able to protect cargo DNA from degradative enzymes. In addition, all thiolated polymers exhibited higher buffering capacities than unmodified PAA, and therefore have a greater potential for endolysosomal escape. Further analysis indicated that the degree of disulfide crosslinking in thiolated polymers significantly impacted these properties. For example, highly crosslinked 5% thiolated polymers demonstrated superior cargo binding over 13% and 20% thiolated carriers, but were unable to release gene cargo. At the same time, 20% thiolated polymers, which had the greatest buffering capacity and potential for endolysosomal escape, were also inefficient at DNA binding and release. Further, 20% thiolated polymers were the least effective in protecting gene cargo. The N/P 20 and 40, 20% thiolated polyplexes were the exception to the 20% polyplex formulations, exhibiting high binding and release kinetics. In the end, the polyplexes with the greatest delivery potential overall, were the 13% thiolated polymers. Although 13% polyplexes showed partial degradation in the presence of DNase, they also achieved approximately twice the buffering capacity of PAA and were typically better at binding and releasing gene cargo.

Despite the positive results obtained from preliminary studies, all thiolated and non-thiolated polymers failed to deliver plasmid DNA to MCF-7 cells. Cell transfection assays showed that free thiols impede polyplex internalization due to polymer-cell surface attachments. The extent of attachment was determined by the concentration of thiols present, with higher concentrated polymers binding more readily to cell surfaces. Thiolated polymers also caused significant toxicity at high N/P ratios. The effects of thiols as determined by this study should be taken under consideration when synthesizing thiol-containing cationic polymers for gene delivery. The high binding between free thiols and polymer cell surfaces impedes internalization but may have potential in other applications such as tissue engineering, medical implants, and biosensors where cell adhesion is necessary.

Bibliography

1.   Jeong, J. H.; Kim, S. W.; Park, T. G., Molecular design of functional polymers for gene therapy. *Progress in Polymer Science* **2007,** 32, (11), 1239-1274.

2.   Pack, D. W.; Hoffman, A. S.; Pun, S.; Stayton, P. S., Design and development of polymers for gene delivery. *Nature Reviews Drug Discovery* **2005,** 4, (7), 581-593.

3.   Dachs, G. U.; Dougherty, G. J.; Stratford, I. J.; Chaplin, D. J., Targeting gene therapy to cancer: a review. *Oncol Res* **1997,** 9, (6-7), 313-25.

4.   Noe, F.; Pool, A. H.; Nissinen, J.; Gobbi, M.; Bland, R.; Rizzi, M.; Balducci, C.; Ferraguti, F.; Sperk, G.; During, M. J.; Pitkanen, A.; Vezzani, A., Neuropeptide Y gene therapy decreases chronic spontaneous seizures in a rat model of temporal lobe epilepsy. *Brain* **2008,** 131, 1506-1515.

5.   Fishbein, I.; Stachelek, S. J.; Connolly, J. M.; Wilensky, R. L.; Alferiev, I.; Levy, R. J., Site specific gene delivery in the cardiovascular system. *Journal of Controlled Release* **2005,** 109, (1-3), 37-48.

6.   Kumar, P.; Wu, H. Q.; McBride, J. L.; Jung, K. E.; Kim, M. H.; Davidson, B. L.; Lee, S. K.; Shankar, P.; Manjunath, N., Transvascular delivery of small interfering RNA to the central nervous system. *Nature* **2007,** 448, (7149), 39-43.

7.   Kaye, D. M.; Preovolos, A.; Marshall, T.; Byrne, M.; Hoshijima, M.; Hajjar, R.; Mariani, J. A.; Pepe, S.; Chien, K. R.; Power, J. M., Percutaneous cardiac recirculation-mediated gene TranSimer of an inhibitory phospholamban peptide reverses advanced heart failure in large animals. *Journal of the American College of Cardiology* **2007,** 50, (3), 253-260.

8.   Janson, C.; McPhee, S.; Bilaniuk, L.; Haselgrove, J.; Testaiuti, M.; Freese, A.; Wang, D. J.; Shera, D.; Hurh, P.; Rupin, J.; Saslow, E.; Goldfarb, O.; Goldberg, M.; Larijani, G.; Sharrar, W.; Liouterman, L.; Camp, A.; Kolodny, E.; Samulski, J.; Leone, P., Gene therapy of Canavan disease: AAV-2 vector for neurosurgical delivery of aspartoacylase gene (ASPA) to the human brain. *Human Gene Therapy* **2002,** 13, (11), 1391-1412.

9.   Tuszynski, M. H.; Thal, L.; Pay, M.; Salmon, D. P.; Sang, U. H.; Bakay, R.; Patel, P.; Blesch, A.; Vahlsing, H. L.; Ho, G.; Tong, G.; Potkin, S. G.; Fallon, J.; Hansen, L.; Mufson, E. J.; Kordower, J. H.; Gall, C.; Conner, J., A phase 1 clinical trial of nerve growth factor gene therapy for Alzheimer disease. *Nature Medicine* **2005,** 11, (5), 551-555.

10.   Romero, N. B.; Braun, S.; Benveniste, O.; Leturcq, F.; Hogrel, J. Y.; Morris, G. E.; Barois, A.; Eymard, B.; Payan, C.; Ortega, V.; Boch, A. L.; Lejean, L.; Thioudellet, C.; Mourot, B.; Escot, C.; Choquel, A.; Recan, D.; Kaplan, J. C.; Dickson, G.; Klatzmann, D.; Molinier-Frenckel, V.; Guillet, J. G.; Squiban, P.; Herson, S.; Fardeau, M., Phase I study of dystrophin Duchenne/Becker plasmid-based gene therapy in muscular dystrophy. *Human Gene Therapy* **2004,** 15, (11), 1065-1076.

11.   Wong, S. Y.; Pelet, J. M.; Putnam, D., Polymer systems for gene delivery-past, present, and future. *Progress in Polymer Science* **2007,** 32, (8-9), 799-837.

12.   Edelstein, M. L.; Abedi, M. R.; Wixon, J., Gene therapy clinical trials worldwide to 2007 - an update. *Journal of Gene Medicine* **2007,** 9, (10), 833-842.

13.   Thomas, M.; Klibanov, A. M., Non-viral gene therapy: polycation-mediated DNA delivery. *Applied Microbiology and Biotechnology* **2003,** 62, (1), 27-34.

14.   Gao, X.; Kim, K. S.; Liu, D. X., Nonviral gene delivery: What we know and what is next. *Aaps Journal* **2007,** 9, (1), E92-E104.

15.   Mintzer, M. A.; Simanek, E. E., Nonviral Vectors for Gene Delivery. *Chemical Reviews* **2009,** 109, (2), 259-302.

16.   Gabrielson, N. P.; Pack, D. W., Acetylation of polyethylenimine enhances gene delivery via weakened polymer/DNA interactions. *Biomacromolecules* **2006,** 7, (8), 2427-2435.

17.   Raper, S. E.; Chirmule, N.; Lee, F. S.; Wivel, N. A.; Bagg, A.; Gao, G. P.; Wilson, J. M.; Batshaw, M. L., Fatal systemic inflammatory response syndrome in a ornithine transcarbamylase deficient patient following adenoviral gene transfer. *Molecular Genetics and Metabolism* **2003,** 80, (1-2), 148-158.

18.   Marshall, E., Clinical research - FDA halts all gene therapy trials at Penn. *Science* **2000,** 287, (5453), 565-+.

19.   Cavazzana-Calvo, M.; Hacein-Bey, S.; Basile, C. D.; Gross, F.; Yvon, E.; Nusbaum, P.; Selz, F.; Hue, C.; Certain, S.; Casanova, J. L.; Bousso, P.; Le Deist, F.; Fischer, A., Gene therapy of human severe combined immunodeficiency (SCID)-X1 disease. *Science* **2000,** 288, (5466), 669-672.

20.   Check, E., Gene therapy: A tragic setback. *Nature* **2002,** 420, (6912), 116-118.
21.   Marwick, C., FDA halts gene therapy trials after leukaemia case in France. *British Medical Journal* **2003,** 326, (7382), 181-181.

22.   Masago, K.; Itaka, K.; Nishiyama, N.; Chung, U. I.; Kataoka, K., Gene delivery with biocompatible cationic polymer: Pharmacogenomic analysis on cell bioactivity. *Biomaterials* **2007,** 28, (34), 5169-5175.

23.   Morille, M.; Passirani, C.; Vonarbourg, A.; Clavreul, A.; Benoit, J. P., Progress in developing cationic vectors for non-viral systemic gene therapy against cancer. *Biomaterials* **2008,** 29, (24-25), 3477-3496.

24.   Kim, S. W.; Kim, T. I., Bioreducible polymers for gene delivery. *Reactive & Functional Polymers* **2011,** 71, (3), 344-349.

25.   Jere, D.; Arote, R.; Jiang, H. L.; Kim, Y. K.; Cho, M. H.; Cho, C. S., Bioreducible polymers for efficient gene and siRNA delivery. *Biomedical Materials* **2009,** 4, (2).

26.   Kim, T.; Rothmund, T.; Kissel, T.; Kim, S. W., Bioreducible polymers with cell penetrating and endosome buffering functionality for gene delivery systems. *Journal of Controlled Release* **2011,** 152, (1), 110-119.

27.   Mastrobattista, E.; Hennink, W. E., Polymers for Gene Delivery Charged for Success. *Nature Materials* **2012,** 11, (1), 10-12.

28.   Varga, C. M.; Wickham, T. J.; Lauffenburger, D. A., Receptor-mediated targeting of gene delivery vectors: Insights from molecular mechanisms for improved vehicle design. *Biotechnology and Bioengineering* **2000,** 70, (6), 593-605.

29.   Brown, M. D.; Schatzlein, A. G.; Uchegbu, I. F., Gene delivery with synthetic (non viral) carriers. *International Journal of Pharmaceutics* **2001,** 229, (1-2), 1-21.

30.   Hou, S.; Yang, K.; Yao, Y.; Liu, Z.; Feng, X.; Wang, R.; Yang, Y.; Wang, C., DNA condensation induced by a cationic polymer studied by atomic force microscopy and electrophoresis assay. *Colloids Surf B Biointerfaces* **2008,** 62, (1), 151-6.

31.   Safinya, C. R.; Koltover, I.; Wagner, K., DNA condensation in two dimensions. *Proceedings of the National Academy of Sciences of the United States of America* **2000,** 97, (26), 14046-14051.

32.   Zhao, Q. Q.; Chen, J. L.; Lv, T. F.; He, C. X.; Tang, G. P.; Liang, W. Q.; Tabata, Y.; Gao, J. Q., N/P Ratio Significantly Influences the Transfection Efficiency and Cytotoxicity of a Polyethylenimine/Chitosan/DNA Complex. *Biological & Pharmaceutical Bulletin* **2009,** 32, (4), 706-710.

33.   Mok, H.; Park, T. G., Functional Polymers for Targeted Delivery of Nucleic Acid Drugs. *Macromolecular Bioscience* **2009,** 9, (8), 731-743.

34.   Bellocq, N. C.; Pun, S. H.; Jensen, G. S.; Davis, M. E., Transferrin-containing, cyclodextrin polymer-based particles for tumor-targeted gene delivery. *Bioconjugate Chemistry* **2003,** 14, (6), 1122-1132.

35.   Kircheis, R.; Wightman, L.; Schreiber, A.; Robitza, B.; Rossler, V.; Kursa, M.; Wagner, E., Polyethylenimine/DNA complexes shielded by transferrin target gene expression to tumors after systemic application. *Gene Therapy* **2001,** 8, (1), 28-40.

36.   Funhoff, A. M.; Van Nostrum, C. F.; Lok, M. C.; Kruijtzer, J. A. W.; Crommelin, D. J. A.; Hennink, W. E., Cationic polymethacrylates with covalently linked membrane destabilizing peptides as gene delivery vectors. *Journal of Controlled Release* **2005,** 101, (1-3), 233-246.

37.   Kirchner, C.; Javier, A. M.; Susha, A. S.; Rogach, A. L.; Kreft, O.; Sukhorukov, G. B.; Parak, W. J., Cytotoxicity of nanoparticle-loaded polymer capsules. *Talanta* **2005,** 67, (3), 486-491.

38.   Yu, J. H.; Huang, J.; Jiang, H. L.; Quan, J. S.; Cho, M. H.; Cho, C. S., Guanidinylated Poly(allyl amine) as a Gene Carrier. *Journal of Applied Polymer Science* **2009,** 112, (2), 926-933.

39.   Fischer, D.; Li, Y. X.; Ahlemeyer, B.; Krieglstein, J.; Kissel, T., In vitro cytotoxicity testing of polycations: influence of polymer structure on cell viability and hemolysis. *Biomaterials* **2003,** 24, (7), 1121-1131.

40.   Zhang, S. B.; Xu, Y. M.; Wang, B.; Qiao, W. H.; Liu, D. L.; Li, Z. S., Cationic compounds used in lipoplexes and polyplexes for gene delivery. *Journal of Controlled Release* **2004,** 100, (2), 165-180.

41.   Synatschke, C. V.; Schallon, A.; Jerome, V.; Freitag, R.; Muller, A. H., Influence of Polymer Architecture and Molecular Weight of Poly(2-(dimethylamino)ethyl methacrylate) Polycations on Transfection Efficiency and Cell Viability in Gene Delivery. *Biomacromolecules* **2011,** 12, (12), 4247–4255.

42.   Xiong, M. P.; Forrest, M. L.; Ton, G.; Zhao, A.; Davies, N. M.; Kwon, G. S., Poly(aspartate-g-PEI800), a polyethylenimine analogue of low toxicity and high transfection efficiency for gene delivery. *Biomaterials* **2007,** 28, (32), 4889-4900.

43.   Godbey, W. T.; Wu, K. K.; Mikos, A. G., Size matters: Molecular weight affects the efficiency of poly(ethylenimine) as a gene delivery vehicle. *Journal of Biomedical Materials Research* **1999,** 45, (3), 268-275.

44.   Georgiou, T. K.; Vamvakaki, M.; Patrickios, C. S.; Yamasaki, E. N.; Phylactou, L. A., Nanoscopic cationic methacrylate star homopolymers: Synthesis by group transfer polymerization, characterization and evaluation as transfection reagents. *Biomacromolecules* **2004,** 5, (6), 2221-2229.

45.   vandeWetering, P.; Cherng, J. Y.; Talsma, H.; Hennink, W. E., Relation between transfection efficiency and cytotoxicity of poly(2-(dimethylamino)ethyl methacrylate)/plasmid complexes. *Journal of Controlled Release* **1997,** 49, (1), 59-69.

46.   Pafiti, K. S.; Mastroyiannopoulos, N. P.; Phylactou, L. A.; Patrickios, C. S., Hydrophilic Cationic Star Homopolymers Based on a Novel Diethanol-N-Methylamine Dimethacrylate Cross-Linker for siRNA Transfection: Synthesis, Characterization, and Evaluation. *Biomacromolecules* **2011,** 12, (5), 1468-1479.

47.   Lv, H. T.; Zhang, S. B.; Wang, B.; Cui, S. H.; Yan, J., Toxicity of cationic lipids and cationic polymers in gene delivery. *Journal of Controlled Release* **2006,** 114, (1), 100-109.

48.   Pathak, A.; Aggarwal, A.; Kurupati, R. K.; Patnaik, S.; Swami, A.; Singh, Y.; Kumar, P.; Vyas, S. P.; Gupta, K. C., Engineered polyallylamine nanoparticles for efficient in vitro transfection. *Pharmaceutical Research* **2007,** 24, (8), 1427-1440.

49.   Godbey, W. T.; Wu, K. K.; Mikos, A. G., Poly(ethylenimine) and its role in gene delivery. *Journal of Controlled Release* **1999,** 60, (2-3), 149-160.

50.   Boussif, O.; Zanta, M. A.; Behr, J. P., Optimized galenics improve in vitro gene transfer with cationic molecules up to 1000-fold. *Gene Therapy* **1996,** 3, (12), 1074-1080.

51.	Kwon, G. S.; Xiong, M. P.; Forrest, M. L.; Ton, G.; Zhao, A.; Davies, N. M., Poly(aspartate-g-PEI800), a polyethylenimine analogue of low toxicity and high transfection efficiency for gene delivery. *Biomaterials* **2007,** 28, (32), 4889-4900.

52.	Park, T. G.; Jeong, J. H.; Kim, S. W., Current status of polymeric gene delivery systems. *Advanced Drug Delivery Reviews* **2006,** 58, (4), 467-486.

53.	Nimesh, S.; Kumar, R.; Chandra, R., Novel polyallylamine-dextran sulfate-DNA nanoplexes: Highly efficient non-viral vector for gene delivery. *International Journal of Pharmaceutics* **2006,** 320, (1-2), 143-149.

54.	Yamagata, M.; Kawano, T.; Shiba, K.; Mori, T.; Katayama, Y.; Niidome, T., Structural advantage of dendritic poly(L-lysine) for gene delivery into cells. *Bioorganic & Medicinal Chemistry* **2007,** 15, (1), 526-532.

55.	Verbaan, F.; van Dam, I.; Takakura, Y.; Hashida, M.; Hennink, W.; Storm, G.; Oussoren, C., Intravenous fate of poly(2-(dimethylamino)ethyl methacrylate)-based polyplexes. *Eur J Pharm Sci* **2003,** 20, (4-5), 419-27.

56.	van de Wetering, P.; Schuurmans-Nieuwenbroek, N. M. E.; Hennink, W. E.; Storm, G., Comparative transfection studies of human ovarian carcinoma cells in vitro, ex vivo and in vivo with poly(2-(dimethylamino)ethyl methacrylate)-based polyplexes. *Journal of Gene Medicine* **1999,** 1, (3), 156-165.

57.	Kim, S. W.; Kim, T.; Rothmund, T.; Kissel, T., Bioreducible polymers with cell penetrating and endosome buffering functionality for gene delivery systems. *Journal of Controlled Release* **2011,** 152, (1), 110-119.

58.	Cho, C. S.; Jere, D.; Arote, R.; Jiang, H. L.; Kim, Y. K.; Cho, M. H., Bioreducible polymers for efficient gene and siRNA delivery. *Biomedical Materials* **2009,** 4, (2).

59.	Peng, Q.; Hu, C.; Cheng, J.; Zhong, Z.; Zhuo, R., Influence of disulfide density and molecular weight on disulfide cross-linked polyethylenimine as gene vectors. *Bioconjug Chem* **2009,** 20, (2), 340-6.

60.	Marschutz, M. K.; Bernkop-Schnurch, A., Thiolated polymers: self-crosslinking properties of thiolated 450 kDa poly(acrylic acid) and their influence on mucoadhesion. *European Journal of Pharmaceutical Sciences* **2002,** 15, (4), 387-394.

61.	Deshpande, M. C.; Garnett, M. C.; Vamvakaki, M.; Bailey, L.; Armes, S. P.; Stolnik, S., Influence of polymer architecture on the structure of complexes formed by PEG-tertiary amine methacrylate copolymers and phosphorothioate oligonucleotide. *Journal of Controlled Release* **2002,** 81, (1-2), 185-199.

62.	Xu, P. S.; Quick, G. K.; Yeo, Y., Gene delivery through the use of a hyaluronate-associated intracellularly degradable crosslinked polyethyleneimine. *Biomaterials* **2009,** 30, (29), 5834-5843.

63.   Giacomelli, C.; Lafitte, G.; Borsali, R., Polycaprolactone-b-poly(ethylene oxide) biocompatible micelles as dynamic light scattering drug delivery nanocarriers: Dynamic light scattering and fluorescence experiments. *Macromolecular Symposia* **2005,** 229, 107-117.

64.   Arima, H.; Kihara, F.; Hirayama, F.; Uekama, K., Enhancement of gene expression by polyamidoamine dendrimer conjugates with alpha-, beta-, and gamma-cyclodextrins. *Bioconjugate Chemistry* **2001,** 12, (4), 476-484.

65.   Tseng, S. J.; Tang, S. C.; Shau, M. D.; Zeng, Y. F.; Cherng, J. Y.; Shih, M. F., Structural characterization and buffering capacity in relation to the transfection efficiency of biodegradable polyurethane. *Bioconjugate Chemistry* **2005,** 16, (6), 1375-1381.

66.   Ou, M.; Wang, X. L.; Xu, R.; Chang, C. W.; Bull, D. A.; Kim, S. W., Novel biodegradable poly(disulfide amine)s for gene delivery with high efficiency and low cytotoxicity. *Bioconjug Chem* **2008,** 19, (3), 626-33.

67.   Cho, C. S.; Yu, J. H.; Huang, J.; Jiang, H. L.; Quan, J. S.; Cho, M. H., Guanidinylated Poly(allyl amine) as a Gene Carrier. *Journal of Applied Polymer Science* **2009,** 112, (2), 926-933.
68.   Ikonen, M.; Murtomaki, L.; Kontturi, K., Controlled complexation of plasmid DNA with cationic polymers: Effect of surfactant on the complexation and stability of the complexes. *Colloids and Surfaces B-Biointerfaces* **2008,** 66, (1), 77-83.

69.   Park, J.; Choi, Y. W.; Kim, K.; Chung, H.; Sohn, D., Aggregation processes of a weak polyelectrolyte, poly(allylamine) hydrochloride. *Bulletin of the Korean Chemical Society* **2008,** 29, (1), 104-110.

70.   Zhou, Y. L.; Li, Y. Z., Studies of interaction between poly(allylamine hydrochloride) and double helix DNA by spectral methods. *Biophysical Chemistry* **2004,** 107, (3), 273-281.

71.   Merdan, T.; Kopecek, J.; Kissel, T., Prospects for cationic polymers in gene and oligonucleotide therapy against cancer. *Adv Drug Deliv Rev* **2002,** 54, (5), 715-58.

72.   Fishbein, I.; Chorny, M.; Levy, R. J., Site-specific gene therapy for cardiovascular disease. *Current Opinion in Drug Discovery & Development* **2010,** 13, (2), 203-213.

73.   Mandzy, N.; Grulke, E.; Druffel, T., Breakage of TiO2 agglomerates in electrostatically stabilized aqueous dispersions. *Powder Technology* **2005,** 160, (2), 121-126.

74.   Muro, S.; Koval, M.; Muzykantov, V., Endothelial endocytic pathways: gates for vascular drug delivery. *Curr Vasc Pharmacol* **2004,** 2, (3), 281-99.

75.   Muro, S. M. V., Affinity and geometry of drug carriers: design parameters for rational control of intracellular delivery. In *Organelle-specific pharmaceutical nanotechnology*, Weissig V., D. S. G., Ed. John Wiley & Sons: Hoboken, NJ, 2010; pp 449-474.

76.   Muro, S.; Wiewrodt, R.; Thomas, A.; Koniaris, L.; Albelda, S. M.; Muzykantov, V. R.; Koval, M., A novel endocytic pathway induced by clustering endothelial ICAM-1 or PECAM-1. *J Cell Sci* **2003,** 116, (Pt 8), 1599-609.

77.   Jeong, S.; Achermann, M.; Nanda, J.; Ivanov, S.; Klimov, V. I.; Hollingsworth, J. A., Effect of the thiol-thiolate equilibrium on the photophysical properties of aqueous CdSe/ZnS nanocrystal quantum dots. *J Am Chem Soc* **2005,** 127, (29), 10126-7.

78.   Williams, R. T.; Bridges, J. W., Fluorescence of Solutions: A Review. *J Clin Pathol* **1964,** 17, 371-94.

79.   Midoux, P.; Pichon, C.; Yaouanc, J. J.; Jaffres, P. A., Chemical vectors for gene delivery: a current review on polymers, peptides and lipids containing histidine or imidazole as nucleic acids carriers. *British Journal of Pharmacology* **2009,** 157, (2), 166-178.

80.   Han, S.; Mahato, R. I.; Sung, Y. K.; Kim, S. W., Development of biomaterials for gene therapy. *Molecular Therapy* **2000,** 2, (4), 302-317.

81.   Samaj, J.; Baluska, F.; Voigt, B.; Schlicht, M.; Volkmann, D.; Menzel, D., Endocytosis, actin cytoskeleton, and signaling. *Plant Physiology* **2004,** 135, (3), 1150-1161.

82.   Gary, D. J.; Puri, N.; Won, Y. Y., Polymer-based siRNA delivery: Perspectives on the fundamental and phenomenological distinctions from polymer-based DNA delivery. *Journal of Controlled Release* **2007,** 121, (1-2), 64-73.

83.   Jachimska, B.; Jasinski, T.; Warszynski, P.; Adamczyk, Z., Conformations of poly(allylamine hydrochloride) in electrolyte solutions: Experimental measurements and theoretical modeling. *Colloids and Surfaces a-Physicochemical and Engineering Aspects* **2010,** 355, (1-3), 7-15.

84.   Song, M. C.; Scheraga, H. A., Formation of native structure by intermolecular thiol-disulfide exchange reactions without oxidants in the folding of bovine pancreatic ribonuclease A. *Febs Letters* **2000,** 471, (2-3), 177-181.

85.   Yang, J.; Zhang, Y.; Gautam, S.; Liu, L.; Dey, J.; Chen, W.; Mason, R. P.; Serrano, C. A.; Schug, K. A.; Tang, L., Development of aliphatic biodegradable photoluminescent polymers. *Proceedings of the National Academy of Sciences of the United States of America* **2009,** 106, (25), 10086-10091.

86.   Wu, C.; Bull, B.; Szymanski, C.; Christensen, K.; McNeill, J., Multicolor Conjugated Polymer Dots for Biological Fluorescence Imaging. *Acs Nano* **2008,** 2, (11), 2415-2423.

87.   Tuncel, D.; Demir, H. V., Conjugated polymer nanoparticles. *Nanoscale* **2010,** 2, (4), 484-494.

88.   Fernando, L. P.; Kandel, P. K.; Yu, J. B.; McNeill, J.; Ackroyd, P. C.; Christensen, K. A., Mechanism of Cellular Uptake of Highly Fluorescent Conjugated Polymer Nanoparticles. *Biomacromolecules* **2010,** 11, (10), 2675-2682.

89.   Forrest, M. L.; Pack, D. W., On the kinetics of polyplex endocytic trafficking: Implications for gene delivery vector design. *Molecular Therapy* **2002,** 6, (1), 57-66.

103

90. Yu, J.; Xiao, J.; Ren, X. J.; Lao, K. Q.; Xie, X. S., Probing gene expression in live cells, one protein molecule at a time. *Science* **2006,** 311, (5767), 1600-1603.

91. Baier, M. C.; Huber, J.; Mecking, S., Fluorescent Conjugated Polymer Nanoparticles by Polymerization in Miniemulsion. *Journal of the American Chemical Society* **2009,** 131, (40), 14267-14273.

92. Kumaraswamy, S.; Bergstedt, T.; Shi, X. B.; Rininsland, F.; Kushon, S.; Xia, W. S.; Ley, K.; Achyuthan, K.; McBranch, D.; Whitten, D., Fluorescent-conjugated polymer superquenching facilitates highly sensitive detection of proteases. *Proceedings of the National Academy of Sciences of the United States of America* **2004,** 101, (20), 7511-7515.

93. You, C. C.; Miranda, O. R.; Gider, B.; Ghosh, P. S.; Kim, I. B.; Erdogan, B.; Krovi, S. A.; Bunz, U. H. F.; Rotello, V. M., Detection and identification of proteins using nanoparticle-fluorescent polymer 'chemical nose' sensors. *Nature Nanotechnology* **2007,** 2, (5), 318-323.

94. Stsiapura, V.; Sukhanova, A.; Artemyev, M.; Pluot, M.; Cohen, J. H. M.; Baranov, A. V.; Oleinikov, V.; Nabiev, I., Functionalized nanocrystal-tagged fluorescent polymer beads: synthesis, physicochemical characterization, and immunolabeling application. *Analytical Biochemistry* **2004,** 334, (2), 257-265.

95. Kushon, S. A.; Ley, K. D.; Bradford, K.; Jones, R. M.; McBranch, D.; Whitten, D., Detection of DNA hybridization via fluorescent polymer superquenching. *Langmuir* **2002,** 18, (20), 7245-7249.

96. McQuade, D. T.; Pullen, A. E.; Swager, T. M., Conjugated polymer-based chemical sensors. *Chemical Reviews* **2000,** 100, (7), 2537-2574.

97. Wang, D. L.; Gong, X.; Heeger, P. S.; Rininsland, F.; Bazan, G. C.; Heeger, A. J., Biosensors from conjugated polyelectrolyte complexes. *Proceedings of the National Academy of Sciences of the United States of America* **2002,** 99, (1), 49-53.

98. Williams, R. T.; Bridges, J. W., Fluorescence of Solutions - Review. *Journal of Clinical Pathology* **1964,** 17, (4), 371-&.

99. Irene Bacalocostantis, V. P. M., Michael S Kang, Addison S Goodley, Silvia Muro, and Peter Kofinas, The effect of thiol pendant conjugates on plasmid DNA binding, release, and stability of polymeric delivery vectors. *Biomacromolecules* **2012**.

100. Jeong, S.; Achermann, M.; Nanda, J.; Lvanov, S.; Klimov, V. I.; Hollingsworth, J. A., Effect of the thiol-thiolate equilibrium on the photophysical properties of aqueous CdSe/ZnS nanocrystal quantum dots. *Journal of the American Chemical Society* **2005,** 127, (29), 10126-10127.

101. Farrar, J. A.; Formicka, G.; Zeppezauer, M.; Thomson, A. J., Magnetic and optical properties of copper-substituted alcohol dehydrogenase: A bisthiolate copper(II) complex. *Biochemical Journal* **1996,** 317, 447-456.

102.   Ghali, M., Static quenching of bovine serum albumin conjugated with small size CdS nanocrystalline quantum dots. *Journal of Luminescence* **2010,** 130, (7), 1254-1257.

103.   Schmaljohann, D., Thermo- and pH-responsive polymers in drug delivery. *Advanced Drug Delivery Reviews* **2006,** 58, (15), 1655-1670.

104.   Fan, C. H.; Wang, S.; Hong, J. W.; Bazan, G. C.; Plaxco, K. W.; Heeger, A. J., Beyond superquenching: Hyper-efficient energy transfer from conjugated polymers to gold nanoparticles. *Proceedings of the National Academy of Sciences of the United States of America* **2003,** 100, (11), 6297-6301.

105.   Fan, C. H.; Plaxco, K. W.; Heeger, A. J., High-efficiency fluorescence quenching of conjugated polymers by proteins. *Journal of the American Chemical Society* **2002,** 124, (20), 5642-5643.

106.   Mishra, S.; Webster, P.; Davis, M. E., PEGylation significantly affects cellular uptake and intracellular trafficking of non-viral gene delivery particles. *European Journal of Cell Biology* **2004,** 83, (3), 97-111.